PETROLOGY AND EMPLACEMENT OF A DIFFERENTIATED SUBVOLCANIC MAFIC SILL COMPLEX IN THE EARLY PRECAMBRIAN FAVOURABLE LAKE VOLCANIC COMPLEX, NORTHWESTERN ONTARIO

A thesis submitted to the

University of Manitoba

in partial fullfilment of the requirements

for the degree

Master of Science

by

Mati Raudsepp

1978 December

Department of Earth Sciences

University of Manitoba

Winnipeg R3T 2N2 Canada

PETROLOGY AND EMPLACEMENT OF A DIFFERENTIATED SUBVOLCANIC MAFIC SILL COMPLEX IN THE EARLY PRECAMBRIAN FAVOURABLE LAKE VOLCANIC COMPLEX, NORTHWESTERN ONTARIO

BY

MATI RAUDSEPP

A dissertation submitted to the Faculty of Graduate Studies of the University of Manitoba in partial fulfillment of the requirements of the degree of

MASTER OF SCIENCE

ABSTRACT

The sill complex is a broadly concordant, multiple, tholeiitic intrusion 4.7 km long and 0.87 km wide that was intruded into the early Precambrian, isoclinally folded Favourable Lake metavolcanic-metasedimentary sequence. It occurs in a vertically dipping, west-facing part of the sequence and the present erosional surface is a cross-section approximately perpendicular to the primary attitude. The cross-sectional area is 3.66 km^2.

The complex comprises three multiple phases that differ in mode and degree of differentiation, and nature of emplacement. These have been designated as phases X, Y, and Z. Each phase marks a discrete intrusive event, with petrologic, geochemical, and intrusive characteristics independent of the others.

Phase X consists of five separate intrusive units each of which comprises a lower ultramafic zone of clinopyroxene and clinopyroxene-olivine cumulates, and an upper mafic zone of plagioclase and clinopyroxene-plagioclase cumulates. The units have very fine-grained mafic chilled border zones averaging 3 m thick. Each unit is either a simple or multiple sill formed by one or more pulses of magma.

Phase Y is a relatively homogeneous, multiple intrusion comprising a succession of mafic sills that are little differentiated. Sills are generally concordant but discordant, transgressive phases are common.

Phase Z comprises five differentiated, multiple, mafic sills, the largest of which consists of a lower ultramafic zone of orthopyroxene-olivine cumulates and an upper mafic zone of subophitic to ophitic gabbro.

All three phases have been metamorphosed to lower to middle greenschist facies and primary mineralogy has been replaced by metamorphic pseudomorphs. Pressure of metamorphism, estimated from the crossite component of Ca-rich amphiboles, was less than 3 kb.

Interpretation of chemical data is hampered by alteration and metamorphism, and by the open-system nature of units in phase X. The observed crystallization sequence of olivine, clinopyroxene, and plagioclase could not be duplicated in the theoretical system olivine-clinopyroxene-plagioclase-silica by ideal fractional crystallization. The cumulate sequence requires the changing of the crystallizing magma composition by additions or deletions of magma in an open system. Such complex petrologic diversity is characteristic of subvolcanic conduits.

Soft-sediment deformation in sedimentary units adjacent to parts of the complex suggests that the complex was emplaced when the country rocks were relatively unlithified, that is, shortly after their formation. This confirms the close association of the sill complex with contemporary volcanism.

TABLE OF CONTENTS

TABLES PAGE

FIGURES

INTRODUCTION

General Statement

Early Precambrian metavolcanic-metasedimentary sequences in the Superior Province of the Canadian Shield are commonly intruded by mafic to ultramafic plutons ranging in composition from diorite to peridotite. Most of these plutons, which include sills, dikes, and stocks, have the following characteristics (Irvine and Ridler, 1972):

(1) They are pre-orogenic, having been metamorphosed and deformed to the same extent as the surrounding volcanic-sedimentary sequence, and are probably an integral part of the volcanism.

(2) Unlike Phanerozoic alpine-type peridotite and ophiolite complexes, they have been emplaced by magmatic processes, rather than by faulting or diapirism.

(3) They are subalkaline. Both the ultramafic and mafic rocks are generally hypersthene-normative and the mafic rocks contain modal hypersthene and quartz.

Such plutons in Canada have been described previously by Naldrett and Mason (1968), MacRae (1969), Irvine and Ridler (1972), among others, and in Australia by Williams (1971; 1972), Williams and Hallberg (1973), and Jacques (1976).

One of these plutons, here termed the Metagabbro Sill Complex, has been examined in the Favourable Lake area of northwestern Ontario about 170 km north of Red Lake (Fig. 1). The sill complex is a composite, tholeiitic intrusion comprising three phases, each of

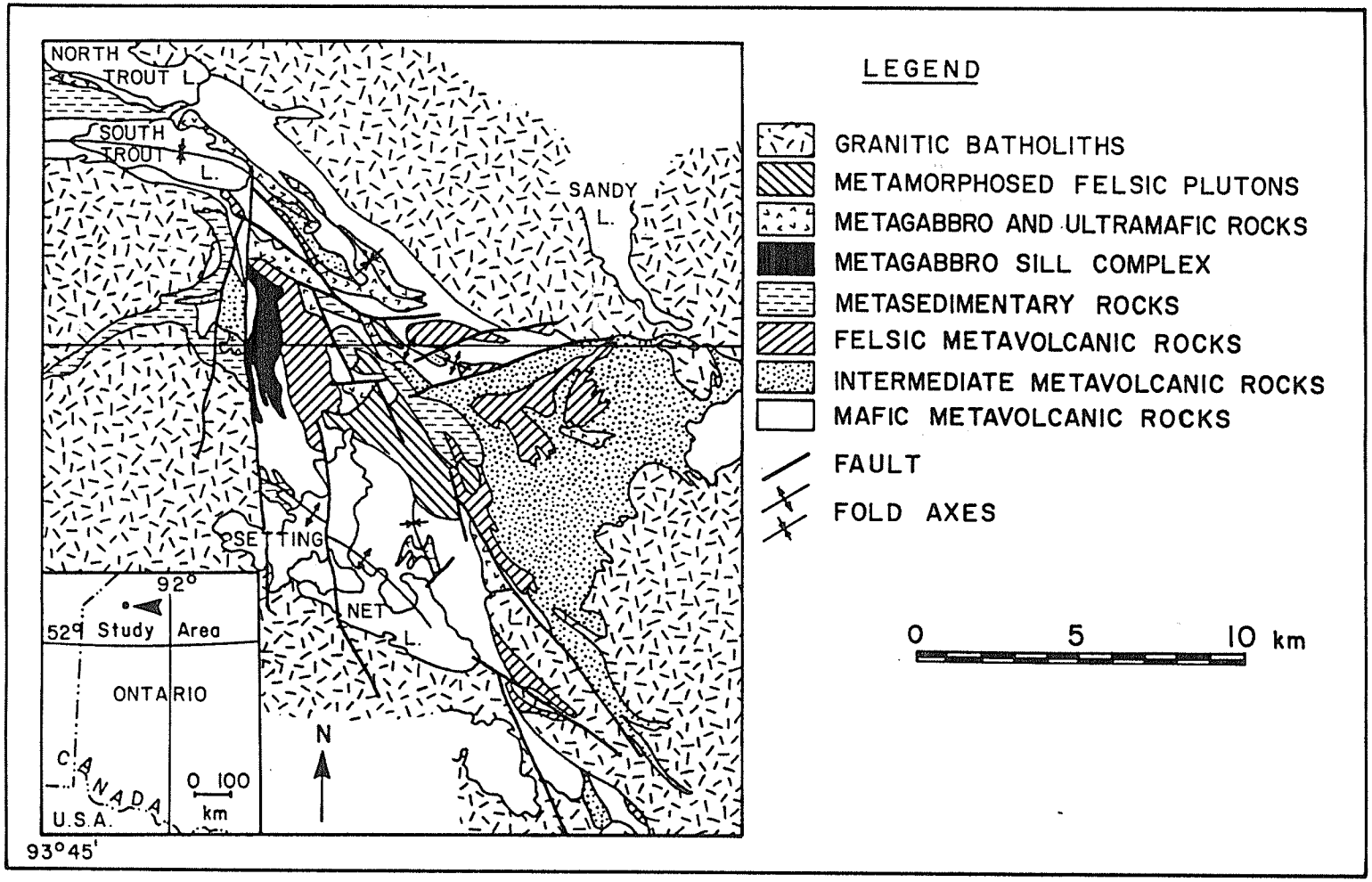

Fig. 1. Generalized geological map and location of the eastern part of the Favourable Lake metavolcanic-metasedimentary belt (Ayres, 1977).

which is petrographically and geographically distinct from the other phases (Fig. 2 (in pocket); Raudsepp, 1975; 1976).. Phase X is a stratiform body formed largely of mafic and ultramafic cumulates; phase Y is a granophyric, mafic, sill-like unit with only minor differentiation, and phase Z is a series of differentiated sills, in part cumulus.

This study was focused on vertical and lateral petrologic and chemical variations in the phases as an aid in determining mechanism of emplacement and nature of differentiation. Special emphasis was placed on phase X, because crystal settling is a major mechanism of differentiation in its five subunits, each of which is a discrete intrusive event, and about 120 m thick. In previous studies of mafic sills of comparable thickness, crystal settling has been found to be minor or absent (e.g. Carmichael et al., 1974).

Mineralogical layering due to crystal settling in stratiform complexes reflects the order of crystallization from the liquid (Irvine, 1970) and it is an indicator of the composition and history of the parent magma. Repetition of segments of the layered sequence record periodic invasions of fresh magma and/or subsequent displacements of the residual liquid (Jackson, 1971). This is especially prevalent if the intrusion was part of an active subvolcanic complex (MacRae, 1969; Irvine and Smith, 1967). Detailed knowledge of the history of these differentiation processes may provide a key to the better understanding of associated, chemically related volcanic rocks.

Method of Study

The Metagabbro Sill Complex was mapped on aerial photographs at a scale of 1:7920 with special areas being mapped at 1:1200 using an existing exploration grid of cut lines. Field work comprised 2 months in 1974 and an additional 3 weeks in 1975. Of 805 samples collected, 315 were studied in thin section and 65 were modally analysed by point counting.

In addition to 2 analyses provided by L. D. Ayres, 31 samples were chemically analysed by rapid methods in the laboratories of the Department of Earth Sciences, University of Manitoba. Si, Al, Fe (total), Mg, Ca, K, Ti, and Mn were determined by X-ray fluorescence spectrometry; Na_2O, MgO, and trace elements by atomic absorption spectrometry; P_2O_5 by colorimetry; FeO by decomposition of the sample in HF and 1:4 H_2SO_4 solution titrated with $K_2Cr_2O_7$ (sodium diphenylamine sulphonate as indicator); and H_2O (total), S, and CO_2 by induction furnace procedures.

Electron microprobe data on amphiboles and plagioclases were obtained on a four-spectrometer ARL-EMX-SM electron microprobe at the State University of New York at Stony Brook. Data were automatically reduced by computer during analysis following the modified technique of Bence and Albee (1968). The electron microprobe was operated at 15 kv. and 0.015 microamperes (on brass).

Acknowledgements

Thanks are due to Dr. L. D. Ayres of the University of Manitoba who suggested the problem, provided direction and encouragement

during its completion, and critically reviewed earlier versions of the manuscript. The author is grateful to Dr. A. C. Turnock of the University of Manitoba and to Dr. A. F. Janzen of the University of Manitoba who improved subsequent manuscripts.

Capable assistance in the field was provided by Catherine McGregor in 1974. Special thanks are due to P. S. Buck who shared camp facilities with the author and provided much fruitful discussion in the field and during subsequent work. Cooperation by fellow students and staff at the University of Manitoba is gratefully acknowledged. Use of the electron microprobe facilities at the State University of New York at Stony Brook was generously provided by A. E. Bence.

Zahavy Mines Ltd. provided free access to the area and furnished diamond drill core.

The study was supported by National Research Council of Canada Grant A8996 and by a University of Manitoba Graduate Fellowship in addition to miscellaneous research funds from the Department of Earth Sciences, University of Manitoba.

Nomenclature

Nomenclature of units in the Metagabbro Sill Complex must consider two diverse mechanisms of crystallization: crystallization of a confined magma progressively inwards from cooler wall rocks, and crystal settling. In addition, regional metamorphism has largely destroyed primary mineralogy and partly destroyed primary textures. Comments on crystallization are based primarily on the relationship of pseudomorphs after primary minerals.

During inward crystallization of a confined, relatively viscous magma in which crystal settling is minor, movement of crystallizing minerals and melt is limited to small displacements of the melt by growing crystals. Although marked differentiation may occur by this process, the differentiation and hence the rock type at a particular stratigraphic level, is a function of these small displacements and of the degree of isolation of early-formed minerals through armouring by later-formed minerals (zoning). A sample from a particular level is a reasonable estimate of the magma composition at that stage in the cooling history. In such rocks, total mineral modes (Table 1A) and/or whole rock chemical analyses may be used as the sole basis for classification.

The classification of rocks formed by crystal settling is more complex because of the mineralogical layering (Jackson, 1961; 1967; 1971). The composition of a rock at a particular level is not the same as the magma originally at that level. The modal classification (Table 1A) can be used, but it does not reflect the cumulus nature of the rocks. An additional textural and modal classification is required.

The mineralogical layering reflects changes in the proportion, grain size, and/or composition of settled crystals (Table 2B) and is caused by changes in supply or dispersal of such crystals at the surface of deposition (Jackson, 1967). Each layer is classified on relative proportions of cumulus phases (Table 1B), the nature and relative proportions of postcumulus material (Table 2A), and the nature of the layering (Table 2B). In addition, post-depositional changes in both the nature and relative proportions of

Table 1. Mineralogical classification of mafic and ultramafic rocks in the Metagabbro Sill Complex

A. Modal Classification[1]

i) Metamorphosed ultramafic rocks (CI 70-100)[2]

- Olivine 0-10
  - Feldspathic metapyroxenite (CI 70-90; quartz absent)
  - Quartz-bearing feldspathic metapyroxenite (CI 70-90; quartz trace-10)
  - Metapyroxenite (CI 90-100)
- Olivine>10
  - Feldspathic metaperidotite (CI 70-90)

ii) Metamorphosed mafic rocks (CI 35-70)

- Metagabbro
- Quartz-bearing metagabbro (quartz trace-10)
- Quartz metagabbro (quartz > 10)
- Granophyric metagabbro (quartz trace to 10; contains granophyric intergrowths of quartz and plagioclase)

B. Classification by cumulus minerals

i) Semiquantitative: cumulus minerals are listed in order of decreasing abundance (e.g. pyroxene-olivine cumulate)

ii) Quantitative: the measured volume proportions of cumulus minerals are listed by subscript (e.g. the proportions of cumulus minerals in the cumulate are $px_{70}ol_{10}$)

[1]Modified after Peterson (1960) and Williams et al. (1954); mode in volume per cent

[2]CI = colour index, per cent volume of mafic minerals

[3]After Jackson (1967); all cumulus minerals in the sill complex have been replaced by metamorphic species - primary species are used in classification

Table 2. Cumulus textures in mafic and ultramafic rocks of the Metagabbro Sill Complex

A. Rocks and textures formed by crystal accumulation[1]

I. Components of rocks formed by crystal accumulation

i) Cumulus crystal = settled crystal - a crystal (mineral) that originated outside of, and previously to, the magmatic sediment of which it now forms a part.

ii) Postcumulus material - primary material that formed in the place it now occupies in the magmatic sediment.

iii) Intercumulus liquid - the liquid that occupied the interstices between cumulus crystals before and during the growth of the postcumulus material.

iv) Adcumulus growth - the extension of the original cumulus crystals by material of the same composition, to give unzoned crystals. The process reduces the amount of intercumulus liquid by mechanically pushing it out.

v) Trapped liquid - that part of the intercumulus liquid, if any, that remains after adcumulus growth.

vi) Pore material - crystallized trapped liquid.

II. Rocks formed by crystal accumulation (see also Table 1B)

i) Cumulate = magmatic sediment - a group name for igneous rocks formed by crystal accumulation through the action of gravity and subsequent modification during solidification.

ii) Orthocumulate - a cumulate consisting essentially of one or more cumulus minerals, together with the products of crystallization of the intercumulus liquid, which necessarily has the composition of the contemporary magma. Adcumulus growth is absent to minor.

iii) Adcumulate - a cumulate modified by adcumulus growth with less than 5 per cent pore material remaining.

iv) Mesocumulate - a cumulate modified by adcumulus growth intermediate in character between orthocumulate and adcumulate end-members.

[1] modified after Jackson (1967; 1971), Wager (1967), Wager et al. (1960).

Table 2 continued

B. Horizons, layers, and groups of layers in cumulates[1,2,3]

I. Horizons[1]

i) Horizon - a reference plane in a cumulate that marks a former surface of deposition

ii) Phase contact - a horizon marked by the appearance or disappearance of a cumulus mineral.

iii) Ratio contact - a horizon marked by a sharp change in the proportions of two cumulus minerals.

iv) Form contact - a horizon marked by a sharp change in the physical properties of a cumulus mineral, such as size or habit.

II. Layers[1]

i) Layer - a continuous sheetlike cumulate that is characterized by uniform or uniformly gradational properties.

ii) Isomodal layer - a layer characterized by a uniform proportion of one or more cumulus minerals.

iii) Mineral-graded layer - a layer characterized by a gradual stratigraphic change in proportions of two or more cumulus minerals.

iv) Size-graded layer - a layer characterized by a gradual stratigraphic change of grain size of one or more cumulus minerals.

v) Chemical-graded layer - a layer characterized by a gradual stratigraphic change in chemical composition of one or more cumulus minerals. Equivalent to "cryptic layering"[2].

vi) Centimeter-scale layering[4] - layering characterized by alternating layers about one centimeter or more thick that are not necessarily cumulus in origin. Analogous to "inch-scale layering" of Hess (1960).

III. Groups of layers[1,3]

i) Zone - an informal, mappable, rock-stratigraphic unit in a layered intrusion, characterized by lithologic homogeneity or distinctive lithologic features.

ii) Member - an informal subdivision of a zone.

iii) Unit - a set of zones which are conveniently grouped together in considering a repetitive pattern.

[1] after Jackson (1967)

[2] after Wager and Deer (1939)

[3] modified after Wager and Brown (1968)

[4] after Morse (1969)

cumulus and postcumulus material must be considered. The terminology of cumulates is given in Table 2.

In the cumulates, names were first assigned according to the total mode (Table 1A) in order to facilitate field mapping and to serve as a guide in outlining similar units. Then, to emphasize their cumulus nature, a classification based on the nature and proportions of cumulus crystals was used (Table 1B).

GENERAL GEOLOGY

Regional Geology

The Favourable Lake metavolcanic-metasedimentary belt (Fig. 1) is an east-southeast-trending, isoclinally folded remnant of a once extensive volcanic-sedimentary terrain (Ayres, 1970; 1972; 1974; 1977). It is separated from other supracrustal remnants by younger intrusive granitic batholiths. The belt extends from Northwind Lake, Ontario, westward to Hudwin Lake, Manitoba, a distance of 155 km. At the east end it has a maximum width of 13 km but it narrows westward; its average width is 4 km. The preserved stratigraphic sequence is at least 7500 m thick; lower units were removed by intrusion of the granitic batholiths, and an erosional surface marks the upper boundary.

Although correlation is hampered by isoclinal folding, extensive faulting, and numerous subvolcanic gabbroic and granitic plutons, 15 metavolcanic-metasedimentary formations have been recognized in the eastern part of the belt (Ayres, 1977). These form 5 incomplete cycles that represent progressive stages in the evolution of coalescing, shield-like volcanoes.

Many multi-phase mafic and ultramafic sills, dikes, and stocks intruded the volcanic-sedimentary sequence prior to major metamorphism and deformation. These plutons range in composition from diorite to peridotite and comprise about 12 percent of the sequence (Ayres, 1974). They are probably related to mafic volcanism and may be, in part, feeder complexes. One of these is the Metagabbro Sill Complex.

This sill complex was emplaced in the lower part of formation J, a mafic flow sequence, at or near the contact with underlying formation I, a heterogeneous clastic and chemical sedimentary unit (Fig. 2). Formation I is the uppermost part of Cycle 2 and is about 5000 m above the base of the preserved stratigraphic section. Here formation I is a lacustrine to alluvial unit deposited within a caldera (Buck, 1978; Ayres, 1977) and the mafic flows of formation J may also be partly filling the caldera. The apparent restriction of the Metagabbro Sill Complex to the area of the caldera may indicate continuing vent activity with the sill complex being a subjacent magma chamber related to volcanism.

Both the volcanic-sedimentary sequence and mafic-ultramafic plutons were regionally metamorphosed under greenschist to amphibolite facies conditions. Metamorphic grade of the sill complex is greenschist facies. Contact metamorphism related to emplacement of the sill complex was either slight or has been obscured by later regional metamorphism. The only contact metamorphic effect observed was minor development of amphibole in metasandstone immediately adjacent to some contacts.

Metagabbro Sill Complex

The Metagabbro Sill Complex is a broadly concordant, composite intrusion of pyroxenite and gabbro, 4.7 km long in a north-south direction, and 0.87 km wide in the central part. It occurs in a vertically dipping, west-facing sequence and the present erosional surface is a cross-section through the complex, approximately perpendicular to the primary attitude of the complex; the cross-

sectional area is 3.66 km^2.

The complex comprises three multiple phases that differ in composition, mode and degree of differentiation, and nature of emplacement. These have been informally designated as phase X, phase Y, and phase Z (Fig. 2), with phase X being the oldest and phase Z the youngest. Chilled margins of all three phases are tholeiitic basalt.

Phase X is strongly differentiated, and comprises five sills consisting largely of layered cumulates. Phase Y comprises numerous, irregular, granophyric mafic sills that lack post-emplacement differentiation. Phase Z consists of five lenticular to sheet-like sills, two of which were locally differentiated by crystal settling.

Individual sills of each phase are generally separated by continuous septa and/or trains of tabular xenoliths although xenoliths are rare in phase Z.

Intrusive contacts with country rocks and among the individual intrusions within the phases are generally abrupt and straight to gently sinuous with local bulbous apophyses. On a formational scale, phases X and Z are concordant but on an outcrop scale, they are as much as 5 to 10 degrees discordant. In phase Y, contacts vary from concordant to strongly discordant and many of the intrusions are irregular or dike-like.

The attitude of the contacts and layering indicates that the sill complex was emplaced into a flat-lying volcanic-sedimentary sequence. Its present subvertical attitude was caused by regional folding. The northern parts of phases X and Z have also been gently warped about a subvertical axis. Mild flexures in layering and

bedding, and minor faults occur throughout the complex and country rocks, but do not markedly disrupt the stratigraphy. In spite of this deformation and the regional metamorphism, primary structures in the sill complex are generally well preserved.

PHASE X

General Relations

Phase X is a tholeiitic multiple sill that forms 42 per cent or 1.54 km^2 of the exposed cross-sectional area of the sill complex (Fig. 2). Its present dimensions are 2.7 km long in a north-south direction and 0.53 km wide. Some shortening or thinning probably occurred during deformation, and the sill is truncated by the Setting Net Lake Fault and phase Z. The smooth, blunt, southern termination, and the generally straight to gently sinuous contacts suggest that the primary cross-sectional shape was a thick lens. Assuming that only several hundred meters were removed from the northern end by the Setting Net Lake Fault, and that folding caused only moderate thinning or shortening, the primary length to width ratio would have been 6:1 to 8:1.

The lower contact is abrupt and straight to gently sinuous with local apophyses and step-like discordancies of 1 to 10 m. Adjacent to thinly bedded, intermediate to mafic metatuff of formation I, the contact is generally irregular with prominent bulbous or wedge-shaped apophyses into the metatuff. Bedding has been contorted, and either wraps around apophyses or is sharply truncated. Some of the contortion was apparently caused by drag during emplacement of the magma; the metatuff probably behaved plastically. Adjacent to thinly to medium bedded metachert and metasandstone, the contact is concordant to discordant and varies from straight to step-like. This country rock was not markedly deformed during emplacement.

There is only a single exposure of the upper contact. Here the phase is adjacent to thinly bedded metachert and the contact is straight and concordant to slightly discordant; country rock deformation is absent.

A very fine-grained, chilled envelope 3 to 6 m wide appears to surround the entire phase, but because of poor exposure along the roof, it is well documented only along the base.

Most of the bulbous southern termination is closely packed, monomictic autobreccia comprising angular to subrounded mafic clasts in a carbonate matrix. The clasts have the same composition as the chilled envelope but are more variable in texture ranging from very fine- to fine-grained. A gradational contact zone several meters wide separates the breccia from the rest of the phase on the north side; on the south side, the breccia is in sharp contact with the chilled envelope. The fine grain size and monomictic nature of the breccia suggests that it is largely an autobreccia produced during emplacement. However, the lack of magmatic matrix and lack of welding of clasts indicates that simple autobrecciation during emplacement could not have produced the breccia. Possibly phreatic activity generated by steam from wet, partly lithified sedimentary host rocks may have aided in production of the breccia. The unusually wide chilled envelope (15 to 30 m) apparently surrounding the southern part of the breccia and the fine grain size of the clasts points to extensive and rapid cooling of the magma by an abundant fluid phase and supports the phreatic explosion mechanism.

The breccia unit may represent coalescence of breccia units formed in advance of each unit of the phase. Similar breccias occur

in sills 1 and 5 of phase Z, but their extent and nature are obscured by lack of exposure and a strong, superimposed mineral foliation, and metamorphic differentiation.

Country Rock Septa and Xenoliths

Country rock xenoliths are rare adjacent to the external contacts. Internally, however, country rock xenoliths are abundant and form septa of long tabular blocks and lenses subparallel to external contacts. Most occur at the boundaries between sills, particularly between the lower three units (Fig. 2). As such, they are not true xenoliths, except at the southern terminations of units 3, 4, and 5, where they form thin lenses within units.

Septa consist only of the lacustrine unit of formation I, namely thinly bedded metachert, ferruginous metachert, metasiltstone and fine metasandstone, and minor intermediate to mafic metatuff. Before intrusion of phase X, the lacustrine unit was about 100 m thick. Successive emplacement of the 5 units of phase X split the upper 50 m along or close to bedding planes, into four inter-unit septa. The best developed septum is between units 1 and 2. It is 17 m thick along section AA' (Fig. 2, 3) and is probably continuous for 1.4 km in the north-south direction. Septa between the other units are restricted to discontinuous trains of lenses and blocks, 1 to 20 m thick and 30 to 285 m long. Some of these septa may be more continuous but lack of outcrop hampers tracing.

Units

Phase X consists of 5 separate intrusive units each of which

comprises a lower ultramafic zone and an upper mafic zone (Table 3); the mafic zone in the uppermost unit is not exposed but is presumed to be present (Fig. 2). The units range in thickness from 17 to 240 m and average about 100 m. Each unit is either a simple or multiple sill formed by one or more discrete pulses of magma. Except at the south end, zones are continuous throughout the exposed lengths of units 1 and 2, but in unit 3, the ultramafic zone pinches out in the north. Units 4 and 5 are truncated by phase Z and the degree of zone continuity is unknown. In the south, mafic zones in all units pinch out between 120 and 200 m north of the breccia. Each unit is surrounded by a very fine-grained mafic chilled border zone that averages 3 m thick.

Autoliths (cognate xenoliths) are rare, although local concentrations do occur. They are generally less than 1 m long, and vary from lenticular to angular. Lenticular autoliths have gradational, in places resorbed, boundaries and are generally cognate to the phase in which they occur. Angular, blocky autoliths have sharp boundaries and are normally from other phases.

Unit 1 is the largest unit and the best expressed and documented (Fig. 3); it is used as the type example. Subsequent discussion of other units focuses on characteristics that are divergent from those of unit 1.

Unit 1 - The Type Unit

General Relations

The unit is confined between a solid floor of formation I

Table 3. Summary of Stratigraphy, Phase X.

unit	thickness (m)	area (km^2)	per cent phase	zones	thickness (m)	rock types (Table 1A)	types of cumulates (Table 1B)
5	90	0.08	5.0[1]	mafic	0-40	-not exposed-	
				ultramafic	50-100	feldspathic metapyroxenite	pyroxene
4	30-150	0.11	7.1[1]	mafic	0-70	metagabbro, quartz-bearing metagabbro	plagioclase - Fe-Ti oxide, pyroxene - plagioclase - Fe-Ti oxide
				ultramafic	30-80	feldspathic metapyroxenite	pyroxene
3	70-160	0.29	18.8	mafic	0-100	metagabbro, quartz-bearing metagabbro	plagioclase - Fe-Ti oxide, pyroxene - plagioclase - Fe-Ti oxide
				ultramafic	0-70	feldspathic metapyroxenite	pyroxene
2	25-110	0.51	33.1	mafic	0-50	metagabbro, quartz-bearing metagabbro	plagioclase - Fe-Ti oxide, pyroxene - plagioclase - Fe-Ti oxide
				ultramafic	15-110	feldspathic metapyroxenite	pyroxene
						metapyroxenite	pyroxene - olivine
1	17-240	0.55	36.0	mafic	0-80	granophyric metagabbro member (2.0)[2]	
						granophyric metagabbro	plagioclase - Fe-Ti oxide
						upper metagabbro member (28.9)	
						quartz-bearing metagabbro	plagioclase - Fe-Ti oxide
						lower metagabbro member (15.1)	
						metagabbro	plagioclase - Fe-Ti oxide
						feldspathic metapyroxenite	pyroxene - plagioclase - Fe-Ti oxide
				ultramafic	17-112	metapyroxenite member (2.6)	
						metapyroxenite, feldspathic metapyroxenite	pyroxene
						feldspathic metapyroxenite member (44.2)	
						feldspathic metapyroxenite,	pyroxene
						feldspathic metaperidotite	pyroxene - olivine
				border	3-6	upper chilled margin member (2.4)	
						feldspathic metapyroxenite	none
						lower chilled margin member (4.9)	
						feldspathic metapyroxenite	none

[1]Minimum value; part of these units were removed by emplacement of phase X.

[2]Volume per cent of member in type section AA' calculated from relative thicknesses. Granophyric metagabbro member volume estimated.

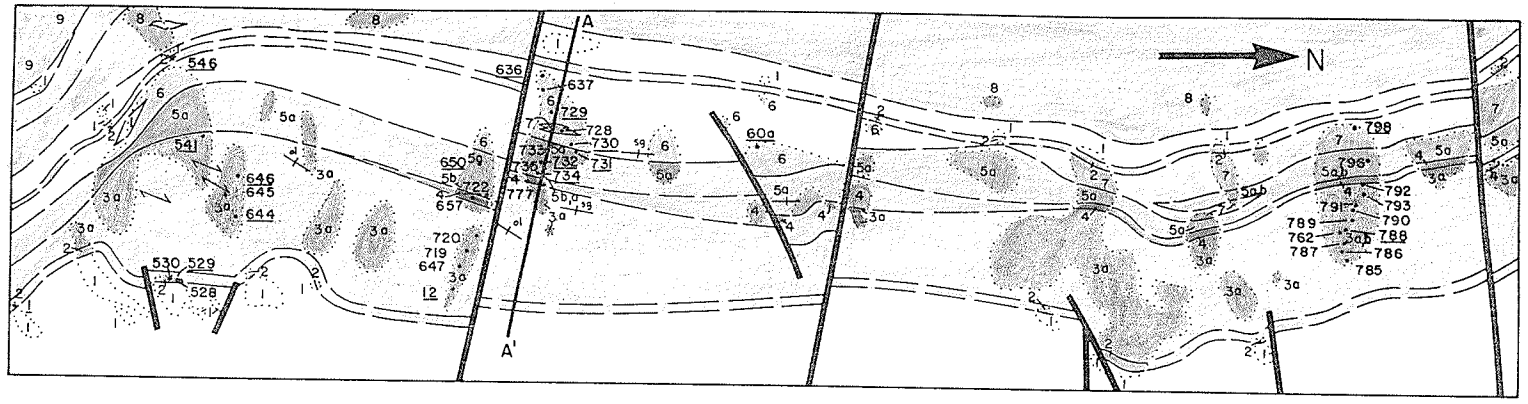

LEGEND

Unit 3

9 unsubdivided

Unit 2

8 unsubdivided

Unit 1

Mafic Zone

Granophyric Metagabbro Member

7 granophyric metagabbro, quartz-bearing metagabbro

Upper Metagabbro Member

6 quartz-bearing metagabbro, metagabbro

Lower Metagabbro Member

5a metagabbro, rare quartz-bearing metagabbro

5b feldspathic metapyroxenite

Ultramafic Zone

Metapyroxenite Member

4 metapyroxenite

Feldspathic Metapyroxenite Member

3a feldspathic metapyroxenite, rare feldspathic metaperidotite

3b feldspathic metaperidotite

Border Zone

Upper and Lower Chilled Margin Members

2 chilled feldspathic metapyroxenite

1 Unsubdivided metavolcanic and metasedimentary rocks

area of rock outcrop

geological boundary (defined, assumed)

fault

· 636 chemically analysed sample

· 637 modally analysed sample

A —— A' section line

cumulus layers (olivine-rich, size-graded), vertical dip

direction of elongation, olivine grains

0 50 100 m

Fig. 3. Relationships in part of unit 1 of phase X. Figure is located on Fig. 2.

metasedimentary rocks, and a country rock septum and unit 2 at the roof. The septum is continuous for at least 1.4 km in the southern part of the unit, but it is apparently absent in the northern part, although it may have been removed by emplacement of unit 2. This structural restriction enabled the development of members within the mafic and ultramafic zone by crystal settling.

In addition to the upper and lower chilled margins, five members occur in the unit and were defined by colour index, mineralogy and texture, and nature of layering (Fig. 3). The ultramafic zone comprises a lower feldspathic metapyroxenite member and an upper metapyroxenite member; the mafic zone comprises a lower metagabbro member, an upper metagabbro member, and a quartz-bearing granophyric metagabbro member.

Section AA' (Fig. 3) is used as the type section because: (1) the members are uniform in thickness, continuous, and well developed, (2) cumulus textures predominate, and (3) the unit was apparently a closed system, at least locally, in the section. Modal and chemical variations in the type section (Fig. 6, 22), are based on samples close to the section, and on samples farther away. Samples away from the section were assigned to the section by calculating the sample's original stratigraphic position in the relevant member as a height to member-thickness ratio, and using this value to plot it on section AA'. This calculation assumes that composition variations are a function of height, and that the composition is the same in all parts of the unit at the same relative stratigraphic position. These assumptions appear valid.

Border Zone

Lower Chilled Margin Member

A lower chilled margin of porphyritic feldspathic metapyroxenite at least 6 m thick is apparently continuous along the base of unit 1. Primary mineralogy has not been preserved, but primary textures are preserved locally by pseudomorphs. Modal analyses, an average mode, and chemical analyses are given in Tables 4, 5, and 11 respectively.

Sparse clinopyroxene phenocrysts up to 1.25 mm that are now pseudomorphed by actinolite occur in an isogranular groundmass of 0.1 mm grain size. The clinopyroxene was identified according to criteria in Williams (1971). Rare olivine phenocrysts, now replaced by 1 mm carbonate pseudomorphs were recognized at one locality (sample 1, Table 4). The groundmass is largely recrystallized to 0.03 to 0.5 mm actinolite, albite, quartz, carbonate, and epidote. The high actinolite content reflects replacement of plagioclase by actinolite and does not represent primary ultramafic composition.

The chilled margin member merges gradually, over an interval of 1 to 2 m, with the fine- to medium-grained cumulates (0.5 to 2.5 mm) at the base of the ultramafic zone.

Upper Chilled Margin Member

The upper chilled margin is only 3 m thick. Adjacent to the overlying metasedimentary septum in the south, the chilled margin is continuous and uniform in thickness. In the north, adjacent to

Table 4. Phase X, Modal Mineralogy (volume per cent)

	Unit 1																								
	Border Zone						Ultramafic Zone																		
	ucm[1]	lower chilled margin member					feldspathic metapyroxenite member																	mpx	
	546	528	529	530	1	486	785	786	787	762	788	789	790	791	793	792	644	645	646	541	12	647	719	720	777	657
actinolite	80.2	85.6	85.5	89.5	77.3	84.0	86.2	81.5	77.0	80.3	76.5	71.8	74.6	69.3	79.5	81.5	81.6	81.5	83.9	79.7	82.3	77.6	79.9	80.9	81.4	84.0
hornblende																										
cummingtonite																										
olivine[3]					0.1[4]		4.0	6.5	5.3	2.1	1.7	10.3	5.1	13.6				4.1	3.4		1.6	3.0	5.7	5.6		
plagioclase	5.8	0.7	1.6	0.2	12.8	10.6	0.3	5.7	11.0	10.0	11.5	9.2	12.9	10.5	9.5		10.8	8.4	6.8	11.2	11.5	13.1	9.1	9.0	0.3	5.2
quartz	2.6				0.5	0.6														0.1					tr	
granophyre																										
Fe-Ti oxides	2.0	1.7	2.4	1.0	1.9	1.6	1.0	0.5	0.8	0.9	1.2	0.6	1.3	1.7	0.8	1.0	1.6	0.8	1.0	1.3	1.7	1.1	1.3	1.1	1.3	2.0
sulphides		tr	0.7	tr	tr	tr	tr	tr	tr			tr		tr	tr	0.5			tr				tr		tr	tr
chlorite	2.4	2.8	3.8	1.0	1.6	tr	tr	0.4	0.1	0.4	0.1	0.8	0.7	0.3	5.6	9.1	0.1	0.1	0.1	1.3	tr	0.9	tr	0.1	10.7	1.7
biotite	0.1	9.1	5.7	7.8	2.3	3.0	tr								tr					2.3	tr	4.3	4.0	tr	3.9	
carbonate	6.9	tr	0.2	0.5	2.7	tr	8.2	5.0	5.1	6.3	9.0	7.2	5.4	4.5	4.6	7.6	5.9	5.1	4.8	4.1	2.9	tr	tr	3.3	2.4	7.1
epidote					0.9	0.1	tr		0.5			0.1		0.1		tr										
sphene		tr	0.1	tr		0.1	0.3	0.4	0.2		tr					0.1						tr	tr			tr
tourmaline		0.1	tr																							
apatite																0.2					tr	tr	tr	tr	tr	tr
colour index[5]	82.7	97.5	95.1	98.3	81.3	87.1	90.5	88.8	82.6	82.8	78.3	82.9	80.4	83.2	85.2	90.7	81.7	85.7	87.4	83.3	83.9	85.8	89.6	86.6	96.0	85.7

[1] Abbreviations: ucm - upper chilled margin member; mpx - metapyroxenite member, UZ - Ultramafic Zone; MZ - Mafic Zone; gmg - granophyric metagabbro member

[2] Data from Ayres (in preparation)

[3] pseudomorphs after cumulus olivine (see Table 6)

[4] trade

[5] colour index = amphibole + olivine + chlorite + biotite + sphene

Table 4 (continued). Modal Mineralogy, Phase X (volume per cent)

	Unit 1																Unit 2				Unit 3		Unit 4
	Mafic Zone																ultramafic zone		mafic zone		UZ	MZ	UZ
	lower metagabbro member								upper metagabbro member						gmg								
	722	734	735	732	733	731	650	796	730	729	637	636	445	60a[2]	728	798	9	21[2]	553	760	5	666	32
actinolite																	80.2	83.5			75.0		81.2
hornblende	68.1	65.5	66.4	72.3	52.5	59.1	50.6	57.0	29.4	35.0	31.3	25.3	32.0	24.4	28.4	48.4			51.8	25.8		22.5	
cummingtonite		tr	tr	tr	tr	tr	9.9		8.4	15.4	11.0	11.2		8.0	6.4				2.6	12.4		22.2	
olivine[3]																	tr				tr		1.4
plagioclase	15.7	29.4	25.2	15.1	31.1	27.5	26.2	36.8	48.7	42.1	47.1	51.0	55.3	56.3	52.2	40.8	13.8	9.6	39.4	46.0	20.8	48.5	13.0
quartz									0.2	0.4	0.5	tr	0.8	0.9	2.1	5.7							
granophyre															1.7	1.2							
Fe-Ti oxides	0.5	1.7	2.1	3.3	4.6	7.5	6.3	4.6	4.7	2.1	2.5	8.8	1.1	8.0	6.3	2.7	1.7	0.9	3.8	6.1	2.5	5.5	1.5
sulphides	0.6	0.2	0.1	tr	tr	tr		tr	tr						tr	tr	0.3		0.4	0.1	0.1	tr	0.1
chlorite	7.6	2.1	2.8	8.2	1.7	3.9	1.0	0.3	1.0	0.3	1.2	0.9	4.8	0.4	0.4	0.6	0.2	0.4	1.2	1.2	tr	0.1	tr
biotite	5.3	tr	1.1	tr			0.8					tr		0.3			0.2			6.2	0.2	0.2	
carbonate	2.2	1.1	tr	1.1	9.0	2.0	4.6	1.3	6.8	4.2	6.1	2.7	3.3	1.7	2.5	0.5	3.6	5.6	0.8	2.2	1.4	1.0	2.8
epdiote	tr	tr	tr	tr	tr	tr	0.4	tr	tr	0.4	0.1	tr	2.7		tr	tr	tr	tr	tr	tr	tr	tr	tr
sphene		tr			tr		0.1	tr		0.1	0.1	0.1			tr	0.1			tr	tr		tr	
tourmaline		tr	2.3		1.1	tr			0.8	tr													
apatite		tr	tr	tr		tr	0.1		tr	tr	0.1	tr		tr	tr		tr		tr	tr		tr	
colour index[5]	81.0	69.5	72.5	83.8	58.8	69.9	58.8	62.0	38.8	50.8	43.6	37.5	36.8	33.1	35.2	49.1	80.6	83.9	53.0	45.6	75.2	45.0	83.9

Table 5. Phase X, Unit 1, Average Modal Analyses (volume per cent)

	border zone		ultramafic zone		mafic zone		
	lower chilled margin member	upper chilled margin member	feldspathic metapyroxenite	metapyroxenite member	lower metagabbro member	upper metagabbro member	granophyric metagabbro member
actinolite	84.4 (4.5)[1]	80.2	79.2 (4.2)	82.7			
hornblende					62.0 (8.2)	29.6 (4.1)	38.4
cummingtonite					1.4	9.0 (5.1)	3.2
olivine[2]	tr[3]		4.0 (3.6)				
plagioclase	5.2 (6.0)	5.8	8.9 (3.7)	2.8	24.5 (6.5)	50.1 (5.3)	46.5
quartz	0.2 (0.3)	2.6	tr			0.5 (0.3)	3.9
granophyre							1.5
Fe-Ti oxides	1.7 (0.5)	2.0	1.1 (0.3)	1.7	3.8 (2.4)	4.5 (3.2)	4.5
sulphides	0.1		tr	tr	0.1 (0.2)	tr	tr
chlorite	1.8 (1.5)	2.4	1.1 (2.4)	6.2	3.9 (2.9)	1.4 (1.7)	0.5
biotite	5.6 (2.9)	0.1	0.6 (1.4)	2.0	1.0 (1.9)	0.1	
carbonate	0.7 (1.1)	6.9	4.9 (2.4)	4.8	2.9 (3.1)	4.1 (2.0)	1.5
epidote	0.2 (0.4)		tr		tr	0.5 (1.1)	tr
sphene	tr		tr	tr	tr	0.1	tr
tourmaline	tr		tr		0.5 (0.9)	0.1	
apatite			tr	tr	tr	tr	
no. of samples	5	1	18	2	8	6	2

[1] one standard deviation

[2] pseudomorphs after cumulus olivine (see Table 6)

[3] trace

unit 2, it is not exposed, but its existence is implied by a grain-size decrease in the mafic zone as the contact is approached. The presence of the chilled margin adjacent to unit 2 implies that unit 2 was intruded along the contact between unit 1 and its roof. The fact that the upper chilled margin is only half the thickness of the lower chilled margin implies that unit 2 must have been emplaced only shortly after unit 1 and it changed the normal cooling pattern at the top of unit 1. If there had been a long hiatus between the emplacement of units 1 and 2, the chilled margins on both top and bottom of unit 1 should have been of equal thickness.

Mineralogically and texturally, the upper and lower chilled margins are essentially identical (Tables 3, 4) although the upper margin has a lower colour index, and higher quartz and carbonate contents. The upper chilled margin merges downward with the top of the mafic zone.

Ultramafic Zone

Feldspathic Metapyroxenite Member

The feldspathic metapyroxenite member ranges in thickness from 18 to 112 m and occurs continuously along the base of the unit, forming 75 to 100 per cent of the ultramafic zone (Fig. 3, 6). It is entirely layered pyroxene and pyroxene-olivine mesocumulates and adcumulates of feldspathic metapyroxenite and rarely feldspathic metaperidotite composition. Primary ferromagnesian minerals were identified according to criteria in Williams (1971). Primary mineralogy was destroyed during regional metamorphism, but primary cumulus

textures are generally well preserved by metamorphic pseudomorphs. Modal analyses of representative samples, an average mode, and chemical analyses are given in Tables 4, 5 and 11 respectively.

Subhedral to euhedral, equant to tabular cumulus clinopyroxene formed 70 to 85 per cent of the feldspathic metapyroxenite, but has been replaced by single or multi-crystal actinolite pseudomorphs (Fig. 4). The pyroxene was relatively constant in abundance through the member (Fig. 6) although grain size varies from 0.5 to 2.5 mm, with rare grains to 3.5 mm. Single-crystal pseudomorphs consist of colourless or pale to medium green actinolite with olive-green to blue-green patches and discontinuous rims. Increasing recrystallization developed multi-crystal pseudomorphs of very fine-grained, acicular actinolite. Grain boundaries become diffuse, and the distinction between cumulus grains and post-cumulus material is less certain.

Olivine was not positively identified. However, local elliptical structures, 1 to 3 mm long consisting of carbonate and actinolite with minor epidote, chlorite, rare iron-titanium oxides, and plagioclase may be altered cumulus olivine (Fig. 5, Table 6). Rarely, these structures mimic primary, euhedral olivine crystal morphology (Fig. 5). Olivine alteration of this kind is relatively unusual in contrast to the more common serpentinization in comparable rocks (e.g. Williams, 1971). However, partial to complete replacement of olivine by both magnesium-rich carbonate and calcite pseudomorphs during sea water alteration does occur in modern submarine basalts (Baragar et al., 1977; Andrews, 1977; Baker and Haggerty, 1968) and in some Tertiary basalts (Fawcett, 1965).

Fig. 4. Pyroxene cumulate. Pyroxene replaced by actinolite pseudomorphs. White interstitial areas are intercumulus plagioclase. Feldspathic metapyroxenite member, ultramafic zone, phase X. Field of view: 4.2 x 2.6 mm. Sample 790. Plane light.

Fig. 5. Carbonate, actinolite, chlorite, and Fe-Ti oxide pseudomorph after cumulus olivine, feldspathic metapyroxenite member, phase X. Arrow points to pseudomorph. Note euhedral outline. Field of view: 4.2 x 2.6 mm. Sample 785. Plane light.

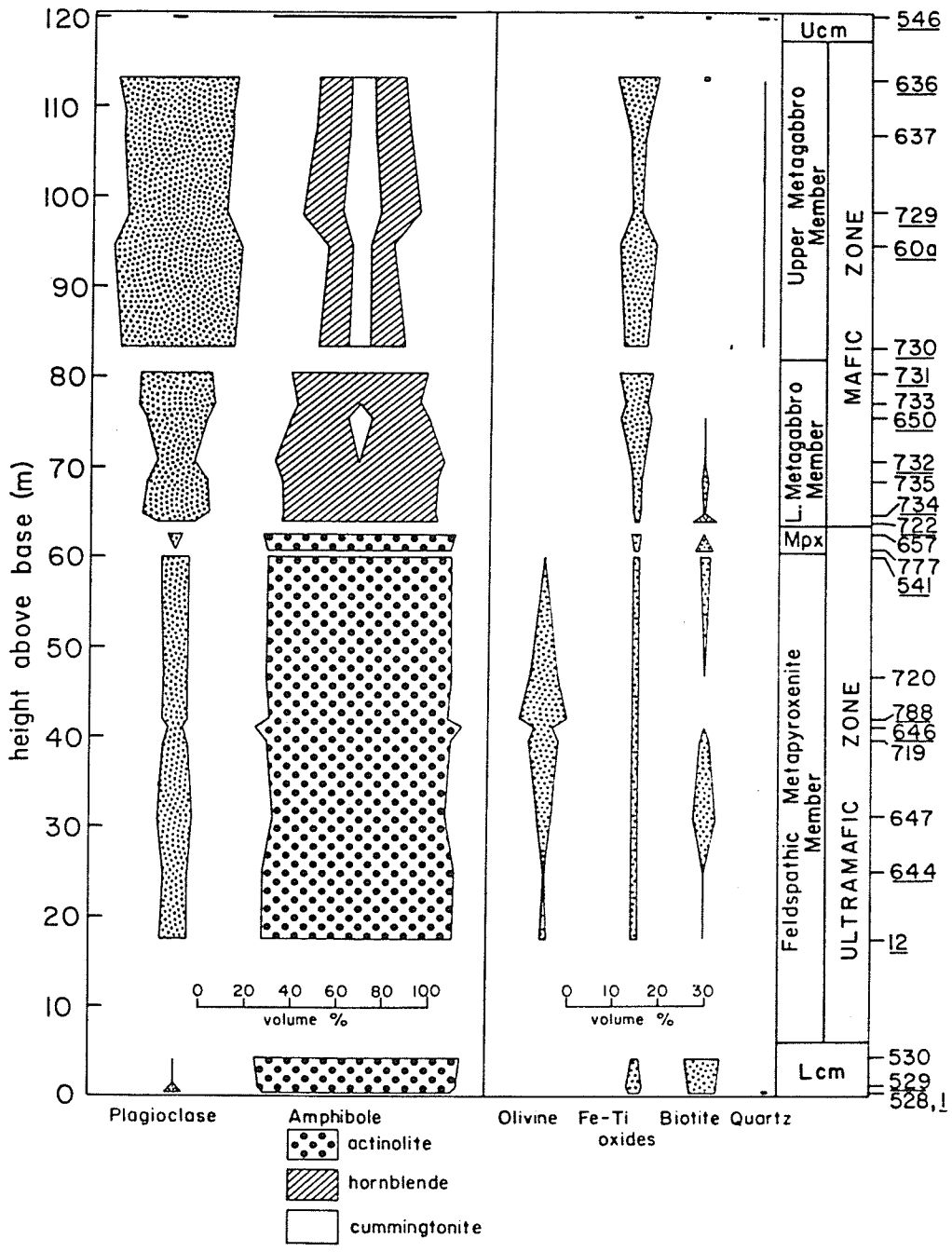

Fig. 6. Variation in metamorphic mineral abundance with stratigraphic height in section AA' of unit 1, phase X. Lcm - lower chilled margin member, Mpx - metapyroxenite member, Ucm - upper chilled margin member. Chemically analyzed samples are underlined.

Table 6. Modal Analyses. Pseudomorphs after cumulus olivine in the feldspathic metapyroxenite member, ultramafic zone.

	carbonate	actinolite	chlorite	Fe-Ti oxides	epidote	plagioclase
646	85.3	14.7	tr	tr	tr	tr
785	85.0	15.0	tr	tr		
786	66.1	30.8	3.1	tr		
787	84.9	9.4	3.8	tr	1.9	
788	82.3	11.8	tr	tr	5.9	
789	70.8	27.2	1.0	tr	1.0	tr
790	75.8	22.6	tr	tr	1.6	tr
791	65.5	30.1	2.2			2.2
average	77.0	20.2	1.3	tr	1.3	0.3

Pseudomorphs after cumulus olivine range in abundance from 0 to 30 per cent and can be readily recognized on outcrop surfaces because they weather to form pits. The olivine/pyroxene ratio is relatively uniform, although it is slightly higher in the center than at the margins (Fig. 6). Rarely, the olivine is concentrated in concordant to discordant layers or lenses. Concordant layers are several meters thick, contain up to 15 per cent olivine, and have gradational phase contacts with olivine-free feldspathic metapyroxenite layers of similar thickness. Discordant layers are 5 to 10 cm thick, contain up to 30 per cent olivine, and are 10 to 15 degrees discordant to member contacts. They have sharp ratio contacts with feldspathic metaperidotite and olivine-bearing feldspathic metapyroxenite of similar thickness. In the discordant layers the pseudomorphs are aligned with their long axes parallel to layering; this is probably a relict igneous lamination.

Other igneous lamination was found only in the top few centimeters of the member where it is defined by aligned prismatic actinolite pseudomorphs subparallel to the upper contact. Centimeter-scale layering is the only other layering observed in the member. It comprises isomodal layers 1 to 2 centimeters thick defined by varying ratios of cumulus pyroxene and intercumulus plagioclase and was observed only in a piece of frost-heaved rubble about 10 m from the southern tip of unit 1.

Postcumulus material forms 10 to 30 per cent of the feldspathic metapyroxenite and comprises altered calcic plagioclase (0 to 13 per cent), altered pyroxene (0 to 20 per cent), minor iron-titanium oxides (0.8 to 1.7 per cent) and rare apatite. Secondary minerals

are albite, and minor epidote, carbonate, actinolite, and chlorite after plagioclase; actinolite and minor chlorite, carbonate, and biotite after pyroxene; and sphene after iron-titanium oxide.

Most of the postcumulus pyroxene apparently formed adcumulus growths on cumulus pyroxene. However, because of the extensive recrystallization, the proportions of cumulus and adcumulus pyroxene could not be precisely determined. Some discrete intercumulus pyroxene is present in a few samples but rarely exceeds 10 per cent.

All of the plagioclase is intercumulus and forms anhedral interstitial grains whose shapes are controlled by the adjacent pyroxene grains. Most grains are 1 to 2 mm in size and occupy one or possibly several adjacent interstices between cumulus pyroxenes. However, in the upper part of the member poikilitic textures are well developed with plagioclase grains up to 8 mm enclosing numerous cumulus pyroxene crystals. Plagioclase is only preserved in the northern part of the member. In the south, it has been largely replaced by actinolite, chlorite, carbonate, and epidote.

Metapyroxenite Member

The metapyroxenite member forms isolated lenses along the top of the ultramafic zone that are up to 15 m thick and 600 m long. At its maximum development (Fig. 3), it forms 25 per cent of the ultramafic zone but is generally less than 5 per cent. It is entirely pyroxene cumulates of metapyroxenite and minor feldspathic metapyroxenite composition, comprising abundant mesocumulates, common orthocumulates, but rare adcumulates. Primary minerals have been replaced by metamorphic pseudomorphs that generally preserve

the primary cumulus textures. However, pervasive recrystallization and grain boundary reactions inhibit interpretation of these textures. Modal analyses and an average mode are given in Tables 4 and 5 respectively.

Mineralogically, the metapyroxenite member is generally similar to the feldspathic metapyroxenite member but has a higher pyroxene content, is coarser in grain size (1.0 to 5.0 mm), and lacks olivine. The contact with the underlying feldspathic metapyroxenite is both a sharp form contact defined by an increase in grain size, and a phase contact defined by the disappearance of olivine.

In the type section AA' (Fig. 3), the metapyroxenite member is 3 m thick and comprises two mineralogically similar layers that differ in grain size and are separated by a sharp form contact marked by abrupt grain size changes. The lower layer is 1.25 m thick and is slightly coarser grained (2 to 5 mm) than the 1.75 m upper layer (1 to 3 mm). Because of poor exposure, these layers could not be traced along strike, but they were identified 435 m north of section AA' and appear to be relatively continuous. There are at least three such layers locally.

The distribution of cumulus pyroxene varied widely among layers. Most of the member was composed of closely packed cumulus crystals (75 per cent), surrounded by intercumulus plagioclase (5 to 10 per cent), pyroxene (15 to 20 per cent), minor iron-titanium oxides, and rare apatite. Locally, however, cumulus pyroxene content is only 40 per cent, with the remainder being intercumulus pyroxene and plagioclase in a 2:1 ratio; the member is then feldspathic metapyroxenite. The amount of adcumulus growth appears to be relatively minor and is

much less than in the feldspathic metapyroxenite member. Igneous lamination is moderately developed with tabular cumulus pyroxenes oriented subparallel to contacts.

Form contacts (Jackson, 1971) are generally produced by mechanical processes such as current velocity changes, rather than by changes in supply of crystals precipitating from the magma. This contention is supported by the local presence of rip-up structures in an area where the metapyroxenite member comprises 3 layers. The rip-ups are in the middle layer and consist of angular blocks of finer metapyroxenite 5 to 15 cm long derived from the lower layer (Fig. 7). Here, the form contact between the two layers is sharp, but jagged due to material plucked during the emplacement of the overlying layer. The rip-ups were probably formed by current flow over partly consolidated pyroxenite.

Mafic Zone

Lower Metagabbro Member

The lower metagabbro member was defined only in the central part of the unit near section AA' (Fig. 3), where outcrop exposure is continuous. Here it is 18 m thick. To the north, the member is poorly exposed and does not appear to be well developed. In the south, the entire mafic zone is less than 12 m thick and members could not be distinguished. The contact with the underlying ultramafic zone is a sharp phase contact defined by the appearance of cumulus plagioclase.

Pyroxene - plagioclase - Fe-Ti oxide cumulates predominate in

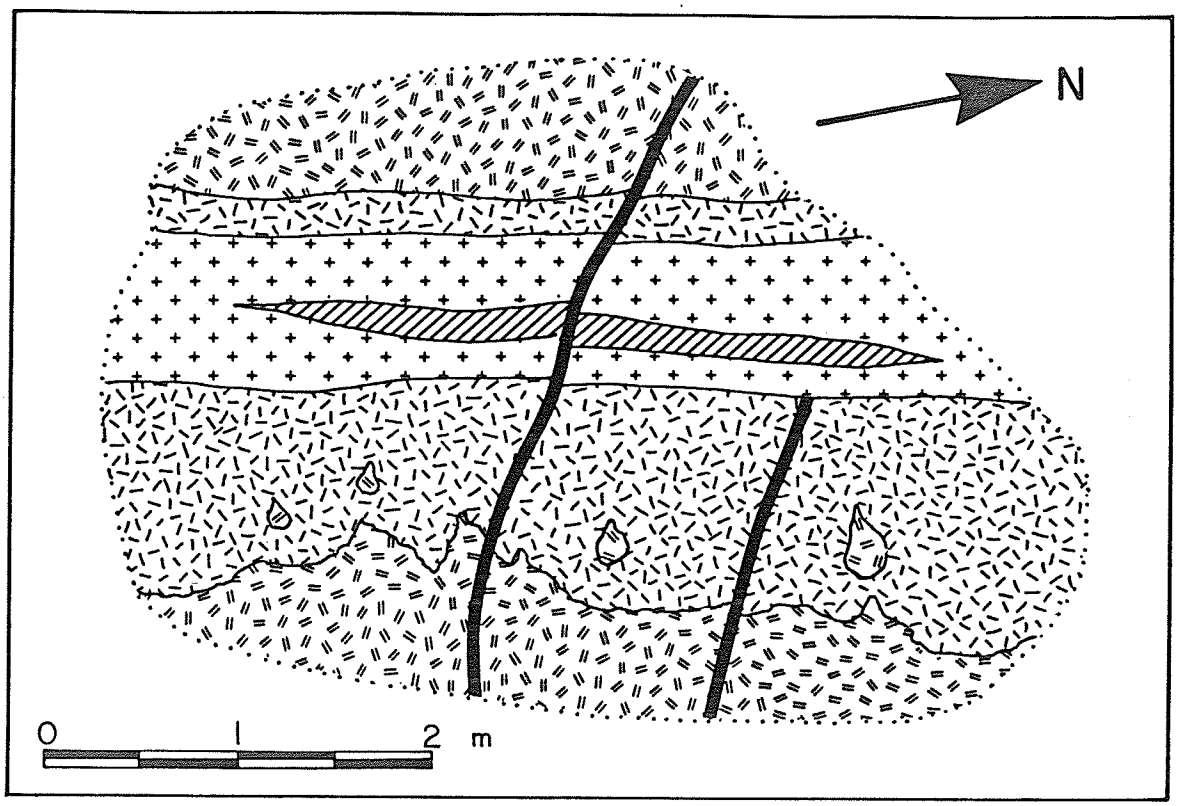

LEGEND

FINE-MEDIUM METAGABBRO
MEDIUM-COARSE METAGABBRO
MINOR SILL
COARSE METAPYROXENITE
MEDIUM METAPYROXENITE
METAPYROXENITE MEMBER
FAULT
LIMIT OF EXPOSURE
GEOLOGICAL BOUNDARY

Fig. 7. Field sketch of rip-ups in the metapyroxenite member of unit 1, phase X. Note jagged contact between lower metapyroxenite and middle metapyroxenite layers. Minor sill is multiple.

the lower part which has colour indices between 70 and 85, and is a feldspathic metapyroxenite. The upper part is less mafic and comprises plagioclase - Fe-Ti oxide cumulates of metagabbro composition. Primary mineralogy was destroyed during regional metamorphism; primary textures were largely destroyed by pervasive recrystallization and grain boundary reactions but are preserved locally by metamorphic pseudomorphs. Modal analyses, an average mode, and chemical analyses are given in Tables 4, 5, and 11 respectively.

Feldspathic metapyroxenite forms the lower 10 m of the member in the type section (Fig. 6). It contains trace to 3 per cent, equant to tabular plagioclase phenocrysts up to 3 mm long that are pseudomorphed by albite aggregates. The groundmass is largely recrystallized but where preserved it consists of albite (25 per cent) and hornblende (35 per cent) single-crystal pseudomorphs after cumulus plagioclase (0.5 to 1.5 mm) and pyroxene (0.5 to 1.0 mm) respectively. Minor cumulus phases included iron-titanium oxides (2 per cent) and apatite (trace). Intercumulus phases comprised pyroxene (28 per cent), now fibrous hornblende and chlorite, and albite pseudomorphs after plagioclase (10 per cent).

In most places, the pyroxene has been replaced by ragged, platy to fibrous masses of medium green to blue green multi-crystal hornblende pseudomorphs that locally contain lamellae or irregular patches of colourless fibrous cummingtonite with very fine lamellar twinning. Actinolite which is the main mineral replacing pyroxene in the ultramafic zone is absent in the mafic zone. Plagioclase was generally replaced by aggregates of albite, chlorite, carbonate, epidote, and rare biotite. Biotite also occurs as scattered interstitial grains

and is intimately intergrown with chlorite and/or hornblende.

A pseudo-chilled margin is locally present in the lower 1 m of the member and reflects more extensive recrystallization. In the upper 2 m of the member, primary grain size (0.5 mm) is slightly reduced.

The feldspathic metapyroxenite is mineral graded with the ratio of cumulus plagioclase to cumulus pyroxene increasing upwards. At the contact with metagabbro, which forms the upper 8 m of the member (Fig. 6), cumulus pyroxene disappears and cumulus plagioclase increases from 21 to 31 per cent.

In the metagabbro most of the plagioclase is subhedral to locally euhedral, blocky laths (Fig. 8), but rounded, equant grains are also present. Many grains are broken and veined by carbonate, and replaced by albite pseudomorphs. The amount of iron-titanium oxides increases markedly from an average of 1.9 per cent in the feldspathic metapyroxenite to 5.8 per cent in the metagabbro. The oxide grains are amoeboid to drop-shaped and have numerous inclusions of actinolite, chlorite, and carbonate. Locally, subhedral to euhedral grains are common, with regular, trellis-like exsolution lamellae now replaced by actinolite, chlorite, and/or carbonate. Sulphides occur in minor amounts and apatite was absent or minor. Intercumulus phases comprised mainly pyroxene (50 per cent), now fibrous hornblende, cummingtonite, and chlorite, and albite pseudomorphs after plagioclase (5 per cent).

Upper Metagabbro Member

The upper metagabbro member comprises quartz-bearing metagabbro

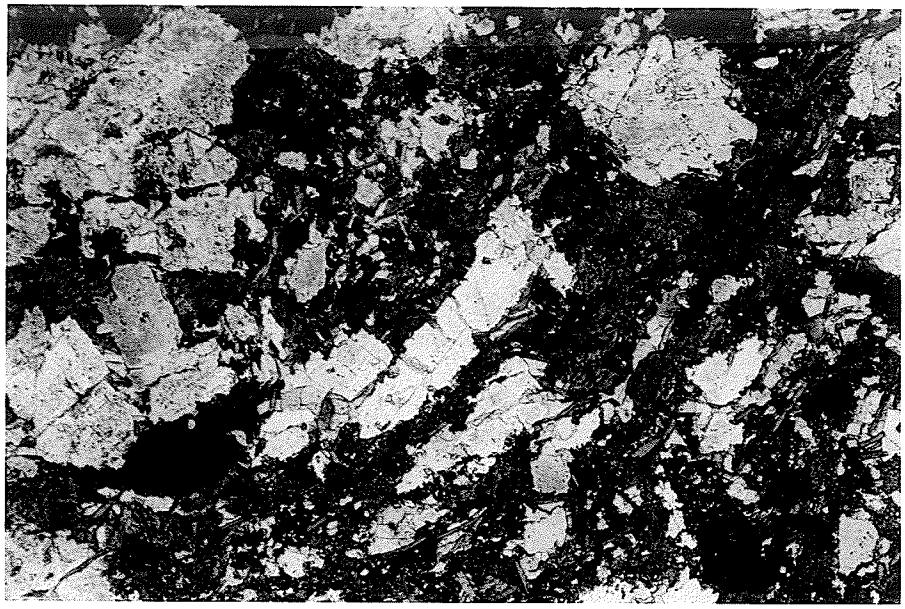

Fig. 8. Plagioclase - Fe-Ti oxide cumulate, metagabbro, lower metagabbro member, phase X. Field of view: 4.2 x 2.6 mm. Sample 733. Plane light.

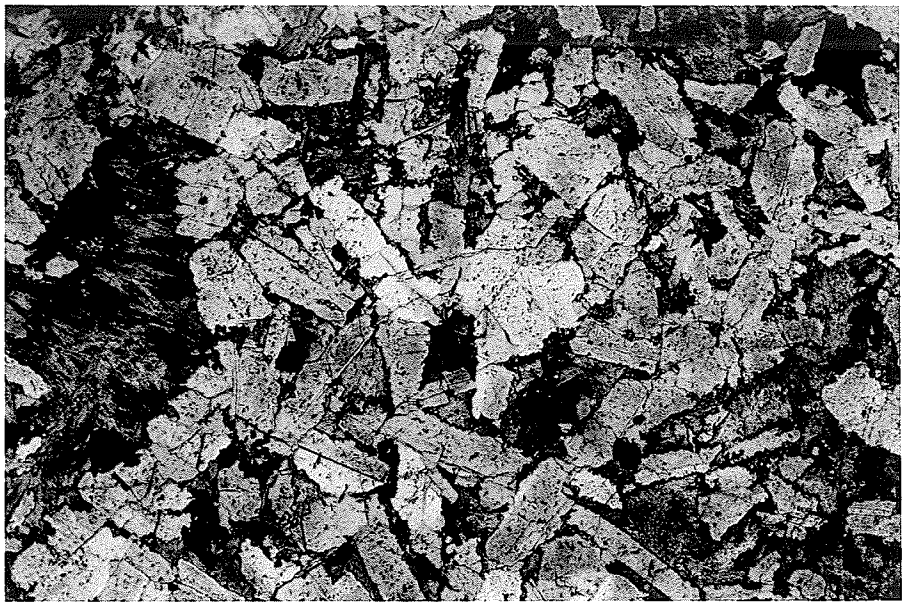

Fig. 9. Plagioclase - Fe-Ti oxide cumulate, quartz-bearing metagabbro, upper metagabbro member, phase X. Note coexisting hornblende (dark grey) and cummingtonite (light grey) at left of photograph. Field of view: 4.2 x 2.6 mm. Sample 636. Plane light.

and is well defined only in the area of Fig. 3 where it forms a lens 40 m thick and 500 m long. In the south, the mafic zone pinches out and members are not defined; in the north, most of the mafic zone is apparently upper metagabbro but it was not differentiated from lower metagabbro because of poor exposure. The upper metagabbro lens (Fig. 3) comprises plagioclase and plagioclase-iron-titanium oxide cumulates; primary textures are partly preserved by metamorphic pseudomorphs. Modal analyses, an average mode, and chemical analyses are given in Tables 4, 5 and 11 respectively.

In section AA' (Fig. 6), the base of the upper metagabbro is marked by a sharp increase in cumulus plagioclase from 31 per cent in the upper part of the lower metagabbro to almost 50 per cent, and a decrease in iron-titanium oxides from 7.5 to 4.7 per cent. Grain size also increases abruptly across the contact from 0.4 mm in the lower metagabbro to 0.7 mm. The contact zone is 1 to 2 m thick.

Cumulus plagioclase has been replaced by single-crystal pseudomorphs of albite (Fig. 9) and was relatively constant in abundance, ranging from 42 to 56 per cent. Most plagioclase forms subhedral to euhedral, tabular grains but anhedral rounded, equant grains are also present and may either represent subhedral or euhedral cumulus grains that underwent post-cumulus enlargement, or rounding by abrasion during movement of partly crystalline material. Many grains are broken and veined by calcite and some lath-like grains are bent. This reflects later deformation and is most common in the central part of the member. Grain size varies from 0.6 to 1.1 mm, with some lath-like grains to 3.0 mm. Primary compositional zoning is reflected by variations in alteration. The central 80 per cent of

most grains contains abundant inclusions of very fine-grained actinolite, chlorite, carbonate, and epidote and probably represents the original cumulus crystal. The rims are less altered and probably represent more sodic plagioclase added by adcumulus growth (cf. Wager and Brown, 1968, p. 33). Minor interstitial finer grained (less than 0.5 mm), anhedral plagioclase is present and is probably intercumulus.

Igneous lamination is locally developed in the lower third of the member, by the orientation of tabular plagioclase crystals subparallel to the floor of the member.

Iron-titanium oxides increase slowly from the base of the member to the center, decrease abruptly and then slowly increase to the top (Fig. 6). They form 0.25 to 1.24 mm, drop-like to amoeboid cumulus grains, generally rimmed by very fine-grained epidote. Subhedral fine-grained (0.4 mm) cumulus apatite is rare.

Pyroxene, which is now replaced by multi-crystal amphibole pseudomorphs, formed 32 to 57 per cent of the member as anhedral, fine to medium-grained (0.5 to 2.0 mm), intercumulus grains and groups of grains (Fig. 9). The secondary amphibole is mainly pale-green to deep blue-green hornblende (25-35 per cent) that is either intergrown with colourless cummingtonite (Fig. 10) (0 to 15 per cent) in fascicular bundles or forms irregular rims on cummingtonite cores. Cummingtonite is most abundant in the central part of the member (Fig. 6).

Quartz was a minor (trace to 1 per cent) fine-grained (0.2 mm) intercumulus phase and has been recrystallized to polycrystalline aggregates.

Fig. 10. Coexisting hornblende (dark to medium grey) and cummingtonite (light grey) in metagabbro, upper metagabbro member, phase X. Note the diamond shape of one of the cummingtonite cores. This shape occurs locally throughout the member but its petrologic significance is unknown. Field of view: 1.7 x 1.0 mm. Sample 726. Plane light.

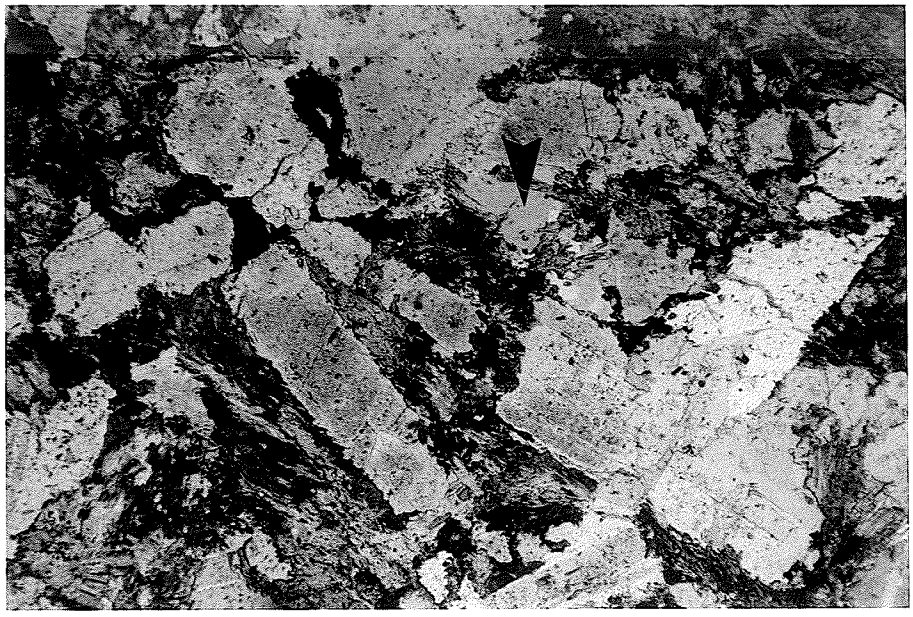

Fig. 11. Plagioclase cumulate, granophyric metagabbro, granophyric metagabbro member, phase X. Arrow points to intercumulus quartz. Field of view: 4.2 x 2.6 mm. Sample 728. Plane light.

Granophyric Metagabbro Member

Granophyric metagabbro occurs locally in the upper metagabbro lens (Fig. 3) as irregular patches a few centimeters to several meters across. Contacts with quartz-bearing metagabbro are gradational over a few centimeters. In the central part of the mafic zone it also forms a complex, lens-like body 25 m thick and at least 250 m long that takes the place of the upper metagabbro (Fig. 3). The lower contact is gradational over a few meters with the lower metagabbro member; the upper contact is not exposed. Modal analyses, an average mode, and chemical analyses are given in Fig. 4, 5 and 11 respectively.

Granophyric metagabbro represents a more advanced stage of differentiation of quartz-bearing metagabbro marked by more intercumulus quartz (2 to 6 per cent) (Fig. 11) and minor complex granophyric intergrowths of plagioclase and quartz (1.2 to 1.7 per cent) (Fig. 12). Mineralogically and texturally it is similar to upper metagabbro but grain size is more variable ranging from 1 to 3 mm and rarely to 10 mm.

Minor Sills

Several fine to medium-grained (0.75 to 2.5 mm) metagabbro and quartz-bearing metagabbro sills 0.1 to 1.0 m thick occur in the metapyroxenite member. They were emplaced either along the contact between layers of the member, or within the upper layer. The sills have very fine-grained chilled margins a few centimeters thick bordering sharp and straight contacts with metapyroxenite. At least

Fig. 12. Granophyric intergrowth of quartz and plagioclase (center of field), granophyric metagabbro, granophric metagabbro member, phase X. Field of view: 1.7 x 1.0 mm. Sample 797. Crossed nicols.

one of the sills is multiple (Fig. 7). Sills occur throughout the exposed length of the metapyroxenite, but individual sills could not be traced for more than a few meters.

The sills consist of 50 per cent albite pseudomorphs after anhedral to subhedral, equant to tabular plagioclase partly enveloped by 42 per cent fibrous hornblende pseudomorphs after subophitic pyroxene, 8 per cent iron-titanium oxides and carbonate, and minor sphene, apatite, chlorite and epidote. Minor interstitial quartz is locally present.

Minor sills occur only in unit 1. They were emplaced after the formation of the metapyroxenite member and probably after the solidification of the entire unit because host rocks must have cooled sufficiently to allow the development of chilled margins. Their relationship to unit 1 and other units is not clear, but they are probably injections of magma that segregated during the crystallization of the mafic zone in one of the overlying units.

Unit 2

The floor of unit 2 is a country rock septum in the south and unit 1 in the north (Fig. 2). The basal contact is poorly exposed, but where observed, it is straight to gently sinuous with a 3 m thick chilled margin of very fine-grained metagabbro that passes upwards into feldspathic metapyroxenite.

The upper contact is poorly exposed but appears to be sinuous. In places, country rock lenses a few meters thick separate units 2 and 3 but generally unit 3 overlies unit 2 directly. A very fine-

grained chilled margin less than 1 m thick was observed in unit 2 against the country rock septum along the roof in the north.

The zones could not be subdivided into members because of lack of continuous exposure, poor textural preservation, and strong secondary mineral foliation. Granophyric metagabbro was not observed. Petrographic data, modal analyses, and chemical analyses are given in Tables 3, 4 and 10 respectively.

Unit 3

Except for local country rock lenses, the unit is bounded by other units but the contacts are not exposed. Much of the upper contact in the north has probably been truncated by phase Z. Petrographic data, modal analyses, and chemical analyses are given in Tables 3, 4 and 11 respectively.

Unlike units 1 and 2, the ultramafic zone pinches out to the north, and the mafic zone merges with the mafic zone of unit 2. Here, the two mafic zones could not be readily distinguished, except for the presence of a country rock septum which was assumed to mark the contact. The mafic zone greatly predominates over the ultramafic zone. Cataclastic textures in the lower two-thirds of the zone generally obscure primary textures; cumulus plagioclase laths are crushed, broken, rounded, and enveloped by fibrous hornblende and cummingtonite pseudomorphs after intercumulus pyroxene. Near the roof, relict subophitic textures are preserved and suggest that the upper part of the zone crystallized <u>in situ</u> and is not cumulus.

The greater volume of the mafic zone, cataclastic texture, and

the presence of normal igneous textures in part of the mafic zone and cumulus textures in other parts implies a more complex crystallization history than in units 1 and 2 which were relatively static, closed systems during crystallization. The cataclastic textures indicate movement of the partly consolidated cumulus zone. The non-cumulus material near the top may represent new magma that was added to the unit, in one or more pulses, during the later stages of crystallization. This addition may have caused the cataclasis. The new magma was gabbroic in composition and must have already undergone some fractionation.

Unit 4

The unit is exposed only in a few outcrops, and the central and northern parts have been removed by intrusion of phase Z. Where the upper contact against country rock lenses is exposed, the metagabbro is fine grained and apparently chilled. The lower contact is not exposed.

Country rock xenoliths are abundant in the mafic zone, especially near the roof. Elsewhere in phase X, country rock lenses normally separate intrusive events. Thus, the country rock lenses in the mafic zone may imply that there were several pulses of gabbro emplacement, with the magma derived from a fractionating system elsewhere. Cataclastic and subophitic textures combined with cumulus textures similar to those in unit 3, support this conclusion. Petrographic data, a modal analysis, and a chemical analysis are given in Tables 3, 4 and 11.

Unit 5

Unit 5 has been largely removed by the intrusion of phase Z and only the ultramafic zone is exposed. The ultramafic rocks are strongly recrystallized with well developed schistosity and local gneissosity. Neither upper nor lower contacts are exposed.

Thin metasedimentary and metavolcanic country rock xenoliths a few meters to over a hundred meters long are common in the ultramafic zone. The unit may actually comprise several thin units separated by country rock lenses.

PHASE Y

General Relations

Phase Y is a relatively homogeneous, multiple intrusion that is exposed for a north-south length of about 3 km and a width of about 0.6 km; the cross-sectional area is 0.90 km^2 (Fig. 2). The width estimate includes 20 to 50 per cent country rock septa.

Phase Y comprises a succession of sills intruded into a meta-sandstone and mafic and felsic metavolcanic sequence at the facies transition between formation I to the north and formation J to the south (Fig. 2). Individual sills vary in thickness from about 30 to 130 m, and in length from 800 to 1500 m. A typical sill consists of medium-grained quartz-bearing feldspathic metapyroxenite and quartz-bearing metagabbro with minor granophyric metagabbro and/or quartz metagabbro in the central or upper parts. Rare pegmatitic patches occur in the thicker sills. All sills have a 1 to 2 m thick, fine-grained chilled margin. Sparse amygdules were observed at one locality which suggests emplacement at shallow depths.

Contacts

Sills are generally concordant to well bedded sandstone in formation I, but discordant, transgressive contacts are common with the flows of formation J. Minor faults occur along many of the discordant contacts.

Contacts with country rocks are sharp and straight to gently

sinuous. Thinly-bedded metasandstone immediately adjacent to the phase is locally highly deformed (Fig. 13). The restriction of this deformation to the vicinity of the phase and the presence of analogous deformation in intermediate metatuff immediately below phase X, suggest that deformation occurred during emplacement. Because the shear stress transmitted to wall rocks by intruding magma is generally low in sills (Pollard, 1973), the presence of the deformation implies that the sediments were still plastic and not entirely lithified. Larger, gently to strongly sinuous folds which affect both the phase and country rocks are also present but are probably related to post-intrusion regional deformation.

Country rocks adjacent to the phase are generally schistose or slaty in a 1 m wide zone. This probably reflects regional metamorphism and deformation of an earlier contact metamorphic zone. Amphibole porphyroblasts to 2 mm occur in metasandstone adjacent to some contacts and reflect this contact metamorphism.

Xenoliths

Lenticular xenoliths of metasandstone, and mafic and felsic metavolcanics from a few meters to several hundred meters long and a few to several tens of meters thick occur throughout the phase. Many of these are septa separating individual sills, but others are concordant raft-like bodies, apparently enclosed completely within a sill. Rarely, the smaller lenses are discordant and were perhaps rotated during magma emplacement.

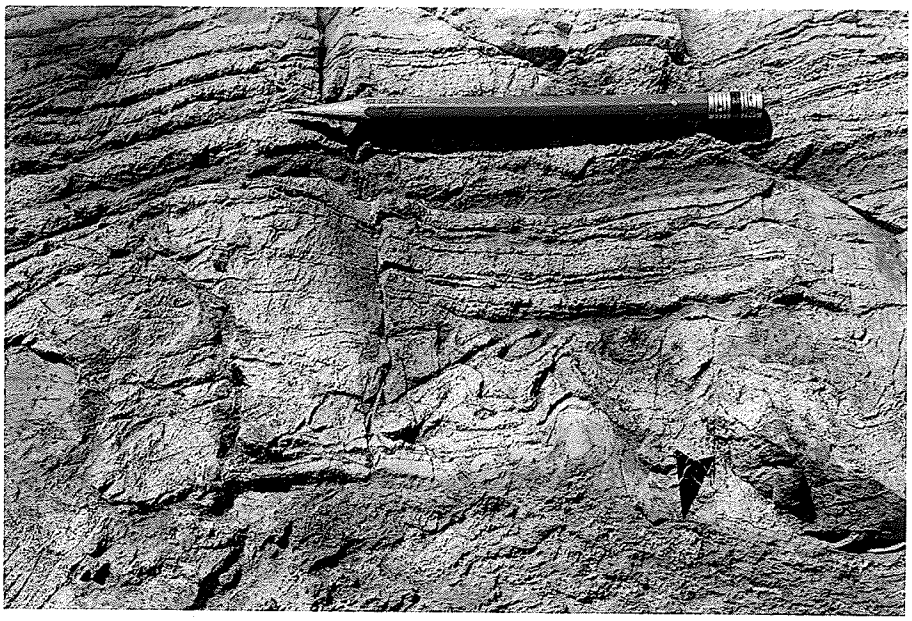

Fig. 13. Deformed metasandstone adjacent to contact with phase Y. Pencil is 15 cm long. Arrow points to metagabbro (bottom) - sandstone (top) contact.

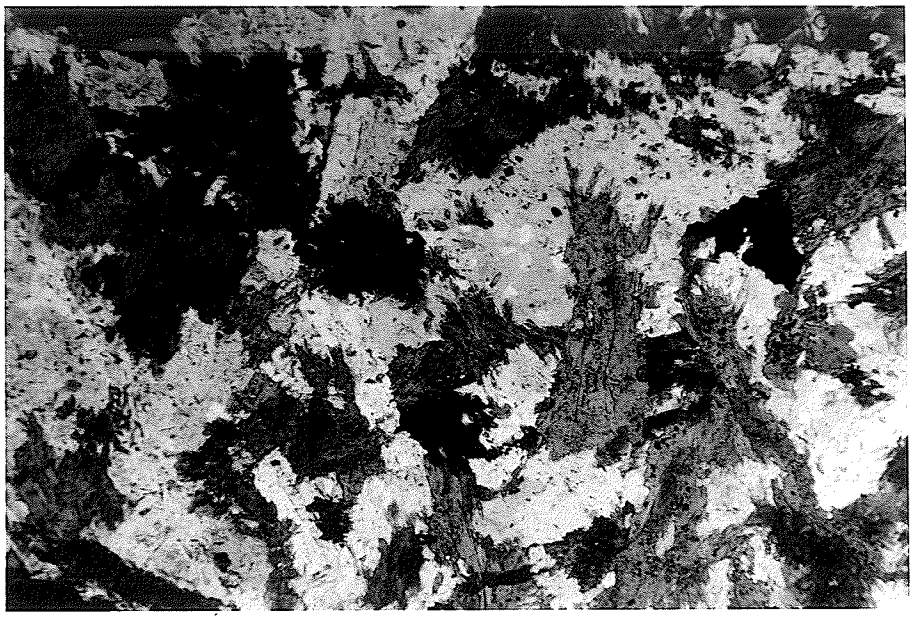

Fig. 14. Quartz-bearing metagabbro, phase Y. Hornblende - dark grey, plagioclase - light grey to white, quartz - medium grey. Field of view: 4.2 x 2.6 mm. Sample 120. Plane light.

Petrography

Chilled Margins

The chilled margins are massive, equigranular, fine-grained (0.1 to 0.5 mm), recrystallized, quartz-bearing metagabbro. Modal and chemical analyses of a typical sample 1 m from the base of a sill are given in Tables 7 and 12 (sample 185).

Quartz-bearing Feldspathic Metapyroxenite and Metagabbro

Quartz-bearing feldspathic metapyroxenite is generally medium-grained and strongly foliated. Primary textures are preserved only locally and are hypidiomorphic-granular to rarely subophitic. Plagioclase ranges in composition from An_{24} to An_{54} and consists of multi-crystal and rarely single-crystal pseudomorphs after primary subhedral, blocky laths and equant grains 0.5 to 1.5 mm in size. Some of the most calcic grains are probably relics close to primary composition. Primary pyroxene is replaced by ragged plates to fibrous bundles of dark green to blue-green hornblende from 0.5 to several mm in size. Quartz forms rounded, strained, isolated grains or patchy mosaics ranging in size from 0.1 to 1.0 mm and is rarely intimately intergrown with plagioclase in what may be a relict granophyric texture. Quartz-bearing metagabbro (Fig. 14) differs from the feldspathic metapyroxenite in its slightly higher plagioclase content. Modal analyses are given in Table 7.

Table 7. Phase Y, Modal Mineralogy (volume per cent)

	cm[1]	qfmpx[1]		qmg[1]			mg[1]		gmg[1]	
	185	122	123	120	242	475	176	184	119	474
hornblende	68.6	72.0	73.1	65.0	68.7	39.6	60.7	60.2	67.0	58.8
cummingtonite					tr	1.0				
plagioclase	25.8	21.2	20.5	24.7	16.2	52.0[2]	28.5	33.6	22.6	28.8
quartz	0.7	0.4	2.1	5.5	6.3	tr			3.7	4.9
granophyre									0.9	1.6
Fe-Ti oxides	1.7	2.2	2.6	2.6	5.5	4.0	4.6	2.9	3.3	3.7
sulphides	1.7	1.0	1.5	2.0	1.0	2.7	4.0	2.5	2.0	tr
chlorite	0.4	3.1	tr	0.2	0.5	0.7	1.4	0.6	0.4	1.5
biotite							0.5	0.1		0.3
carbonate	1.0	0.1	0.2	tr	0.6	tr	0.3	0.1	tr	tr
epidote	tr	tr	tr	tr	tr	tr	tr	tr	0.1	0.4
sphene			tr							
tourmaline					1.2		tr			tr
apatite	0.1		tr	tr						tr
colour index[3]	69.0	75.1	73.1	65.2	69.2	41.3+	62.6	66.3	67.4	60.6

[1] cm - chilled margin; qfmpx - quartz-bearing feldspathic metapyroxenite; qmg - quartz-bearing metagabbro; mg - metagabbro; gmg - granophyric metagabbro (see Table 1A)

[2] includes abundant very fine-grained hornblende, chlorite, epidote, and carbonate.

[3] colour index = amphibole + chlorite + biotite + sphene

Other Rock Types

Well preserved granophyric metagabbro is relatively rare (Fig. 15). It is mineralogically and texturally similar to quartz-bearing metagabbro and feldspathic metapyroxenite but contains up to 2 per cent granophyre. Modal and chemical analyses (sample 474) are given in Tables 7 and 12.

Quartz metagabbro was found at only one locality. It is similar to quartz-bearing metagabbro but is slightly less mafic and contains more than 10 per cent quartz.

Quartz-free metagabbro is generally less mafic and more oxide-rich than quartz-bearing varieties. Modal and chemical analyses are given in Tables 7 and 12.

Differentiation

Lithologic and textural homogeneity, and relict subphitic texture suggest that the magma crystallized in situ and was not markedly differentiated, especially by crystal settling, during or after emplacement. This is supported by the chemical similarity of chilled feldspathic metapyroxenite from the margin of one sill and granophyric metagabbro about 20 m from the contact of another sill (samples 185 and 474, Table 12).

Fig. 15. Granophyric metagabbro, phase Y. Field of view: 1.7 x 1.0 mm. Sample 124. Plane light.

PHASE Z

General Relations

Phase Z comprises five differentiated, concordant, multiple mafic sills. Age relationships between sills could not be determined but sill 1, the uppermost and largest, is the type sill (Fig. 2, Table 8). All sills are enveloped by fine-grained chilled margins 1 to 2 m thick. The phase is 4.6 km long in the north-south direction and is 0.3 km thick; it has a cross-sectional area of 1.22 km^2.

Sills 1 and 5 consist of a lower cumulus metapyroxenite zone and an upper subophitic to ophitic metagabbro zone that crystallized largely in situ. Sills 2, 3 and 4 are entirely metagabbro with massive, subophitic to ophitic and hypidiomorphic granular textures; there is only minor evidence of crystal settling but differentiation by crystal fractionation is probably marked. The northern termination of sill 1 and the southern part of sill 5 contain autobreccia similar to that in phase X.

Contacts

The relationship of phase Z to host rocks is relatively simple. Both upper and lower contacts are sharp, gently sinuous and broadly concordant with formation J flows, but the phase is discordant to units 4 and 5 of phase X. Where inter-sill contacts are exposed, thin lenticular metasedimentary septa commonly separate the sills; septa also locally occur within sills. The septa are all part of

Table 8. Summary of Stratigraphy, phase Z.

sill	thickness (m)	length (m)	zones	thickness (m)	rock types (Table 1A)	Primary texture	Types of cumulates (Table 1B)
5	40-120	2200+	mafic	90	upper metagabbro member		
					metagabbro	subophitic to hypidiomorphic-granular	
				0-30	lower metagabbro member		
					metagabbro	subophitic to ophitic	
			ultramafic		metapyroxenite	cumulus	orthopyroxene, orthopyroxene-olivine
4	50-160	1300	mafic only		metagabbro	not preserved	
3	50-80	2500+	mafic only		metagabbro	not preserved	
2	40-100	1900+	mafic only		metagabbro, chilled feldspathic metapyroxenite	subophitic equigranular	
1	35-260	2700	mafic	20-140	upper metagabbro member		
					metagabbro	subophitic to hypidiomorphic-granular	
				40-120	lower metagabbro member		
					metagabbro	subophitic to ophitic	
			ultramafic	0-30	metapyroxenite	cumulus	orthopyroxene, orthopyroxene-olivine

the lacustrine unit of formation I and are identical to the septa in phase X.

At the base of sill 5, the contact with intermediate tuff and lapilli-tuff of formation I is more complex. It is generally sharp and smooth to interdigitating but locally there are bulbous protuberances of chilled metagabbro (Fig. 16). The tuff and lapilli-tuff are contorted and strongly schistose and appear to have been plastic during intrusion of the gabbro; the metagabbro is massive and apparently undeformed. The metagabbro has a wider chilled zone than elsewhere. It has a very fine-grained chilled selvage 1 cm thick, and is still fine-grained 20 m from the contact.

Sill 1

Chilled Margin

The basal chilled zone is a completely recrystallized feldspathic metapyroxenite (Table 9) which has a strong mineral foliation parallel to the contact. This zone is about 2 m thick and passes abruptly upwards into the ultramafic zone. The top chilled zone was not directly observed but grain size in the upper metagabbro member decreases towards the contact, and is fine-grained a few meters from the contact.

Ultramafic Zone

The ultramafic zone is exposed only in the southern part of sill 1, but is probably present along most of the base, except at the

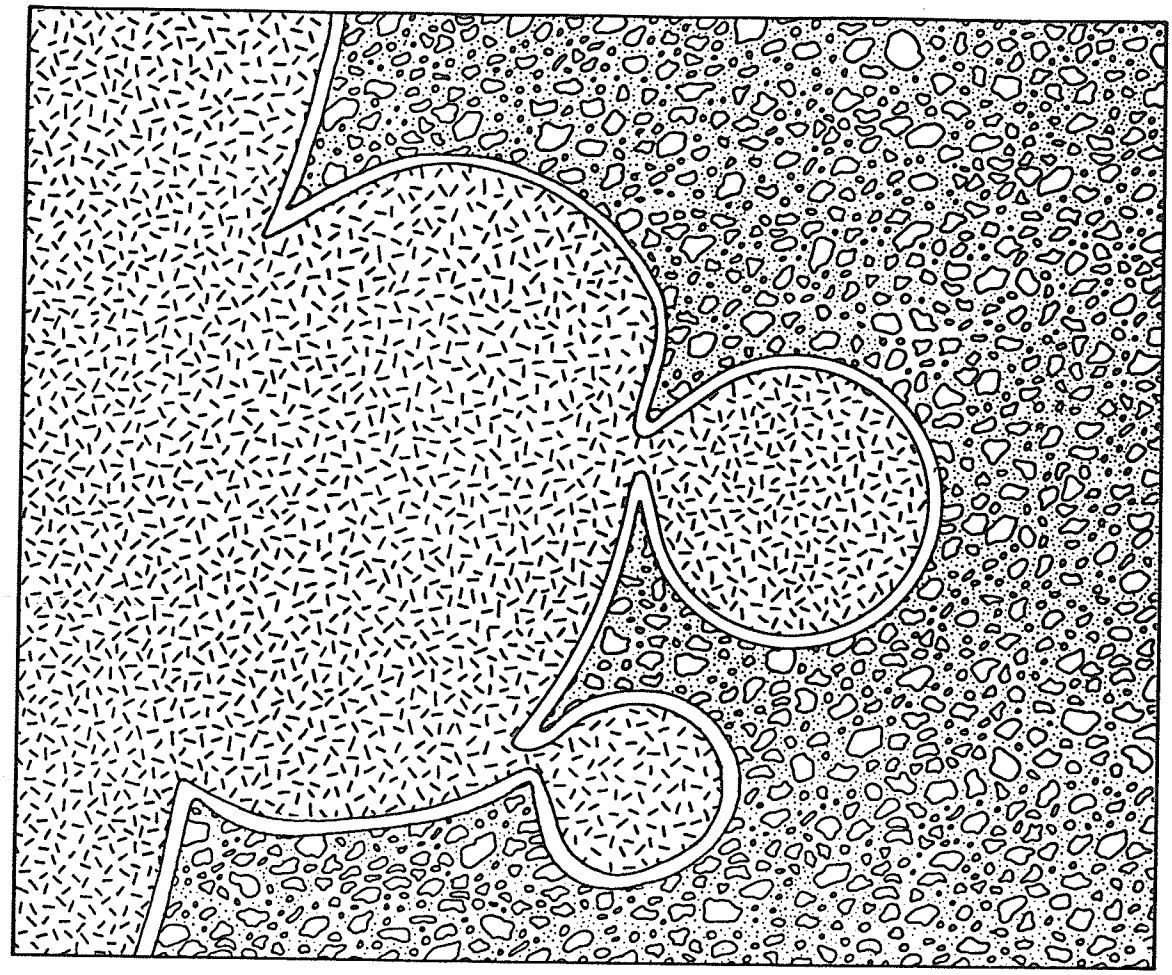

LEGEND

VERY FINE-GRAINED CHILLED SELVAGE

MASSIVE FINE-GRAINED METAGABBRO

INTERMEDIATE TUFF AND LAPILLI-TUFF

0 0.5 m

Fig. 16. Field sketch showing bulbous protrusions of chilled, massive metagabbro into intermediate tuff andlapilla-tuff at the base of sill 5, phase Z.

Table 9. Phase Z, Modal Mineralogy (volume per cent)

	Sill 1													Sill 2
	cm[1]	Ultramafic Zone		Mafic Zone										cm[1]
				lower metagabbro member					upper metagabbro member					
	198	200	202	166	167	168	169	136	205	206	207	140	141	142	622
actinolite	73.0			49.6	48.1	47.0	42.3	54.3							74.4
tremolite		35.8	36.0												
hornblende									41.5	64.5	59.5	60.1	54.6	67.4	
olivine[2]		0.2	2.7												
plagioclase	14.2			44.5	49.2	48.2	53.8	35.8	53.7	33.5	36.5	35.7	34.7	20.0	22.7
quartz										0.1				1.0	
Fe-Ti oxides	1.7	1.0	0.7	1.0	0.5	0.6	0.5	0.9	1.0	0.6	1.8	0.9	1.2	1.2	2.3
sulphides	1.8	tr	tr	tr			tr	tr		tr	1.5		tr		tr
chlorite	4.7			2.2	1.5	2.2	2.3	7.5	0.3	0.4	0.2	1.8	1.2	0.1	0.3
biotite						tr	1.0		1.8	0.6	tr				tr
carbonate	tr	tr	tr	tr	tr	tr	tr	tr	tr	tr	tr	0.1	0.1	tr	0.3
epidote	4.3			2.6	0.5	1.6	0.1	1.5	1.7	0.3	0.5	1.4	8.2	10.3	
sphene	0.3			0.2	0.2	0.4	tr					tr	tr		
apatite													tr		
mesostatis[3]		63.0	60.6												
colour index[4]	78.0	98.8[5]	96.6[5]	52.0	49.8	49.6	44.6	61.8	43.6	65.5	61.5	61.9	55.8	67.5	74.7

[1] cm - chilled margin

[2] chlorite pseudomorphs

[3] very fine-grained fibrous tremolite and chlorite with minor carbonate

[4] colour index = amphibole + olivine + chlorite + biotite + sphene

[5] includes trace amounts of carbonate

extreme south, where the mafic zone occurs both above and below the ultramafic zone. The ultramafic zone is generally in sharp contact with the chilled zone below and apparently with the mafic zone above, although the latter contact is obscured by a 5 m wide covered interval. Most of the zone is strongly foliated metapyroxenite and primary textures are poorly preserved. Primary minerals are not preserved. Modal analyses, average modes, and chemical analyses are given in Tables 9, 10 and 12 respectively.

Typical metapyroxenite consists of 30 to 50 per cent colourless to very pale-green tremolite single crystal pseudomorphs after cumulus orthopyroxene (0.5 to 4.0 mm) in a fine-grained, strongly foliated fibrous intercumulus mesostasis of tremolite, chlorite and iron-titanium oxides (Fig. 17, Table 9). Rounded to amoeboid aggregates (0.5 to 1.0 mm) of very fine-grained chlorite in or partly enclosed by tremolite grains may be multi-crystal pseudomorphs after primary cumulus olivine. Some of these pseudomorphs mimic primary subhedral to euhedral olivine crystal morphology (Fig. 17). Iron-titanium oxides are generally restricted to the margins of tremolite pseudomorphs where they form a very fine-grained opaque-rich rim. This may reflect zoning in primary orthopyroxene with the rims being more iron-rich. No evidence of primary plagioclase was observed.

The zone is a size-graded, isomodal layer; grain size of the pseudomorphs after cumulus orthopyroxene increases from 0.5 to 2.0 mm at the base to 3.0 or 4.0 mm at the top, but modal abundance of pyroxene and olivine do not change. Rarely, pyroxene is concentrated in concordant layers several centimeters thick, alternating with layers of normal metapyroxenite. These layers have sharp contacts marked by abrupt changes in orthopyroxene abundance.

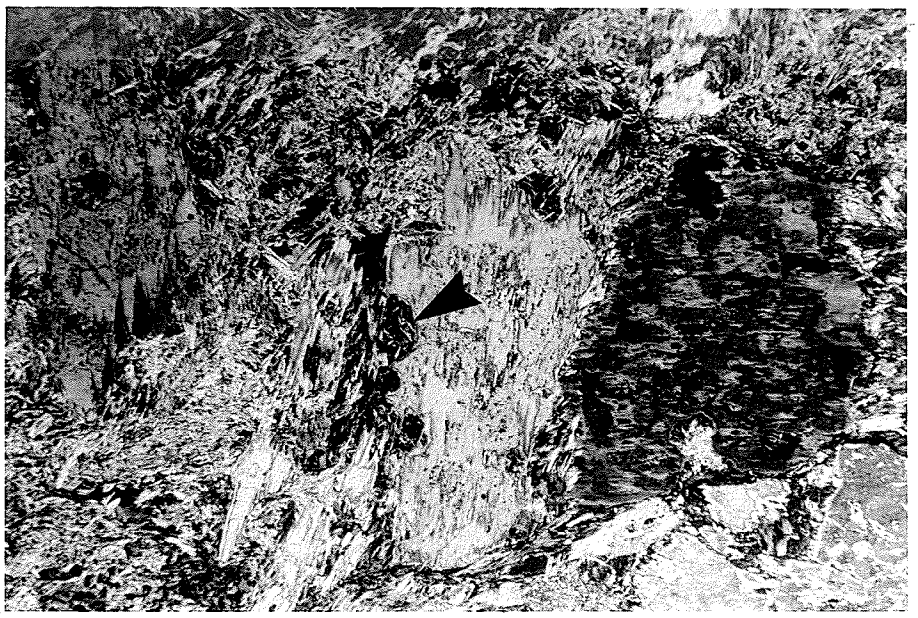

Fig. 17. Orthopyroxene - olivine cumulate, ultramafic zone, phase Z. Arrow points to chlorite pseudomorph after cumulus olivine, partly enclosed by cumulus orthopyroxene (tremolite pseudomorph). Sill 1. Field of view: 4.2 x 2.6 mm. Sample 202. Crossed nicols.

Fig. 19. Subophitic to ophitic metagabbro, upper part of lower metagabbro member, sill 1, phase Z. Field of view: 4.2 x 2.6 mm. Sample 169. Crossed nicols.

Table 10. Phase Z, Sill 1, Average Modal Analyses (volume per cent)

	chilled margin	ultramafic zone	mafic zone	
			lower meta-gabbro member	upper meta-gabbro member
actinolite	73.0		48.3 (4.3)[1]	
tremolite		35.9		
hornblende				57.9 (9.2)
olivine[2]		1.5		
plagioclase	14.2		46.3 (6.7)	35.7 (10.7)
quartz				0.2
Fe-Ti oxides	1.7	0.9	0.7 (0.2)	1.1 (0.4)
sulphides	1.8		tr	0.3
chlorite	4.7		3.1 (2.5)	0.7 (0.7)
biotite			0.2	0.4
carbonate	tr	tr	tr	tr
epidote	4.3		1.3 (1.0)	3.7 (4.4)
sphene	0.3		0.2 (0.2)	tr
apatite				tr
mesostatis[3]		61.8		
colour index[4]	78.0	98.1[5]	51.6 (6.3)	59.3 (8.7)
no. of samples	1	2	5	6

[1] one standard deviation

[2] chlorite pseudomorphs

[3] very fine-grained fibrous tremolite and chlorite with minor carbonate

[4] colour index = amphibole + olivine + chlorite + biotite + sphene

[5] includes trace amounts of carbonate

Mafic Zone

Lower Metagabbro Member

The member is present everywhere except at the southern end. Along the base, the contact with metapyroxenite is a sharp phase contact, marked by the disappearance of cumulus olivine and orthopyroxene, and the appearance of cumulus clinopyroxene and plagioclase. At the top, the contact with upper metagabbro is gradational over 15 m. Modal analyses, average modes, and chemical analyses are given in Tables 9, 10 and 12 respectively.

Texture and composition are functions of stratigraphic height (Fig. 18). In the basal 40 m the metagabbro has ophitic to locally subophitic texture formed by 3 to 15 mm anhedral very pale-green, slightly pleochroic actinolite pseudomorphs after clinopyroxene that enclose subhedral laths and more rarely, equant, primary plagioclase grains (0.1 to 1.0 mm). The plagioclase grains are normally zoned; core composition is An_{82} and rims are An_{59}. Interstitial to these ophitic grains is a fine-grained mixture of fibrous actinolite and chlorite, and flow-oriented subhedral plagioclase laths that are more blocky to equant and generally coarser-grained than the enclosed grains (0.25 to 1.25 mm). Interstitial plagioclase is unzoned with composition An_{57}.

With increasing height in the member, large ophitic grains decrease in both size and abundance, and are rare near the top. Here, the lower metagabbro member is typically medium-grained and subophitic (Fig. 19).

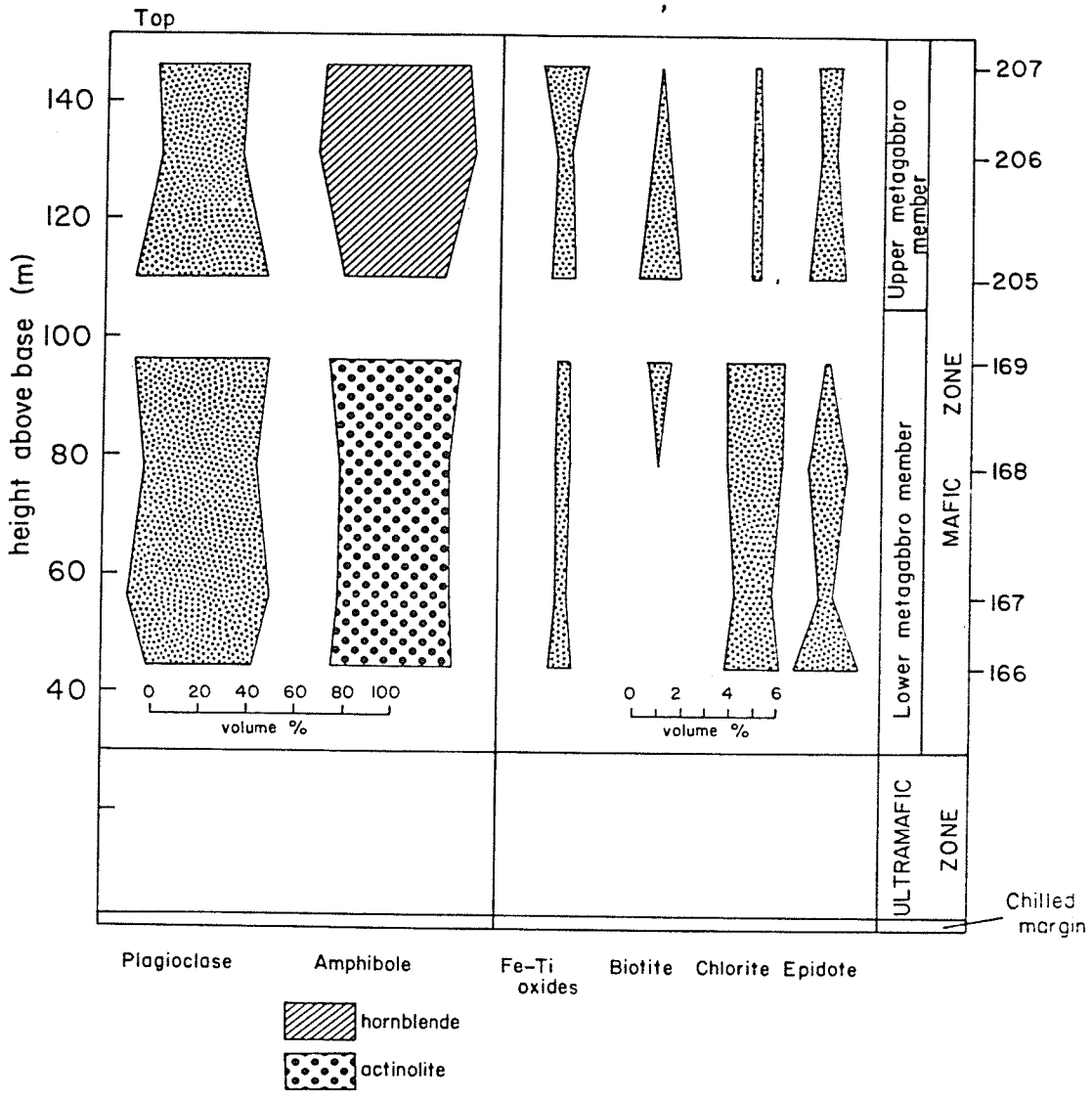

Fig. 18. Variation of metamorphic mineralogy with stratigraphic height along section BB' in sill 1, phase Z.

Upper Metagabbro Member

The upper metagabbro is distinguished from lower metagabbro by a relatively abrupt decrease in hornblende pseudomorph grain size and the predominance of subophitic and hypidiomorphic-granular textures over ophitic texture. Modal analyses, an average mode, and chemical analyses are given in Tables 9, 10 and 12 respectively. Hornblende forms pale green, anhedral, 0.5 to 1.5 mm pseudomorphs after clinopyroxene that either partly enclose 0.3 to 1.0 mm equant grains and blocky laths of probably primary plagioclase (An_{60}) in subophitic texture, or form hypidiomorphic-granular texture. These two textures are intergradational. Biotite occurs as scattered interstitial grains or intimately intergrown with chlorite and/or hornblende. Chlorite generally occurs as very fine-grained inclusions in plagioclase but also as ragged interstitial grains. Quartz is a rare interstitial phase.

From bottom to top, the upper metagabbro becomes more mafic (Fig. 18), more uniformly subophitic and finer grained. Hornblende pseudomorphs after clinopyroxene decrease in size from several millimeters to less than one, but plagioclase decreases only slightly. These trends reflect rapid cooling at the top of the sill and progressive crystallization (and differentiation) downwards from the upper contact.

Pegmatitic Metagabbro

Pegmatitic, quartz-bearing metagabbro forms irregular pods up to 120 m long and 40 m thick in the lower third of the upper

metagabbro member. They are texturally and mineralogically similar to adjacent metagabbro with which they are gradational but contain up to 10 per cent quartz and are coarse grained (5 to 10 mm). They occur in the least mafic and most differentiated part of the sill.

Sill 2

Sill 2 comprises a very fine grained chilled margin of equigranular feldspathic metapyroxenite up to 1.5 m thick, surrounding fine to medium-grained subophitic metagabbro. Primary textures are not preserved in the chilled zone but are preserved in the interior, which is similar to upper metagabbro in sill 1 (colour index 60) and is less mafic than the chilled margin (colour index 75). A pod of pegmatitic, quartz-bearing metagabbro 100 m long and 10 m thick occurs in the center of the sill. Modal and chemical analyses of the chilled margin are given in Tables 8 and 12.

Metamorphosed Ultramafic Intrusive Rocks

Several discordant, lenticular to arcuate, ultramafic bodies 5 to 20 m thick and 50 to 100 m long occur in phases X and Z (Map unit 12, Fig. 2). They are mainly metapyroxenites composed of fine-grained fibrous tremolite, chlorite, carbonate, and minor iron-titanium oxides with local metaperidotite containing up to 20 per cent elliptical pseudomorphs of very fine-grained chlorite after primary olivine. Primary textures and structures have been largely destroyed.

They are in sharp intrusive contact with sill complex rocks and

in places are characterized by well developed polygonal jointing. They are apparently unrelated to sill complex magma.

CHEMISTRY

Introduction

Major elements and selected trace elements of 26 samples from phase X, 3 from phase Y, and 4 from phase Z are given in Tables 11 and 12. Volatile-free Barth-Niggli cation norms were calculated by removing H_2O (total), CO_2, and S, and recalculating analyses to 100 per cent. Fe_2O_3/FeO is abnormally high in 12 of the samples and Fe_2O_3 was adjusted according to the method of Irvine and Baragar (1971).

Several problems were encountered in interpreting the chemistry. These mainly reflect the nature and extent of original submarine alteration and burial metamorphism, the subsequent regional metamorphic overprint, and the fact that part of the sill complex was not a closed system after emplacement.

General Classification - Rock Series

All three phases of the sill complex are tholeiitic (Fig. 20). According to Irvine and Baragar's (1971) classification, the chilled margins are tholeiitic basalt (samples 1, 529, 546, 185, and 622; Tables 11 and 12).

Metamorphism and Alteration

The sill complex intruded both lacustrine volcanogenic clastic and chemical sedimentary rocks (formation I) and submarine mafic

Table 11. Phase X, Chemical Analyses[1]

	Unit 1																	
	Border Zone			Ultramafic Zone					Mafic Zone									
	lcm[2]		ucm	feldspathic metapyroxenite member					lower metagabbro member					upper metagabbro member				gmg
	1	529	546	12	644	646	788	541	722	734	732	650	731	730	729	636	60a[3]	445	798
Major Elements (weight per cent)																			
SiO_2	49.80	47.55	47.45	50.50	50.40	51.00	49.75	48.60	45.55	49.00	44.20	46.65	46.40	47.40	50.35	51.40	53.00	49.60	53.50
Al_2O_3	9.10	8.76	8.62	3.66	4.62	4.22	3.82	6.76	11.37	13.22	13.61	11.34	12.42	13.01	13.30	12.66	13.00	15.22	13.76
Fe_2O_3	2.32	2.88	1.39	1.96	1.16	1.24	2.18	1.49	2.68	2.68	4.47	3.10	3.52	2.76	2.96	4.90	5.42	2.79	2.92
FeO	9.39	13.20	13.28	9.36	9.56	9.56	8.92	12.76	13.56	12.04	15.76	14.76	15.16	11.81	15.16	12.64	12.10	9.00	13.20
FeO*[4]	11.48	15.79	14.53	11.12	10.60	10.68	10.88	14.10	15.97	14.45	19.78	17.55	18.33	14.29	17.82	17.05	16.98	11.51	15.83
MgO	11.10	11.88	10.80	13.85	14.90	14.10	13.75	11.50	9.03	7.15	6.00	7.38	5.65	2.93	3.70	2.23	1.99	5.08	2.35
CaO	12.10	9.93	11.80	13.35	12.60	13.10	13.65	11.40	9.27	8.60	7.85	8.35	7.60	8.70	5.18	4.65	4.73	8.35	4.95
Na_2O	0.79	0.82	0.93	1.43	1.30	1.14	1.46	1.11	2.43	3.19	2.79	2.84	3.81	5.70	4.73	6.28	5.47	4.63	4.70
K_2O	0.26	0.74	0.10	0.02	nd[5]	0.02	0.01	0.54	0.72	0.22	0.16	0.48	0.16	0.06	0.14	0.08	0.39	0.08	0.26
TiO_2	0.63	0.76	0.77	0.49	0.41	0.42	0.49	0.75	0.51	0.56	1.19	1.08	1.62	1.21	0.91	1.37	1.31	0.99	1.23
P_2O_5	0.02	0.18	0.16	0.12	0.11	0.10	0.10	0.10	0.15	0.16	0.15	0.16	0.17	0.15	0.26	0.22	0.14	0.08	0.14
MnO	0.39	0.30	0.28	0.22	0.23	0.22	0.25	0.28	0.26	0.23	0.22	0.24	0.24	0.24	0.25	0.21	0.22	0.18	0.24
CO_2	1.92	0.20	1.89	2.77	1.92	2.22	3.29	2.13	1.12	0.44	0.71	1.34	1.11	4.36	0.74	2.04	1.62	1.63	0.66
H_2O	2.02	2.51	2.49	1.97	2.38	2.18	2.00	2.24	3.02	2.15	2.68	2.33	2.19	1.54	1.99	1.28	0.74	2.29	1.61
S	-[6]	0.026	0.017	0.034	0.018	0.011	0.008	0.009	0.077	0.003	0.002	0.066	0.006	0.008	0.004	0.013	0.010	0.004	-
total	99.81	99.74	99.98	99.73	99.61	99.53	99.68	99.67	99.75	99.64	99.79	100.12	100.06	99.88	99.67	99.97	100.10	99.92	99.52
Trace Elements (ppm)																			
Co	-	119	70	80	68	83	74	93	124	96	77	106	73	67	68	51	40	58	-
Cu	-	191	74	8	83	60	41	36	493	15	8	428	10	8	20	22	20	51	-
Ni	-	308	174	245	342	268	222	176	190	172	187	140	60	11	11	9	20	48	< 20
Pb	-	nd	6	nd	8	5	12	11	12	18	nd	nd	41	6	17	17	30	13	-
Rb	-	52	10	3	< 10	< 10	3	31	40	11	< 10	24	12	< 10	8	< 10	20	3	-
Zn	-	176	121	59	117	81	67	110	145	118	153	143	121	116	142	51	80	151	-

Table 11 (continued). Phase X, Chemical Analyses, Volatile-free[7]

	Unit 1																	
	Border Zone			Ultramafic Zone					Mafic Zone									
	lcm[2]		ucm	feldspathic metapyroxenite member					lower metagabbro member					upper metagabbro member				gmg
	1	529	546	12	644	646	788	541	722	734	732	650	731	730	729	636	60a[3]	445	798
	Major Elements (weight per cent)																	
SiO_2	51.95	49.02	49.64	53.18	52.89	53.62	52.77	51.00	47.68	50.49	45.85	48.40	47.96	50.44	51.94	53.19	54.20	51.67	55.01
Al_2O_3	9.49	9.03	9.02	3.85	4.85	4.44	4.05	7.09	11.90	13.62	14.12	11.77	12.84	13.84	13.72	13.10	13.30	15.85	14.15
Fe_2O_3	2.42	2.97	1.45	2.06	1.22	1.30	2.31	1.56	2.81	2.76	4.64	3.22	3.64	2.94	3.05	5.07	5.54	2.91	3.06
FeO	9.76	13.61	13.89	9.86	10.03	10.05	9.45	13.39	14.19	12.41	16.35	15.31	15.67	12.57	15.64	13.08	12.37	9.38	13.57
FeO*	11.94	16.28	15.20	11.71	11.13	11.22	11.53	14.79	16.72	14.89	20.53	18.21	18.95	15.22	18.39	17.64	17.36	12.00	16.32
MgO	11.58	12.25	11.30	14.59	15.64	14.82	14.57	12.07	9.45	7.15	6.22	7.66	5.84	3.12	3.82	2.31	2.04	5.29	2.42
CaO	12.62	10.24	12.35	14.06	13.22	13.77	14.46	11.96	9.70	8.86	8.14	8.66	7.86	9.26	5.34	4.81	4.84	8.70	5.09
Na_2O	0.82	0.85	0.97	1.51	1.36	1.20	1.55	1.16	2.54	3.29	2.89	2.95	3.94	6.07	4.88	6.50	5.59	4.82	4.82
K_2O	0.27	0.76	0.10	0.02	nd	0.02	0.01	0.57	0.75	0.23	0.17	0.50	0.17	0.06	0.14	0.08	0.40	0.08	0.27
TiO_2	0.66	0.78	0.81	0.52	0.43	0.44	0.52	0.79	0.53	0.58	1.23	1.12	1.67	1.29	0.94	1.42	1.34	1.03	1.26
P_2O_5	0.02	0.19	0.17	0.13	0.12	0.11	0.11	0.10	0.16	0.16	0.16	0.17	0.18	0.16	0.27	0.23	0.14	0.08	0.14
MnO	0.41	0.31	0.29	0.23	0.24	0.23	0.26	0.29	0.27	0.24	0.23	0.25	0.25	0.26	0.26	0.22	0.22	0.19	0.25
	Volatile-free Barth-Niggli Norms																	
Quartz	3.41																		3.86
Orthoclase	1.62	4.59	0.63	0.13		0.12	0.06	3.40	4.51	1.35	1.01	3.01	1.00	0.38	0.87	0.50	2.42	0.49	1.62
Albite	7.49	7.72	8.89	13.52	12.17	10.75	13.88	10.61	23.08	29.80	26.79	27.01	36.18	37.53	44.75	59.36	51.52	43.27	44.47
Anorthite	21.66	18.92	20.29	3.70	7.06	6.66	4.07	12.63	19.04	21.97	25.82	17.78	17.26	10.44	15.44	6.45	10.25	21.36	16.53
Nepheline														10.39					
Diopside	23.56	15.93	20.02	39.11	34.38	36.06	40.37	23.87	12.63	9.02	4.87	9.94	7.52	9.68	2.52	3.22	2.42	9.32	1.82
Hedenbergite	9.70	9.30	12.74	13.09	11.53	12.70	13.19	13.63	10.25	8.06	6.96	10.07	9.64	18.14	5.36	9.84	8.31	7.66	4.89
Enstatite	20.56	20.61	18.82	19.73	21.02	22.86	16.21	18.13		7.63	2.59	4.53	0.70		5.42	0.16	4.15	0.01	5.93
Ferrosilite	8.47	12.03	11.98	6.61	7.05	8.05	5.30	10.35		6.82	3.71	4.60	0.90		11.51	0.48	14.29	0.01	15.97
Forsterite		4.37	2.19	0.74	3.52		2.84	2.80	15.05	6.30	9.52	9.07	9.03	2.87	3.06	3.54	0.30	7.45	
Fayalite		2.55	1.39	0.25	1.18		0.93	1.60	12.21	5.64	13.61	9.19	11.57	5.39	6.50	10.80	1.04	6.12	
Magnetite	2.56	2.48	1.55	2.16	1.27	1.36	2.20	1.66	2.22	2.24	3.01	2.86	3.45	3.04	2.66	3.16	3.08	2.71	3.01
Ilmenite	0.93	1.11	1.14	0.72	0.60	0.62	0.72	1.11	0.75	0.81	1.77	1.60	2.39	1.81	1.34	2.01	1.91	1.44	1.81
Apatite	0.04	0.40	0.36	0.27	0.24	0.22	0.22	0.22	0.33	0.35	0.34	0.36	0.38	0.34	0.57	0.49	0.31	0.17	0.31
Specific Gravity	3.00	3.13	3.06	3.01	3.06	3.02	2.98	3.09	3.06	2.99	3.11	3.05	3.07	2.90	2.88	2.93	-	-	2.98

Table 11. Phase X, Chemical Analyses[1] (continued)

	Unit 2				Unit 3		Unit 4
	UZ		MZ		UZ	MZ	UZ
	9	21[3]	553	760	5	666	32
	Major Elements (weight per cent)						
SiO_2	49.50	50.80	52.15	49.75	50.50	53.05	48.50
Al_2O_3	7.14	5.52	13.47	13.81	7.98	12.20	6.80
Fe_2O_3	1.85	1.11	1.77	2.93	1.86	2.30	2.20
FeO	10.72	10.40	12.36	13.68	11.56	15.96	11.00
FeO*	12.39	11.40	13.95	16.32	13.23	17.43	12.98
MgO	12.30	12.00	5.30	3.98	11.05	3.37	11.10
CaO	11.20	12.70	6.35	5.00	10.55	3.34	13.00
Na_2O	1.81	1.46	4.44	5.35	1.90	5.50	1.80
K_2O	0.08	0.10	0.10	0.72	0.20	0.08	0.08
TiO_2	0.61	0.58	1.12	1.09	0.66	1.31	0.54
P_2O_5	0.12	0.01	0.06	0.12	0.07	0.25	0.05
MnO	0.27	0.25	0.25	0.22	0.25	0.29	0.25
CO_2	2.00	2.40	0.57	1.67	0.94	0.64	2.81
H_2O	2.38	1.06	1.61	1.49	1.93	1.61	1.92
S	0.035	0.060	-	-	-	0.006	-
total	100.02	98.45	99.55	99.81	99.45	99.90	100.05
	Trace Elements (ppm)						
Co	81	60	-	-	-	53	-
Cu	86	50	-	-	-	7	-
Ni	253	210	85	60	205	13	180
Pb	11	30	-	-	-	nd	-
Rb	< 10	10	-	-	-	3	-
Zn	134	150	-	-	-	178	-

Table 11 (continued). Phase X, Chemical Analyses, Volatile-free

	Unit 2				Unit 3		Unit 4
	UZ		MZ		UZ	MZ	UZ
	9	21[3]	553	760	5	666	32
	Major Elements (weight per cent)						
SiO_2	51.78	53.48	53.56	51.47	52.29	54.33	50.88
Al_2O_3	7.47	5.81	13.83	14.29	8.26	12.49	7.13
Fe_2O_3	1.94	1.17	1.82	3.03	1.93	2.36	2.31
FeO	11.21	10.95	12.69	14.15	11.97	16.34	11.54
FeO*	12.96	12.00	14.28	16.88	13.71	18.46	13.62
MgO	12.87	12.63	5.44	4.12	11.44	3.45	11.64
CaO	11.72	13.37	6.52	5.17	10.92	3.42	13.64
Na_2O	1.89	1.54	4.56	5.54	1.97	5.63	1.89
K_2O	0.08	0.11	0.10	0.74	0.21	0.08	0.08
TiO_2	0.64	0.61	1.15	1.13	0.68	1.34	0.57
P_2O_5	0.13	0.01	0.06	0.12	0.07	0.26	0.05
MnO	0.28	0.26	0.26	0.23	0.26	0.30	0.25
	Volatile-free Barth Niggli Norms						
Quartz		0.72					
Orthoclase	0.50	0.63	0.61	4.45	1.24	0.49	0.50
Albite	17.03	13.87	41.29	47.82	17.80	51.60	17.09
Anorthite	11.66	8.69	17.13	12.06	13.21	8.75	10.83
Nepheline							
Diopside	25.45	32.08	5.63	3.86	21.45	1.64	30.32
Hedenbergite	11.16	14.25	6.45	6.57	11.31	3.85	15.32
Enstatite	17.64	19.01	10.04		20.08	7.69	8.80
Ferrosilite	7.73	8.44	11.49		10.59	17.98	4.45
Forsterite	3.92		1.73	7.16	0.77	0.91	6.34
Fayalite	1.72		1.98	12.18	0.41	2.12	3.20
Magnetite	2.03	1.23	1.92	2.83	2.03	2.51	2.26
Ilmenite	0.89	0.86	1.62	1.59	0.96	1.91	0.80
Apatite	0.26	0.02	0.13	0.26	0.15	0.55	0.11
Specific Gravity	-	-	-	-	-	-	-

[1] Modal analyses in Table 4; sample locations on Fig. 2 and 3.

[2] Abbreviations: lcm - lower chilled margin member; ucm - upper chilled margin member; gmg - granophyric metagabbro member; UZ - Ultramafic Zone; MZ - Mafic Zone.

[3] Data from Ayres (in preparation)

[4] Total Fe as FeO

[5] Not detected

[6] Not analysed

[7] Analyses minus CO_2, H_2O, and S recalculated to 100 per cent.

Table 12. Phases Y and Z, Chemical Analyses[1]

	Phase Y			Phase Z			
				Sill 1			Sill 2
	cm[2]	qmg	gmg	UZ	MZ		cm
					lmg	umg	
	185	475	474	202	136	142	622
	Major Elements (weight per cent)						
SiO_2	52.00	51.30	51.90	44.30	46.90	50.40	48.60
Al_2O_3	13.81	15.15	12.94	7.92	15.46	13.94	14.56
Fe_2O_3	3.13	2.78	2.98	1.99	1.73	1.80	2.23
FeO	10.88	12.52	11.60	9.74	8.52	9.64	9.28
FeO*[3]	13.70	15.02	14.28	11.53	10.08	11.26	11.29
MgO	4.90	4.18	5.60	20.75	11.90	7.50	8.50
CaO	8.73	4.97	8.28	7.46	10.50	10.20	11.53
Na_2O	2.68	3.82	2.85	0.04	1.07	2.39	1.58
K_2O	0.14	0.10	0.14	0.01	0.10	0.33	0.04
TiO_2	1.46	1.63	0.99	0.40	0.34	0.67	0.64
P_2O_5	0.29	0.23	0.20	0.04	0.09	0.14	0.13
MnO	0.23	0.23	0.23	0.17	0.19	0.23	0.22
CO_2	0.16	0.31	0.18	0.13	0.22	0.15	0.29
H_2O	1.36	2.50	1.68	6.38	3.46	2.18	1.85
S	0.022	0.211	0.159	0.006	0.107	0.025	0.009
total	99.77	99.87	99.73	99.40	100.01	99.60	99.46
	Trace Elements (ppm)						
Co	53	52	61	52	78	66	70
Cu	15	106	163	20	85	33	10
Ni	51	58	70	740	320	94	174
Pb	nd[4]	nd	nd	nd	12	4	nd
Rb	5	<10	3	10	<10	13	2
Zn	118	119	84	71	68	74	77

[1] Modal analyses in Tables 7 and 8; sample locations on Fig. 2 and 3.

[2] Abbreviations: cm - chilled margin; qmg - quartz-bearing metagabbro; gmg - granophyric metabbro; UZ - Ultramafic Zone; MZ - Mafic Zone; lmg - lower metagabbro member; umg - upper metagabbro member.

[3] Total Fe as FeO

[4] Not detected

[5] Analyses minus CO_2, H_2O, and S recalculated to 100 per cent.

Table 12 (continued). Phases Y and Z, Chemical Analyses, Volatile-free.[5]

	Phase Y			Phase Z			
				Sill 1			Sill 2
	cm^2	qmg	gmg	UZ	MZ		cm
					lmg	umg	
	185	475	474	202	136	142	622
Major Elements (weight per cent)							
SiO_2	52.93	52.97	53.12	47.73	48.74	51.83	49.94
Al_2O_3	14.06	15.64	13.24	8.53	15.46	14.34	14.96
Fe_2O_3	3.19	2.87	3.05	2.14	1.80	1.85	2.29
FeO	11.07	12.93	9.54	10.49	8.85	9.64	9.54
FeO*	13.94	15.51	14.62	12.42	10.47	11.58	11.60
MgO	4.99	4.32	5.73	22.36	12.37	7.71	8.73
CaO	8.89	5.13	8.47	8.04	10.91	10.20	11.85
Na_2O	2.73	3.94	2.92	0.04	1.11	2.46	1.62
K_2O	0.14	0.10	0.14	0.01	0.10	0.34	0.04
TiO_2	1.49	1.68	1.01	0.43	0.35	0.69	0.66
P_2O_5	0.30	0.24	0.20	0.04	0.09	0.14	0.13
MnO	0.23	0.18	0.23	0.18	0.20	0.24	0.23
Volatile-free Barth-Niggli Norms							
Quartz	6.93	4.03	4.90			0.54	0.64
Orthoclase	0.87	0.62	0.87	0.06	0.61	2.02	0.25
Albite	25.15	36.17	26.79	0.38	9.92	22.23	14.71
Anorthite	26.39	24.42	23.15	22.49	36.68	27.29	33.73
Diopside	6.81		7.30	10.43	9.72	11.85	12.92
Hedenbergite	6.72		7.50	2.48	3.50	7.50	6.86
Enstatite	10.74	12.17	12.54	33.60	21.71	15.52	17.88
Ferrosilite	10.60	16.30	12.89	7.98	7.81	9.83	9.50
Forsterite				16.03	5.52		
Fayalite				3.81	1.98		
Magnetite	3.24	3.07	2.73	2.09	1.87	1.95	2.32
Ilmenite	2.13	2.40	1.44	0.59	0.49	0.97	0.93
Apatite	0.64	0.51	0.44	0.09	0.20	0.30	0.28
Corundum		0.32					

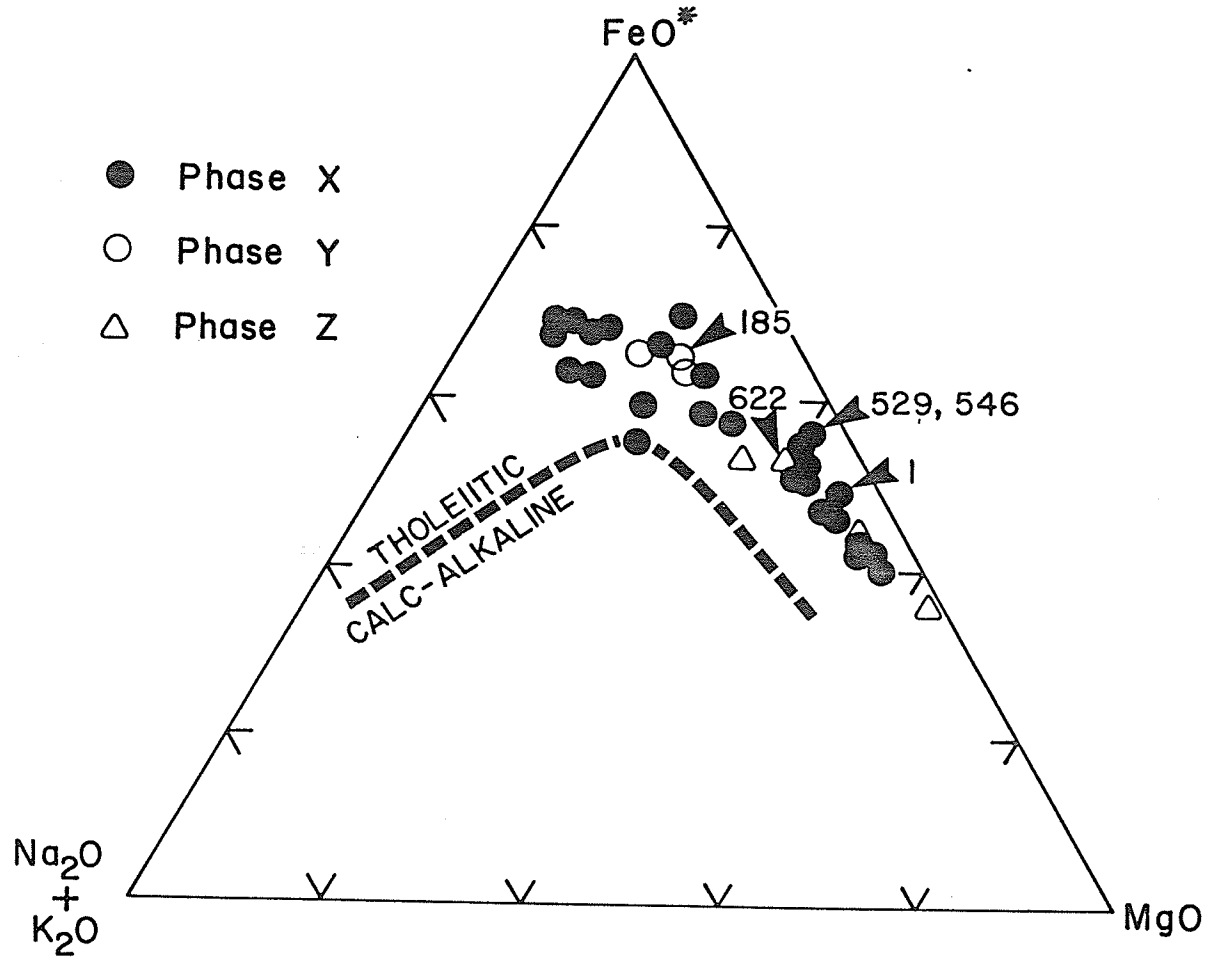

Fig. 20. $(Na_2O + K_2O)$ - FeO* - MgO diagram of sill complex rocks. Dashed line is boundary between tholeiitic and calc-alkaline fields (Irvine and Baragar, 1971). Arrows point to chilled margin compositions. FeO* is all Fe as FeO (weight per cent).

flows (formation J) that may have been only slightly older than the sill complex. The country rocks were probably saturated with sea water or open to sea water ingress, and the sill complex may have been altered by interaction with this sea water. The presence of an abundant external fluid phase during and after emplacement is suggested by several factors: (1) the presence of brecciated, very fine-grained, apparently chilled metagabbro (phreatic breccias) in marginal parts of phases X and Z that may have formed by interaction of hot magma with cold, water-saturated sedimentary rocks during emplacement, (2) filling of interstices in these breccias by abundant and pervasive carbonate and silica, possibly by circulation of hydrothermal fluids (cf. Andrews, 1977), (3) soft-sediment deformation in sandstone adjacent to phases Y and Z, suggesting that the sandstone was unlithified and therefore a probable source of water during emplacement, and (4) complete replacement of cumulus olivine in phase X by calcite pseudomorphs accompanied by minor actinolite, chlorite, and iron-titanium oxides, an alteration characteristic of some sea water interaction with basalts (Andrews, 1977).

It is not possible to assess in detail the extent and nature of original submarine alteration because these assemblages have been re-equilibrated by later burial and regional metamorphism. Alteration is evidenced mainly by scatter in the plotted chemical data. However, low-pressure burial and petrographically similar higher-pressure regional metamorphism might be distinguished by crystal chemical data. Because of the relatively sluggish nature of regional metamorphic reactions at low temperatures, particularly in the absence of an abundant fluid phase, low-pressure assemblages may have

been preserved.

The pressure of metamorphism, and therefore the approximate depth, can be estimated from the amount of crossite component in Ca-amphibole (Brown, 1977). The amphibole composition depends on the reaction (Brown, 1974):

Ca-amphibole + iron oxide + albite + chlorite + H_2O ($\pm$ stilpnomelane, quartz)
= crossite + epidote + ($\pm$ muscovite, quartz)

The reaction between crossite and Ca-amphibole is continuous in the greenschist facies with the two amphiboles being mixed as a single solid solution. Therefore, Ca-amphibole that coexists with albite + iron oxide + chlorite should have a fixed amount of Na-amphibole in solution at any given pressure and temperature. The amount of crossite component can be estimated by the amount of sodium in the M4 site.

Forty-two amphibole grains from the sill complex were analysed on the electron microprobe (Table 13). Pressure of formation of the amphiboles was tentatively estimated from a plot of sodium in M4 (NaM4) versus tetrahedral aluminum (Al^{iv}) (Fig. 21). Precautions in the interpretation of these data are discussed by Brown (1977). Sill complex amphiboles plot in the same general field as amphiboles from the low-pressure Hidaka belt, Japan (Grapes, 1975), Sierra batholith contact aureoles (Compton, 1958; Hietanen, 1974), and Oman ophiolite dike complex (Brown, 1977). The estimated pressure of formation is less than 3 kb, and probably less than 2 kb, because the rocks that give the higher estimate are more recrystallized and thus probably more equilibrated to regional metamorphic conditions. This implies that the present metamorphic mineral

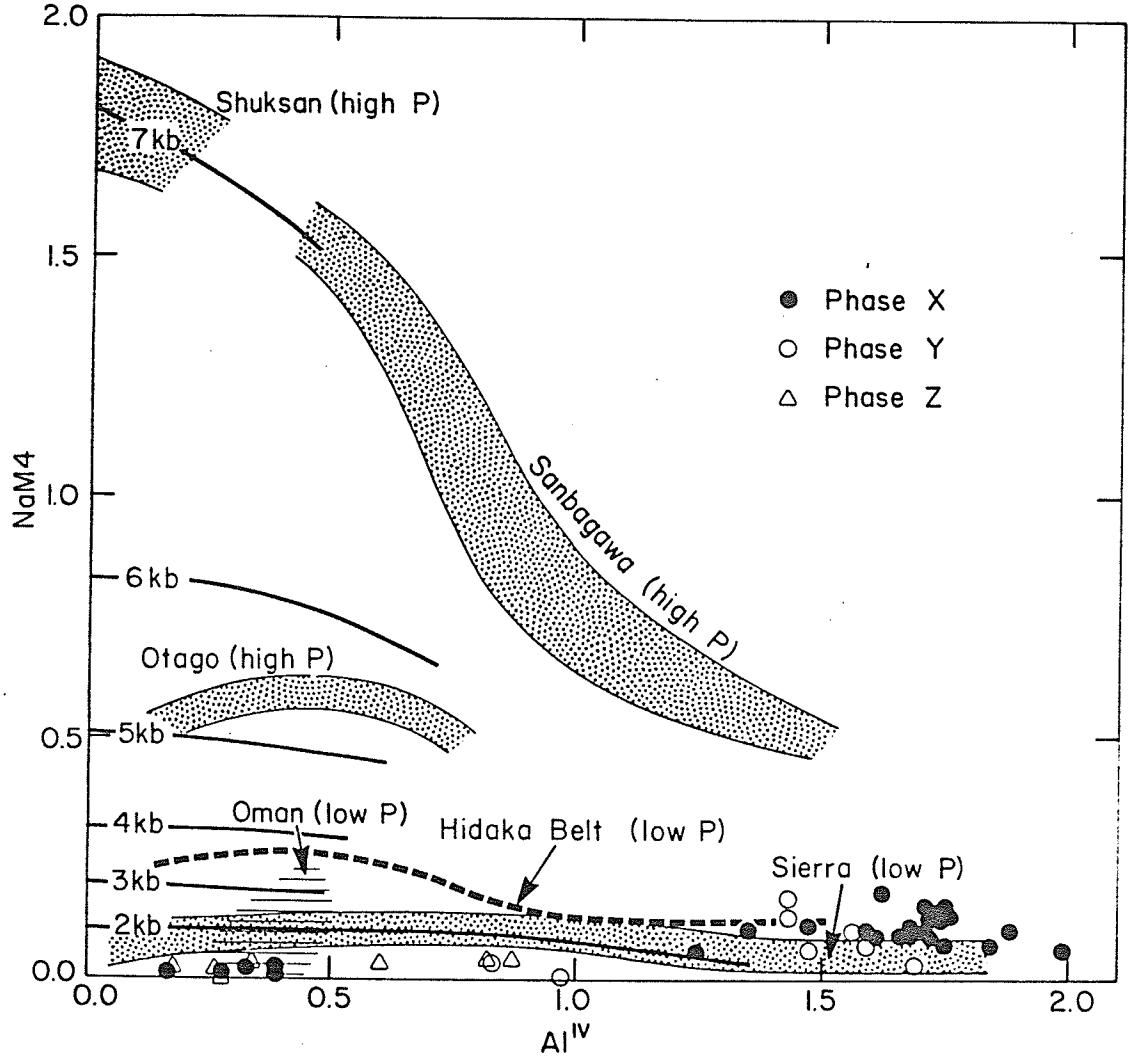

Fig. 21. Al^{iv} versus NaM4 diagram (Brown, 1977) showing estimated relationship between pressure of metamorphism and NaM4. Amphibole formulas were calculated with Fe_2O_3 midway between maximum possible Fe_2O_3 and minimum Fe_2O_3 (Papike et al., 1974). Amphibole analyses are listed in Table 13. Data for Shuksan from Misch (1959, 1966) and Brown (1974); Sanbagawa from Banno (1964); Otago from Brown (1977) and Hutton (1940); Sierra batholith contact aureoles from Compton (1958), Klein (1968) and Hietanen (1974); Hidaka belt from Grapes (1975); and Oman ophiolite dike complex from Brown (1977).

Table 13. Amphibole Analyses[1], Metagabbro Sill Complex.

		Phase X																				
		666-1	666-2	666-3	666-4	666-5	666-6	666-7	729-1	729-2	729-3	729-4	732-1	732-2	732-3	650-1	650-2	650-3	445-1	445-2	445-3	445-4	445-5
SiO_2		41.16	41.25	40.96	41.54	40.93	40.24	40.72	41.26	41.11	42.62	41.00	41.96	41.65	41.45	42.40	42.19	44.08	40.03	41.33	45.68	43.64	42.28
Al_2O_3		13.70	14.52	15.31	14.07	14.65	16.21	15.32	14.80	14.83	11.88	14.26	13.60	13.45	14.25	13.07	13.23	11.49	17.13	16.06	10.58	14.51	15.07
TiO_2		0.36	0.30	0.24	0.21	0.20	0.28	0.24	0.22	0.22	0.19	0.14	0.23	0.33	0.32	0.34	0.24	0.30	0.21	0.29	0.28	0.31	0.34
FeO		26.09	24.99	25.38	26.09	25.85	26.12	25.95	25.24	25.71	24.83	25.76	21.72	21.34	22.16	23.53	23.58	22.11	22.04	21.96	20.32	21.65	21.95
MnO		0.10	0.12	0.13	0.13	0.15	0.12	0.17	0.10	0.07	0.12	0.15	0.15	0.08	0.15	0.13	0.10	0.11	0.24	0.24	0.30	0.20	0.23
MgO		4.17	3.76	3.33	3.86	3.50	3.04	3.23	4.21	4.01	5.26	3.88	7.49	7.08	6.40	5.84	5.73	6.96	5.35	5.76	8.42	7.39	6.35
CaO		11.07	11.04	10.80	9.76	11.05	11.17	10.71	10.94	10.62	10.91	11.16	10.62	11.06	10.82	11.25	11.19	11.18	11.66	11.68	11.90	11.82	11.74
Na_2O		1.46	1.42	1.56	1.26	1.49	1.51	1.61	1.79	1.67	1.56	1.59	1.78	1.66	1.90	1.54	1.46	1.39	1.61	1.48	1.07	1.03	1.38
K_2O		0.33	0.30	0.28	0.36	0.32	0.32	0.30	0.26	0.27	0.22	0.37	0.20	0.21	0.20	0.26	0.29	0.21	0.29	0.32	0.21	0.26	0.33
Cr_2O_3		0.01	0.00	0.00	0.00	0.00	0.03	0.01	0.00	0.00	0.00	0.00	0.00	0.00	0.00	0.00	0.02	0.01	0.00	0.00	0.04	0.04	0.00
total		98.45	97.70	97.99	97.28	98.14	99.04	98.26	98.82	98.45	97.59	98.31	97.75	96.86	97.65	98.36	98.03	97.84	98.56	99.12	98.81	100.85	99.67
Tet.	Si	6.29	6.34	6.28	6.38	6.28	6.12	6.24	6.26	6.25	6.53	6.28	6.29	6.32	6.27	6.41	6.39	6.65	6.01	6.16	6.76	6.32	6.25
	Al	1.71	1.66	1.72	1.62	1.72	1.88	1.76	1.74	1.75	1.47	1.72	1.71	1.68	1.73	1.59	1.61	1.35	1.99	1.84	1.24	1.68	1.75
	total	8.00	8.00	8.00	8.00	8.00	8.00	8.00	8.00	8.00	8.00	8.00	8.00	8.00	8.00	8.00	8.00	8.00	8.00	8.00	8.00	8.00	8.00
Oct. M_{1-3}	Ti+Cr	0.04	0.03	0.03	0.02	0.02	0.03	0.03	0.03	0.03	0.02	0.02	0.03	0.04	0.04	0.04	0.03	0.03	0.02	0.03	0.03	0.03	0.04
	Al	0.75	0.96	1.04	0.93	0.93	1.02	1.00	0.91	0.91	0.68	0.86	0.69	0.73	0.81	0.74	0.76	0.69	1.04	0.98	0.61	0.80	0.88
	Fe^{3+}	0.58	0.35	0.36	0.57	0.44	0.48	0.43	0.44	0.53	0.47	0.47	0.72	0.55	0.51	0.47	0.50	0.36	0.51	0.47	0.34	0.45	0.48
	Fe^{2+}	2.75	2.86	2.90	2.78	2.88	2.84	2.89	2.77	2.74	2.72	2.84	2.00	2.16	2.29	2.51	2.49	2.43	2.25	2.29	2.18	1.97	2.24
	Mg	0.95	0.86	0.76	0.88	0.80	0.69	0.74	0.95	0.91	1.20	0.89	1.67	1.60	1.44	1.32	1.29	1.56	1.20	1.28	1.86	1.60	1.40
	Mn	0.01	0.02	0.02	0.02	0.02	0.02	0.02	0.01	0.01	0.02	0.02	0.02	0.01	0.02	0.02	0.01	0.01	0.03	0.03	0.04	0.02	0.03
	total	5.09	5.09	5.10	5.21	5.09	5.08	5.11	5.10	5.13	5.10	5.08	5.14	5.09	5.11	5.08	5.09	5.09	5.06	5.06	5.05	5.08	5.06
M_4	Ca	1.81	1.82	1.77	1.61	1.82	1.82	1.76	1.78	1.72	1.79	1.83	1.71	1.80	1.75	1.82	1.82	1.81	1.88	1.87	1.89	1.83	1.86
	Na	0.10	0.09	0.13	0.18	0.09	0.10	0.13	0.12	0.15	0.11	0.09	0.15	0.11	0.14	0.10	0.09	0.10	0.06	0.07	0.06	0.09	0.07
	total	2.00	2.00	2.00	2.00	2.00	2.00	2.00	2.00	2.00	2.00	2.00	2.00	2.00	2.00	2.00	2.00	2.00	2.00	2.00	2.00	2.00	2.00
A	Na	0.33	0.33	0.34	0.20	0.34	0.35	0.35	0.41	0.34	0.35	0.38	0.37	0.38	0.42	0.36	0.34	0.30	0.41	0.36	0.25	0.20	0.32
	K	0.06	0.06	0.05	0.07	0.06	0.06	0.06	0.05	0.05	0.04	0.07	0.04	0.04	0.04	0.05	0.06	0.04	0.06	0.06	0.04	0.05	0.06
	total	0.39	0.39	0.39	0.26	0.40	0.41	0.41	0.46	0.39	0.39	0.45	0.41	0.42	0.46	0.41	0.41	0.34	0.47	0.42	0.29	0.25	0.38

Table 13 (continued). Amphibole Analyses, Metagabbro Sill Complex

		Phase X					Phase Y								Phase Z						
		788-1	788-2	788-3	788-4	788-5	474-1	474-2	474-3	474-4	474-5	475-1	475-2	475-3	136-1	136-2	136-3	136-4	142-1	142-2	142-3
SiO_2		52.79	54.27	54.43	55.96	53.98	43.47	42.79	47.61	48.84	42.54	44.05	43.11	43.75	54.19	54.54	54.04	55.08	49.28	49.98	50.68
Al_2O_3		2.50	2.99	2.80	2.28	2.22	12.35	14.42	8.01	7.22	14.55	11.24	12.47	11.38	2.62	3.06	3.72	2.61	7.54	7.69	5.50
TiO_2		0.02	0.04	0.11	0.04	0.04	0.27	0.12	0.29	0.22	0.24	0.18	0.23	0.23	0.08	0.12	0.06	0.04	0.15	0.10	0.25
FeO		11.93	12.19	12.29	11.72	11.84	20.35	20.40	18.59	18.26	20.69	21.26	21.12	21.25	9.79	9.84	10.57	10.06	15.60	14.94	14.46
MnO		0.08	0.08	0.07	0.08	0.08	0.28	0.31	0.24	0.21	0.22	0.21	0.23	0.18	0.16	0.11	0.18	0.22	0.20	0.22	0.25
MgO		16.20	16.71	16.74	16.73	16.57	7.65	6.75	9.83	10.43	7.00	8.43	7.93	8.22	17.42	17.27	16.49	16.86	12.27	12.72	13.16
CaO		13.03	12.80	12.33	12.46	12.50	11.66	11.64	12.96	12.17	12.26	11.02	11.22	10.43	12.68	12.49	12.63	12.51	12.43	12.44	12.41
Na_2O		0.14	0.14	0.12	0.04	0.12	1.09	1.39	0.00	0.69	1.47	1.01	1.37	1.39	0.03	0.09	0.15	0.09	0.56	0.42	0.42
K_2O		0.04	0.02	0.04	0.01	0.04	0.29	0.16	0.19	0.16	0.19	0.12	0.13	0.13	0.05	0.04	0.05	0.04	0.17	0.13	0.09
Cr_2O_3		0.15	0.10	0.06	0.06	0.11	0.00	0.00	0.00	0.04	0.00	0.00	0.02	0.00	0.00	0.00	0.00	0.00	0.31	0.00	0.00
total		97.73	99.24	98.93	99.32	97.39	97.72	98.20	99.21	98.24	99.21	97.52	97.83	96.96	97.02	97.56	97.89	97.51	98.51	98.64	97.22
Tet.	Si	7.71	7.61	7.67	7.83	7.72	6.53	6.41	7.03	7.19	6.31	6.57	6.44	6.57	7.72	7.73	7.66	7.82	7.13	7.18	7.40
	Al	0.39	0.39	0.33	0.17	0.28	1.47	1.59	0.97	0.81	1.69	1.43	1.56	1.43	0.28	0.27	0.34	0.18	0.87	0.82	0.60
	total	8.00	8.00	8.00	8.00	8.00	8.00	8.00	8.00	8.00	8.00	8.00	8.00	8.00	8.00	8.00	8.00	8.00	8.00	8.00	8.00
Oct. M_{1-3}	Ti+Cr	0.02	0.02	0.02	0.01	0.02	0.03	0.01	0.03	0.03	0.03	0.02	0.03	0.03	0.01	0.01	0.01	0.00	0.05	0.01	0.03
	Al	0.04	0.11	0.13	0.21	0.09	0.72	0.95	0.43	0.64	0.86	0.54	0.63	0.59	0.16	0.24	0.29	0.25	0.42	0.48	0.34
	Fe^{3+}	0.28	0.26	0.16	0.00	0.16	0.44	0.33	0.44	0.17	0.37	0.79	0.67	0.70	0.09	0.01	0.04	0.00	0.26	0.26	0.13
	Fe^{2+}	1.16	1.18	1.29	1.37	1.26	2.11	2.23	1.86	2.08	2.19	1.86	1.97	1.97	1.08	1.15	1.21	1.19	1.62	1.53	1.63
	Mg	3.48	3.49	3.51	3.49	3.53	1.71	1.51	2.16	2.29	1.55	1.87	1.77	1.84	3.70	3.65	3.49	3.57	2.65	2.72	2.86
	Mn	0.01	0.01	0.01	0.01	0.01	0.04	0.04	0.03	0.03	0.03	0.03	0.03	0.02	0.02	0.01	0.02	0.03	0.02	0.03	0.03
	total	4.99	5.06	5.12	5.09	5.07	5.06	5.06	4.95	5.04	5.02	5.11	5.10	5.15	5.06	5.08	5.05	5.04	5.03	5.04	5.03
M_4	Ca	2.01	1.92	1.86	1.87	1.92	1.88	1.87	2.05	1.92	1.95	1.76	1.80	1.68	1.94	1.90	1.92	1.90	1.93	1.92	1.94
	Na	0.00	0.02	0.02	0.01	0.01	0.06	0.07	0.00	0.04	0.03	0.13	0.10	0.17	0.00	0.02	0.03	0.02	0.04	0.04	0.03
	total	2.01	2.00	2.00	1.97	2.00	2.00	2.00	2.05	2.00	2.00	2.00	2.00	2.00	2.00	2.00	2.00	1.97	2.00	2.00	2.00
A	Na	0.04	0.02	0.02	0.00	0.02	0.26	0.33	0.00	0.15	0.39	0.16	0.29	0.23	0.01	0.00	0.01	0.00	0.12	0.08	0.09
	K	0.01	0.00	0.01	0.00	0.01	0.06	0.03	0.04	0.03	0.04	0.02	0.02	0.02	0.01	0.01	0.01	0.01	0.03	0.02	0.02
	total	0.05	0.02	0.03	0.00	0.03	0.32	0.36	0.04	0.18	0.43	0.18	0.31	0.25	0.02	0.01	0.02	0.01	0.15	0.10	0.11

[1] Amphibole formulas calculated according to Papike et al., (1974).

assemblage was either formed during low-pressure burial metamorphism, or that the regional metamorphism occurred at low pressures and at burial depths of less than 9 km. Considering the high thermal gradients in the Early Precambrian and the unstable downsinking and intrusion by granitic batholiths of greenstone belts, regional metamorphism to greenschist facies was reached at relatively shallow depths of 7 to 8 km (Ayres, 1978). Since this corresponds to the depth based on amphibole composition, the amphiboles probably formed during the regional metamorphism, but may be petrographically and crystal-chemically similar to those formed by prior burial metamorphism.

Phase X, Unit 1

General Relations

Of the 19 analyses in Table 11, 18 are plotted against height in Figure 22. One of the analyses (sample 445) is omitted from the plot because its stratigraphic position cannot be accurately extrapolated to the type section AA'. In section AA', granophyric metagabbro occurs as irregular pods in the lower third of the upper metagabbro member, however, it was plotted as a separate unit at the top of the upper metagabbro so that trends in this member would not be distorted.

The interpretation of chemical variations with height is hampered for five reasons: (1) secondary mineral assemblages obscure primary cryptic variation, (2) the rocks are largely cumulates containing variable proportions of cumulus minerals and pore material,

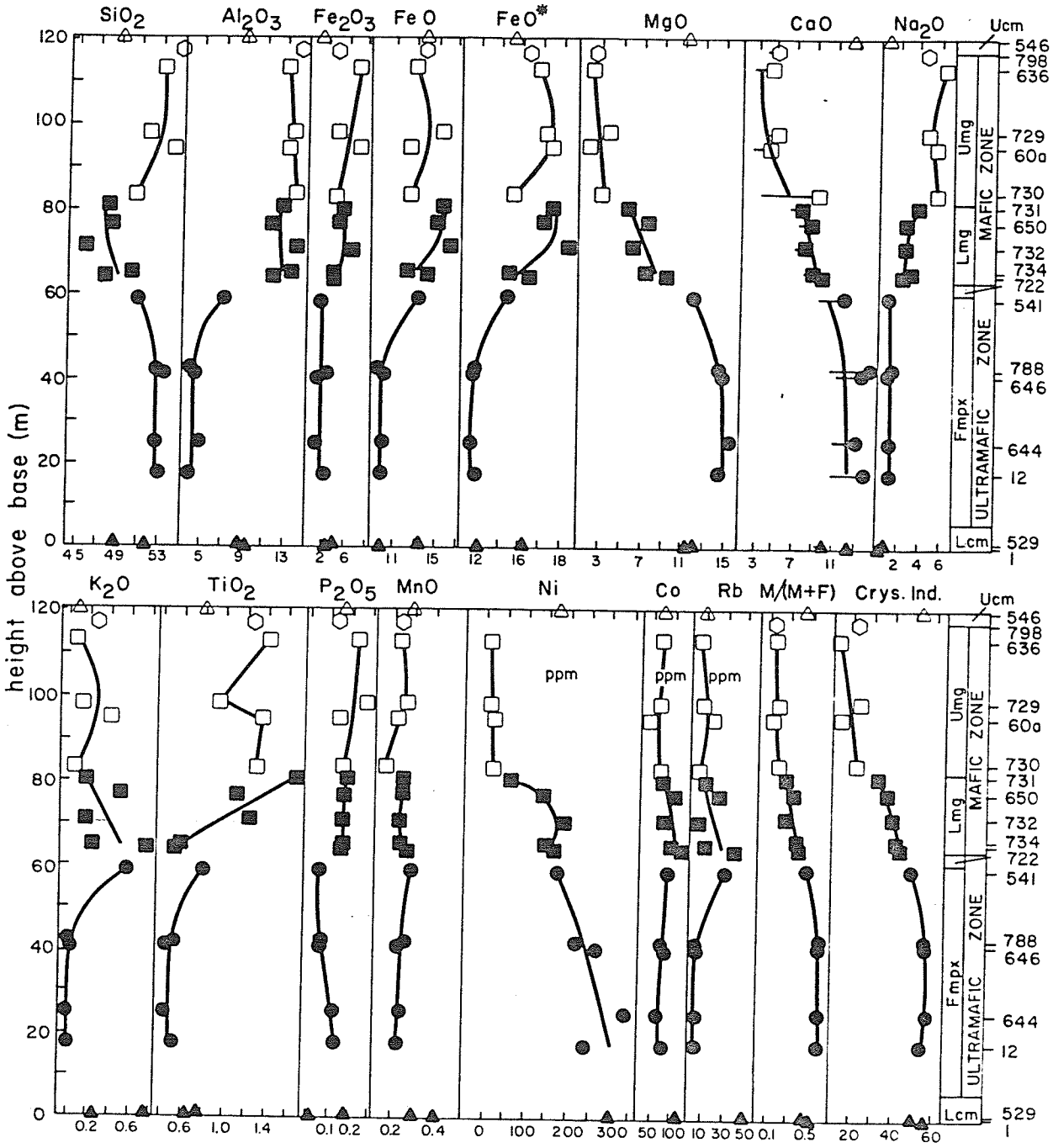

Fig. 22. Variation in major and trace element abundances with stratigraphic height through unit 1 of phase X along section AA'. See text for explanation of granophyric metagabbro (798) sample position. Volatile-free compositions (Table 10) were used. Horizontal lines on CaO data show position of plotted points if CaO in calcite is removed. Abbreviations: Lcm - lower chilled margin member, Fmpx - feldspathic metapyroxenite member, Mpx - metapyroxenite member, Lmg - lower metagabbro member, Umg - upper metagabbro member, Ucm - upper chilled margin member, M/(M+F) - MgO/(MgO+FeO), Crys. Ind. - crystallization index.

(3) although samples were chosen to represent average rocks, the total sample population is small, (4) the variable development of mafic zone members in unit 1 suggests that the unit was not a closed system during differentiation with material being added and/or subtracted after initial emplacement, and (5) the high volatile contents, especially CO_2, indicate some metasomatism which may have affected other elements.

In order to compensate for the small number of samples and to offset the effect of local compositional variation, smooth curves were drawn by inspection for most of the data in Figure 22. The average composition of a cumulate, therefore, at any desired level in the unit, may be read directly from the graph.

High CO_2 contents in most samples reflect abundant modal calcite. This creates problems in the interpretation of element trends, particularly for CaO, because the CaO in calcite may have been added from outside the system, or it might have been derived from alteration of primary Ca-bearing minerals in the sample. If the CaO is added from outside the system then CaO in calcite should be subtracted from the analysis to derive the primary CaO. If the CaO is part of the rock, then no adjustment is necessary. The source of the CaO is unknown but on Figure 22 both corrected and uncorrected CaO values are shown. The true CaO value probably lies between these values and the CaO trend is drawn to average these results.

To properly evaluate post-emplacement differentiation processes, the composition of the continually changing residual liquids must be known. This information is not directly available from rock compositions but can be calculated from average rock compositions

if weighted volumes of individual members are known. In addition, changing liquid compositions and amounts can be inferred from the behaviour of some incompatible elements that are enriched preferentially in liquids. For elements enriched preferentially in crystals relative to liquid, trends in Figure 22 broadly indicate their changing behavior.

Composition of the Chilled Magma

Three chilled samples collected within 1 m of the contact probably represent the quenched magma at the time of intrusion (Table 11) but all samples have suffered some metasomatism. Samples 1 and 546 were rejected because they have secondary quartz and carbonate, and a higher degree of metamorphic recrystallization than sample 529. Sample 529, has abnormally high K_2O which is reflected by the presence of 5.7 per cent biotite, and some of the K_2O may have been derived from the adjacent biotite-rich sandstone. Sample 546, which is adjacent to relatively non-reactive metachert probably has a primary K_2O value. If K_2O in sample 529 is adjusted to the value in sample 546 (0.10 per cent), the composition of sample 529 is probably the best estimate of chilled magma composition (sample L1, Table 14). This choice is supported by the absence of major phenocryst phases in this sample although sparse pyroxene phenocrysts were present. In addition, the similarity of the MgO/(MgO + FeO) ratio in the lower and upper chilled zones suggests that the lower chilled margin does not contain abundant early Mg-rich cumulus phases. Higher Ni content in the base, however, suggests the presence of at least some cumulus olivine.

Feldspathic Metapyroxenite Member

Chemical variation with height (Fig. 22) is remarkably smooth despite the fact that the section comprises samples from several different locations. Except for Ni, smooth curves representing average rock compositions can be closely fitted to the data by inspection. Except for some scatter in the Ni data, the chemistry is relatively constant in the lower and central part of the member, but at the top, Al_2O_3, FeO*, TiO_2, Rb, K_2O, MgO/(MgO + FeO), and crystallization index increase and SiO_2, MgO, and CaO decrease. Na_2O is relatively constant throughout, MnO and Co increase gradually, and P_2O_5 decreases gradually with height. These trends suggest that marked differentiation occurred only in the upper part. Furthermore, the petrographic similarity of all samples implies that much of the compositional changes may be due to cryptic variation in pyroxene. However, the data are conflicting and do not indicate any clear-cut processes. For example, the increase in Al_2O_3 does not agree with the relatively constant abundance of plagioclase, or with the Na_2O, CaO or K_2O trends. These inconsistencies may reflect alteration.

If magmas contain more than 50 to 60 per cent crystals, the crystals begin to touch and weld (Jackson, 1971). The feldspathic metapyroxenite averages 80 to 85 per cent cumulus pyroxene and much of this must reflect postcumulus enlargement. P_2O_5 is almost entirely enriched in liquid relative to crystals and is, therefore, a measure of differentiation and of the amount of pore material. Since P_2O_5 decreases with height in spite of increasing differentia-

tion, the amount of pore material must have decreased upwards because of an increasing amount of adcumulus pyroxene growth (Wager and Brown, 1968).

The relatively low degree of scatter in the data and the fact that primary textures are generally well preserved suggest either that the feldspathic metapyroxenite samples represent primary compositions, or that uniform chemical alteration affected all samples. The generally high CO_2 (1.92 to 3.29 per cent) implies that uniform alteration has occurred. This is supported by the inconsistencies between some of the observed chemical trends and model differentiation trends.

Lower Metagabbro Member

Considerable scatter is present in data from the lower metagabbro (Fig. 22). Relatively smooth variation with height is shown by CaO, Na_2O, P_2O_5, MnO, MgO/(MgO + FeO) ratio, and crystallization index. SiO_2, Al_2O_3, and K_2O show wide scatter; data for the other elements are also scattered but general trends are apparent. The appearance of cumulus plagioclase and apatite are responsible for the abrupt increases in Al_2O_3, Na_2O, and P_2O_5. The increase in FeO* and TiO_2 upward reflect the concentration of iron-titanium oxides in the upper part of the member.

The destruction of primary textures by recrystallization in most samples suggests that the scatter could reflect secondary alteration. Such alteration is indicated by the high normative olivine content of all samples. Modal olivine is absent and high

normative olivine content could reflect depletion of SiO_2 or enrichment of alkalies or CaO.

The recrystallization is particularly intense in the lowermost sample which contains high CO_2 and H_2O, and abundant modal biotite and chlorite (cf. Tables 4 and 11, sample 722). In addition, the underlying metapyroxenite member and the uppermost part of the feldspathic metapyroxenite member are also strongly altered and are rich in secondary biotite, chlorite, H_2O, and CO_2.

In spite of the apparently strong alteration, both MgO/(MgO + FeO) ratio and crystallization index are a smooth continuation of the differentiation trend in the feldspathic metapyroxenite member. This suggests that cumulus processes in the lower metagabbro are an extension of those operating in the ultramafic zone.

Upper Metagabbro Member

For many oxides there is considerable scatter in the data and only general trends can be defined. The scatter is best documented by the differences between the two samples in the center of the member which are stratigraphically close together (Fig. 22). These differences must be due to either alteration or local compositional variations. Local compositional variation is the most probable reason because the two samples differ modally and sample 60a was extrapolated to the type section. SiO_2, Na_2O, P_2O_5, and MnO increase upwards; Al_2O_3, MgO, CaO, Ni, MgO/(MgO + FeO), and crystallization index decrease; and Rb and Co are relatively constant. K_2O, TiO_2, and FeO* show much scatter and lack coherent trends.

All samples contain normative olivine (Table 11) and sample 730 contains normative nepheline, minerals that are not present in the samples. The occurrence of these minerals in the norm could reflect depletion of SiO_2 or enrichment of alkalies or CaO during alteration.

There is no evidence that crystallization trends were reversed near the top of the upper metagabbro by cold roof rocks. With the exception of the upper chilled margin, differentiation apparently increased upwards throughout the exposed section. The chemical trends generally reflect continuation of lower metagabbro variation as cumulus plagioclase, iron-titanium oxides, and apatite increase in abundance. Ni is almost totally depleted.

Granophyric Metagabbro Member

Only one sample of granophyric metagabbro was analysed (Table 11). Although it normally occurs in the lower third of the upper metagabbro, it is plotted in Figure 22 as the highest sample in the type section because its position in the unit is variable, and it is probably the closest approach to the final liquid composition in unit 1.

The occurrence of granophyric metagabbro pods in the lower third of the upper metagabbro in section AA' is puzzling because they probably recrystallized <u>in situ</u>, suggesting that the chemical trends above this level should be reversed. This does not occur and the granophyric metagabbro pods could represent only local developments of advanced differentiation. To the north (Fig. 3), however,

granophyric metagabbro forms the upper part of the mafic zone and probably represents the culmination of differentiation.

Units 2, 3 and 4

Only seven samples were analysed from these units (Table 11); unit 5 was not sampled because of abundant carbonate enrichment and strong fabric deformation. Comparison with unit 1 shows that these units are generally similar in composition to stratigraphic equivalents in unit 1. A notable exception is Al_2O_3 in the ultramafic zones which averages only 4.86 per cent (volatile-free) in unit 1, but 7.17 in units 2, 3, and 4. This reflects higher intercumulus plagioclase content.

Phase Y

Three samples were analysed from this phase (Table 12). A sample of chilled tholeiitic basalt collected 1 m from the contact of a 65 m thick sill represents the original magma. The other two samples are granophyric metagabbro and quartz-bearing metabaggro from opposite sides of another sill about 75 m thick. Although there are considerable modal differences, chemical variations are small (Fig. 20).

Phase Y chilled magma is more differentiated than the chilled margin of phase X. It is higher in SiO_2, Al_2O_3, Na_2O, K_2O, TiO_2, and P_2O_5; lower in FeO*, MgO, CaO, and MnO, and shows more iron enrichment (Fig. 20).

Phase Z

Four samples were analysed from this phase (Table 12). The composition of the original magma is not known because the chilled margins are either unexposed or visibly altered. Chilled sample 622 (Table 12) is about 2 m from the top of sill 2, but is slightly differentiated and transitional in composition to the mafic zone. However, it is probably the closest approach to original magma composition. It is slightly more differentiated than phase X chilled magma, being higher in SiO_2, Al_2O_3, and total alkalies and Na_2O, but lower in MgO and slightly more iron enriched (Fig. 20).

DIFFERENTIATION

Introduction

Fractional crystallization was the major mechanism of differentiation in the sill complex. In phases X and Z, this involved sinking of early formed crystals and armouring of the crystals by successive layers of crystallizing material during cooling (zoning) thereby preventing reaction of early-formed parts of crystals with coexisting liquid. In phase Y, the major process was probably zoning. Some filter differentiation with crystals being separated from the melt by sieving (Propach, 1976) may also have occurred but cannot be evaluated.

In order to trace the course of differentiation, the following must be known (Mueller and Saxena, 1977): (1) composition of the original magma including intratelluric phases and volatile content, (2) compositions and proportions of minerals separating from the magma, (3) position of appearance and disappearance of each mineral, (4) nature of residual liquids and volatiles in the differentiation sequence, and (5) temperature and total pressure at each stage of crystallization.

These parameters can be documented in varying detail for unit 1 of phase X but are essentially unknown for the other units and phases of the sill complex. For unit 1, the composition of the original magma can be estimated from the chilled margin (sample L1, Table 14). Proportions of crystallizing phases and positions of appearance and disappearance can be estimated from modal variations

Table 14. Average Member and Calculated Liquid Compositions — Unit 1, Phase X

	average member compositions						calculated liquids				
	uz	lmg	umg	gmg	lcm	ucm	bc	L1	L2	L3	L4
SiO_2	52.69	48.12	52.52	55.01	50.67	49.64	51.81	49.35	51.93	51.13	52.69
Al_2O_3	4.86	12.86	13.51	14.15	9.30	9.02	9.02	9.09	9.00	13.32	13.55
Fe_2O_3	1.65	2.59	2.81	3.06	2.29	1.45	2.17	2.99	2.18	2.74	2.81
FeO	10.56	15.54	14.64	13.57	12.11	13.89	12.70	13.70	12.70	14.91	14.58
MgO	14.34	7.31	2.82	2.42	11.96	11.30	9.61	12.33	9.44	4.33	2.79
CaO	13.49	8.65	6.07	5.09	11.12	12.35	10.37	10.31	10.27	6.90	6.00
Na_2O	1.36	3.13	5.77	4.82	0.84	0.97	2.90	0.85	3.06	4.83	5.71
K_2O	0.12	0.36	0.17	0.27	0.52	0.10	0.19	0.10	0.18	0.24	0.18
TiO_2	0.54	1.03	1.25	1.26	0.72	0.81	0.84	0.79	0.85	1.18	1.25
P_2O_5	0.11	0.17	0.20	0.14	0.11	0.17	0.15	0.19	0.15	0.19	0.20
MnO	0.25	0.25	0.24	0.25	0.36	0.29	0.25	0.31	0.25	0.24	0.25
total	100.0	100.0	100.0	100.0	100.0	100.0	100.0	100.0	100.0	100.0	100.0
density	3.03	3.06	2.90	2.98	3.07	3.06					
wt. %[1]	47.2	15.4	27.9	2.0	5.0	2.5					

explanation (see text for method of liquid calculation)

uz - average ultramafic zone, samples 12, 644, 646, 788, 541

lmg - average lower metagabbro member, samples 722, 734, 732, 650, 731

umg - average upper metagabbro member, samples 730, 729, 636, 60a

gmg - granophyric metagabbro member, sample 798

lcm - average lower chilled margin member, samples 529, 1

ucm - upper chilled margin member, sample 546

bc - bulk composition

[1]wt. % - weight per cent members, based on relative volume and density

of pseudomorphs, but the compositions of these phases are unknown. In closed systems, successive liquids produced during fractionation can be calculated from volumetric proportions and densities of members. Because the sill complex is a high level intrusion, pressures would have been low and cooling rates moderate to fast. Other parameters are unknown.

Phase X - Unit 1

Calculated Liquids and Bulk Composition

The chilled margin composition (L1, Table 14), which represents the initial liquid is known directly. Other liquid compositions and bulk composition must be calculated from chemical and stratigraphic data (Tables 3 and 11) with the following assumptions:

(1) The mafic and ultramafic zones of unit 1 are cumulates, crystallized in a static magma chamber (closed system). In closed systems, the calculated bulk composition is the same as the chilled margin composition. If magma has been added or subtracted these compositions will be different.

(2) The thickness of each member in the type section AA' is proportional to its volume in the unit. Unknown variations in member thickness and volume both in the third dimension and laterally would produce errors in member weighting. In most closed-system layered intrusions, zones and members are relatively uniform in thickness throughout (e.g. Wager and Brown, 1968). The irregular stratigraphy in unit 1 (Fig. 2 and 3) thus suggests open-system behavior, i.e. addition and subtraction of magma. However, the type section AA'

is probably a relic of the primary layering because members are well developed, uniform in thickness and continuous, and preserves, at least partly, the original stratigraphy.

(3) The average composition of each member is the mean of the analysed samples (Table 14).

(4) The average density of each member is the mean of the measured densities of the analysed samples. Densities are lower than original densities because of the replacement of primary mafic minerals by less dense, hydrous phases. This difference is probably greater in the ultramafic rocks than for gabbroic members, but a density difference of 0.1 gcm^{-3} in feldspathic metapyroxenite produces only 1.8 per cent difference in member weighting.

(5) The average composition of the ultramafic zone is based only on analyses of the feldspathic metapyroxenite member because analyses of the metapyroxenite are not available, but the volume of the ultramafic zone is the sum of the volumes of both members.

The bulk composition (bc), and three liquid compositions (L2, L3, L4) (Table 14) were calculated. Component oxides of the liquids (e.g. ox_{L2}) were calculated from oxides (e.g. ox_{uz}) of average rocks (Table 14) according to the equations (see Table 14 for abbreviations):

$$ox_{bc} = (47.2\ ox_{uz} + 15.4\ ox_{lmg} + 27.9\ ox_{umg} + 2.0\ ox_{gmg} + 5.0\ ox_{lcm} + 2.5\ ox_{ucm})\ /\ 100$$

$$ox_{L2} = \frac{47.2\ ox_{uz} + 15.4\ ox_{lmg} + 27.9\ ox_{umg}\ 2.0\ ox_{gmg}}{47.2 + 15.4 + 27.9 + 2.0}$$

$$ox_{L3} = \frac{15.4\ ox_{lmg} + 27.9\ ox_{umg} + 2.0\ ox_{gmg}}{15.4 + 27.9 + 2.0}$$

$$ox_{L4} = \frac{27.9\ ox_{umg} + 2.0\ ox_{gmg}}{27.9 + 2.0}$$

where coefficients of ox are weight percentages of members (Table 14). These are the liquids remaining after the crystallization of the border zone (L2), the ultramafic zone (L3), and the lower metagabbro member (L4).

The most significant result of these calculations is the large difference between chilled margin and bulk compositions (L1 and bc, Table 14). If the system was closed, these two compositions should be the same. The differences are too large to be caused entirely by alteration. The chilled margin would be the most susceptible to alteration because of its very fine grain size and proximity to country rocks, but as previously shown, it is probably close to primary composition. Differences between L2 and L1 compositions, especially the lower MgO/FeO ratio in L2 suggest that the border zone was differentiated during crystallization.

Thus the differences between chilled magma and bulk composition mean that this unit was probably an open system during crystallization, and that the calculated liquids do not represent accurately the composition changes with time in the differentiating magma. However, the proximity of the calculated liquid trends to rock trends on the (Na_2O+K_2O) - FeO* - MgO diagram (Fig. 23) suggests that the calculated liquids are probably close to the actual liquid compositions at comparable differentiation stages, at least with respect to alkali, FeO*, and MgO variation. The general validity of this relationship was observed by Hess (1960). The composition of the granophyric metagabbro, except for SiO_2, is close to L4, the

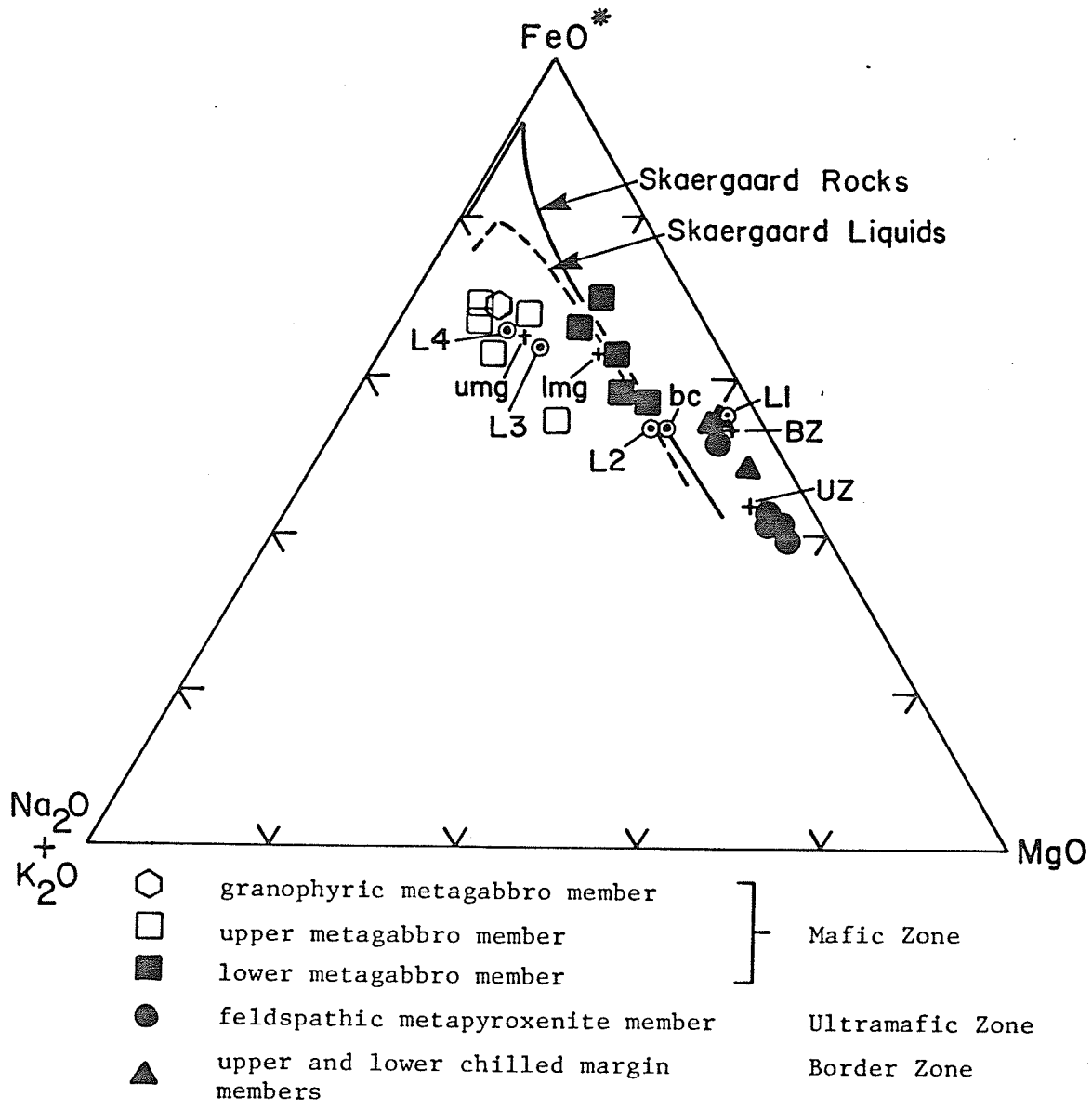

Fig. 23. $(Na_2O + K_2O)$ - FeO* - MgO diagram showing rock, average rock, and calculated liquid compositions of unit 1, phase X. Skaergaard rocks and liquids (Wager and Brown, 1968) are shown for comparison. Abbreviations: Ll to L4 - calculated liquids, Table 14; umg, lmg, UZ (+) - average rocks, Table 14; bc - bulk composition, Table 14; BZ - average border zone (average of lcm and ucm, Table 14).

liquid formed after crystallization of the lower metagabbro member. This indicates that the difference between the final fractionation phase (granophyric metagabbro) and upper metagabbro is largely textural, rather than chemical, except for more abundant SiO_2 in the granophyric metagabbro.

Iron Enrichment

The calculated liquids show the typical iron-enrichment trend of tholeiitic magmas with the liquids having more alkali enrichment than the rock units crystallizing from the liquids (Fig. 23). Compared to Skaergaard trends, unit 1 has less iron enrichment and lacks the strong alkali enrichment in the final stages of fractionation (Fig. 23). Average rock compositions lag behind the liquid compositions, reflecting the enrichment of the successive liquids in iron.

Crystallization Sequence

The observed cumulus crystallization sequence as inferred from metamorphic pseudomorphs is olivine (ol), clinopyroxene (cpx), plagioclase (pl) which produced cpx-ol, cpx, cpx-pl, and pl cumulates. Fe-Ti oxides are not considered here because their occurrence as primary phase could not always be confirmed. The olivine - clinopyroxene order is not clear but according to Irvine (1970), the order clinopyroxene - olivine has not been documented from intrusions or volcanic series. Indeed, he states that under normal conditions magmas of appropriate composition precipitate clinopyroxene before olivine do not exist, at least in the orthopyroxene-normative range. Orthopyroxene was not observed in unit 1 but may have been destroyed by metamorphism.

As an aid to understanding crystallization paths in layered intrusions, a tetrahedral phase model based on the system olivine-clinopyroxene-plagioclase-silica was constructed by Irvine (1970). The liquidus boundaries were based on melting relations of average basaltic rocks at one atmosphere pressure. Unit 1 liquids and rocks were plotted in the tetrahedron by projecting them from the olivine apex to the intermediate join clinopyroxene-plagioclase-orthopyroxene (Fig. 24). The most notable features of this plot are the large scatter of mafic zone rocks, large difference between bulk composition and chilled magma composition, and the lack of any coherent trends in calculated liquids. Rocks from the feldspathic metapyroxenite member, however, form a relatively tight group.

Under ideal conditions of fractional crystallization, eighteen

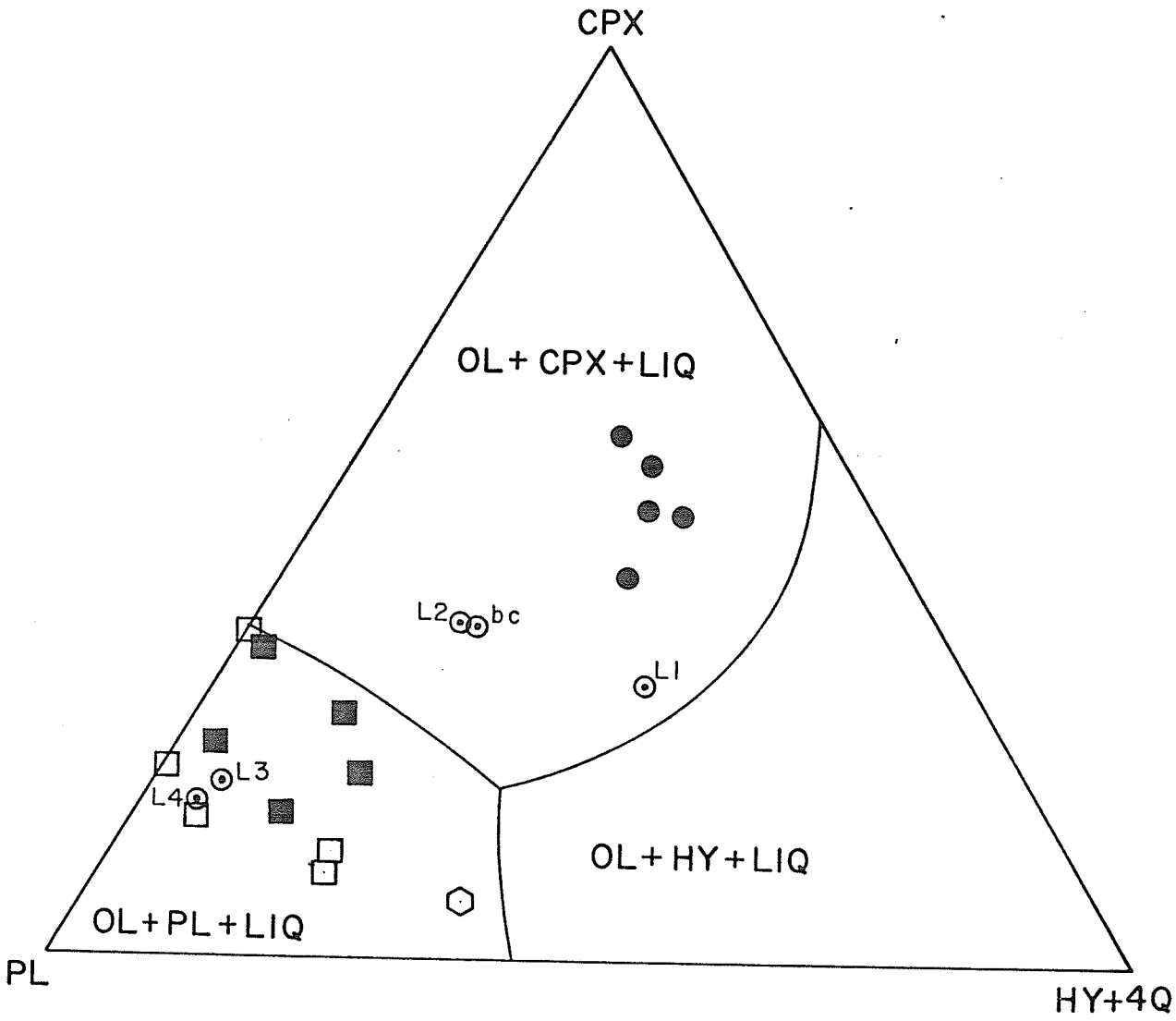

Fig. 24. Olivine (OL) projection (cation equivalents) in tetrahedral system olivine-clinopyroxene-plagioclase-silica, after Irvine (1970). Unit 1, phase X rocks and calculated liquids were plotted by projecting from the olivine apex. Norms were not adjusted to exclude Fe_2O_3, TiO_2, and P_2O_5. See text for explanation of liquidus boundaries. Symbols are the same as for Fig. 23. PL = normative plagioclase; CPX = normative clinopyroxene; HY = normative orthopyroxene; Q = normative quartz; LIQ = liquid.

different crystallization sequences are theoretically possible from the same starting composition in the tetrahedron, each producing particular sequences of cumulates (Irvine, 1970). In this system, the observed sequence of cumulates in unit 1 can be obtained only from a starting composition near or left of the five-phase point in Figure 24, with cotectic crystallization of olivine and clinopyroxene, and of olivine and plagioclase, and later reaction of olivine to form orthopyroxene. This crystallization sequence is unlikely because the starting composition (L1) is not in the correct place, and orthopyroxene should be produced late in the sequence; no evidence of orthopyroxene was observed.

From the chilled magma composition, ideal fractional crystallization could produce the ultramafic zone cumulates, but successive liquids and mafic zone rocks could not have formed without changing the composition or physical conditions of the system. Thus unit 1 cumulates were apparently formed by a complex sequence of events involving additions and/or deletions of magma in an open system and probably involving reversals in crystallization order, and reaction among phases.

These conclusions, however, are not unequivocal because the phase boundaries in the model were constructed for average, generally Phanerozoic basaltic rocks. Crystallization conditions may have been different in the early Precambrian sill complex, especially with respect to vapour phase composition.

MODE OF EMPLACEMENT

Introduction

The sill complex was intruded along and immediately above the contact between cycles 2 and 3, an important break in the volcanism of the Favourable Lake complex. Cycle 2 represents the end of a mafic, largely subaqueous edifice-building stage that was terminated by the subaerial development of a caldera filled by felsic to intermediate flows and pyroclastic rocks of formation H and fluvial and lacustrine sedimentary rocks of formation I (Ayres, 1977; Buck, 1978). Cycle 3 was initiated by renewed mafic volcanism that expanded the volcanic complex northwestwards. The caldera was then apparently submerged and was buried by mafic flows of formation J and intercalated clastic sedimentary rocks of the upper part of formation I (Ayres, 1977). The sill complex intruded formation J and the upper part of formation I and appears to be restricted to the area immediately above the caldera. Stratigraphy above the sill complex is poorly known because formation J is truncated by the Setting Net Lake fault (Fig. 2).

The stratigraphy prior to intrusion of the sill complex was approximated by subtracting sill complex rocks (Fig. 25). This reconstruction does not give accurate pre-intrusion relationships because strain induced during emplacement was not considered. The upper clastic unit of formation I was apparently deposited at the same time as mafic flows of formation J were erupted. They formed a north-sloping sequence that was probably bounded by the south wall

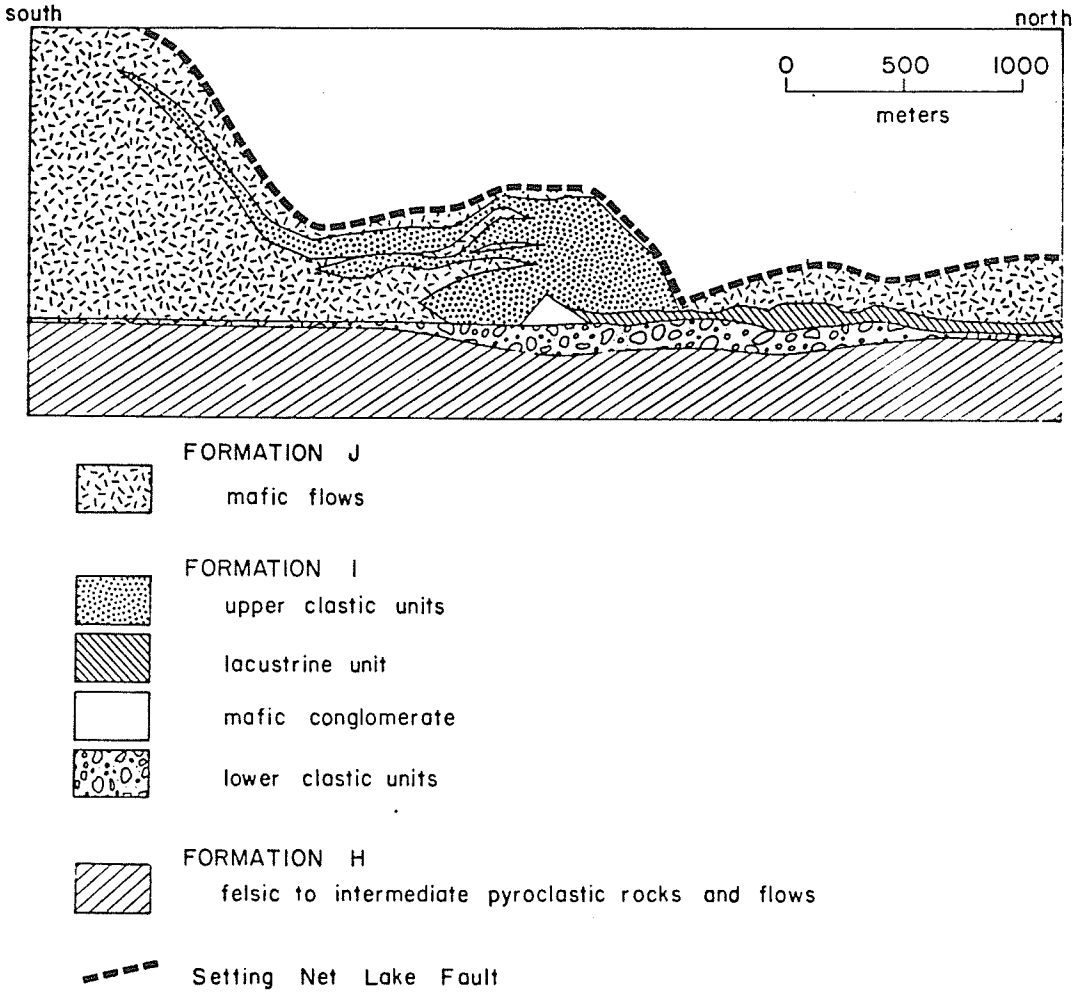

Fig. 25. Reconstruction of stratigraphy prior to intrusion of sill complex. No correction has been made for regional deformation.

of the caldera. The rather blunt terminations of the lower tongue of the upper clastic unit must reflect either the steep front of a flow sequence or north-south shortening.

The order of emplacement of the phases is poorly documented. Phase Z apparently truncated phase X and is, therefore, younger, but the contact is poorly exposed. Phase Y is not in contact with the other two phases.

Phase X

The emplacement model for phase X must satisfy the following constraints:

(1) Units are either in contact or are separated by thin septa of thinly-bedded metachert and fine-grained clastic rocks or trains of lenses of such rocks. Where units are in contact, there is no truncation; units do not intrude each other, nor are they separated by thick septa. Units were, therefore, emplaced at discrete stratigraphic levels with the upper units being younger than lower units, and emplacement was controlled by the nature of the host rock.

(2) Each of the five units is surrounded by a well developed chilled margin which could only form if the host materials were at temperatures of less than 300^{o}C (Jaeger, 1958). This implies that the preceding unit had cooled and partly crystallized prior to emplacement of the next unit.

(3) Cooling periods for each unit were sufficiently long for ultramafic cumulates to develop by crystal settling.

(4) Autoclastic monomictic breccia comprising angular fragments

identical in composition and in part, texture, to the chilled margins of units and cemented by carbonate occurs in the southern termination of phase X. It may represent intrusion of magma into water-saturated sedimentary rocks, forming a wedge of steam and magma (phreatic breccia) ahead of the sill (cf. Grapes et al., 1974).

Unit 1 was intruded into metachert and fine-grained clastic rocks of the lacustrine unit of formation I, splitting the sequence along or at low angles to bedding and lifting the upper half of the sedimentary sequence and overlying formation J to form a continuous roof. At the southern termination, the mafic conglomerate lens and associated sandstones of the upper clastic unit of formation I apparently acted as a barrier to the advance of magma and were deformed into their present shape by the advancing magma (cf. Fig. 25).

The sandstone and mafic conglomerate are wrapped around the termination of phase X apparently as a result of direct southward pushing by the magma. Sandstone for several hundred meters above the termination, has localized, extremely complex, outcrop scale folding and faulting that probably reflects a combination of uplift and a shear couple produced by emplacement of phase X. The small scale, complex nature of this deformation and the lack of associated axial planar mineral foliation consistent with east-west regional trends, suggests that emplacement of phase X and deformation occurred while the rocks were relatively soft and unlithified, and thus still water-saturated.

Emplacement of succeeding units, probably sequentially, occurred in the same way as unit 1 and caused more deformation of the southern sedimentary unit. Septa decrease in size and abundance upwards

because the available septum material was reduced markedly in thickness by the emplacement of each unit.

Phase Y

The internal structure of phase Y is poorly known, but its emplacement is constrained by the following points:

(1) It comprises numerous thin sills, some of which are transgressive. Individual sills are generally thinner than those in phases X and Z, resulting in faster cooling and lack of differentiation.

(2) Chilled margins against country rocks are generally well developed, but inter-sill contacts were not observed.

(3) The phase was emplaced into a sequence of interlayered mafic flows and sandstone that was probably largely unlithified and water saturated as evidenced by local, complex deformation northwest of Borthwick Lake and adjacent to some contacts (Fig. 13).

(4) Rare amygdules imply emplacement at shallow depth.

Emplacement of phase Y at slightly higher stratigraphic levels than phase X may have acted as part of a shear couple to further deform the sedimentary units between the phases (Fig. 2).

Phase Z

In phase Z, the thinner sills are fine-grained, subophitic to ophitic, and unfractionated, implying quick cooling. The thicker sills show some differentiation by crystal settling, but the predominance of subophitic and ophitic textures and fine-grained

marginal phases suggests relatively quick cooling also. The phase is partly discordant and its emplacement was not controlled by specific stratigraphic horizons as in phase X and to a lesser extent, in phase Y.

The unusual bulbous protuberances into intermediate metatuff at the base of sill 5 (Fig. 16) suggest that country rocks, at least at this locality, were still relatively unlithified and plastic during emplacement. This implies that phase Z was intruded shortly after the emplacement of the other phases. Monomictic breccias similar to phreatic autobreccias in phase X indicate that sills 1 and 5 probably came into contact with formational water in unlithified country rocks.

CONCLUSIONS

The sill complex is a broadly concordant multiple high-level intrusion comprising three distinct, multiple phases that differ in mode and degree of differentiation, and nature of emplacement. In spite of the small size, and restricted spatial and probably temporal association of these phases, some exhibit marked and complex differentiation.

Previously, this broad spectrum of composition and physical characteristics had not been generally recognized in early Precambrian mafic plutons of similar size. Such plutons are important because they are samples of magmas parent to associated lavas. Deciphering the inter-relationships among these plutons and their differentiation histories is an aid to the understanding of magmatic evolution in early Precambrian volcanic complexes.

Phase X, the largest, best exposed, and most complex of the three phases, comprises five units, generally separated by thin country-rock septa. Although primary mineralogy has been destroyed by metamorphism, primary igneous textures, predominantly cumulus, have been preserved by metamorphic pseudomorphs. Each unit is enveloped by a chilled border zone and is a discrete intrusive event; units were emplaced sequentially upwards and cooled sufficiently slowly to allow the formation of abundant mafic and ultramafic cumulates. Layered ultramafic cumulates are well developed in all units, but mafic cumulates are best developed in lower units. In the upper units, concordant intrusive phases apparently identical in composition to mafic cumulates locally predominate.

Layering of cumulus pyroxene and minor cumulus olivine is common throughout the ultramafic zone, but pyroxene layering is especially well developed near the top of the zone. Rip-up structures in pyroxene cumulates and orientation of anisotropic olivine crystals implies active magma flow during cooling. Units were open systems and magma was added and/or subtracted during cooling.

Interpretation of chemical data is hampered by alteration and metamorphism, and by the obvious open-system nature of units. The tholeiitic nature and marked iron-enrichment trend with differentiation, however, are preserved. The observed crystallization sequence of olivine, clinopyroxene, and plagioclase which produced clinopyroxene-olivine, clinopyroxene, clinopyroxene-plagioclase, and plagioclase cumulates cannot be duplicated theoretically in the system olivine-clinopyroxene-plagioclase-silica by ideal fractional crystallization, except for the ultramafic cumulates. Subsequent cumulates require the changing of the crystallizing magma composition by additions or deletions of magma in an open system, and probably involved reversals in crystallization order and reaction among phases. Such petrologic complexity is characteristic of subvolcanic conduits.

In phase Y, there was only minor differentiation because the sills were relatively thin and cooled quickly. The emplacement of numerous sills, however, implies a nearby active magma source. Limited crystal settling occurred in the thickest phase Z sills but these sills are mainly subophitic to ophitic and cooled relatively quickly with moderate differentiation.

Soft-sediment deformation adjacent to phases X and Y and to part of phase Z, indicates that the sill complex was emplaced when the country rocks were relatively unlithified, that is, shortly after their formation. This close temporal association of the sill complex with country rocks confirms the close association of the sill complex with contemporary volcanism.

REFERENCES

Andrews, A. J. 1977. Low temperature fluid alteration of oceanic layer 2 basalts, DSDP leg 37. Can. J. Earth Sci., 14, p. 911-926.

Ayres, L. D. 1970. Setting Net Lake area. Ontario Dept. Mines Prelim. Map P538.

Ayres, L. D. 1972. Northwind Lake. Ontario Dept. Mines N. Aff. Prelim. Map p. 756.

Ayres, L. D. 1974. Geology of the Trout Lakes area. Ontario Div. Mines, Geol. Rept. 113, 199 p.

Ayres, L. D. 1977. Importance of stratigraphy in early Precambrian volcanic terranes: cyclic volcanism at Setting Net Lake, northwestern Ontario. p. 243-264 in Baragar, W. R. A., Coleman, L. C., and Hall, J. M. (ed), Volcanic regimes in Canada. Geol. Assoc. Canada, Spec. Paper 16.

Ayres, L. D. 1978. Metamorphism in the Superior Province of northwestern Ontario and its relationship to crustal development. in Geol. Surv. Canada Paper 78-10, Metamorphism in the Canadian Shield.

Baker, I. and Haggerty, S. E. 1967. The alteration of olivine in basaltic and associated lavas. Part II: Intermediate and low temperature alteration. Contr. Mineral. Petrol., 16, p. 258-273.

Banno, S. 1964. Petrologic studies on Sanbagawa crystalline schists in the Bessi-Ino district, central Sikoku, Japan. J. Fac. Sci. Tokyo Univ., Sec. II, 15, p. 203-219.

Baragar, W. R. A., Plant, A. G., Pringle, G. J. and Schau, M., 1977. Petrology and alteration of selected units of mid-Atlantic

ridge basalts sample from sites 332 and 335, DSDP. Can. J. Earth Sci., 14, p. 837-874.

Bence, A. E. and Albee, A. L. 1968. Empirical correction factors for the electron microanalysis of silicates and oxides. J. Geol., 76, p. 382-403.

Brown, E. H. 1974. Comparison of the mineralogy and phase relations of blueschists from the north Cascades, Washington, and greenschists from Otago, New Zealand. Geol. Soc. Amer., Bull., 85, p. 333-344.

Brown, E. H. 1977. The crossite content of Ca-amphibole as a guide to pressure of metamorphism. J. Petrology, 18, p. 53-72.

Buck, P. S. 1978. A caldera sequence in the Early Precambrian, Favourable Lake volcanic complex, northwestern Ontario. Unpublished M.Sc. thesis, University of Manitoba.

Carmichael, I. S. E., Turner, F. J. and Verhoogen, J. 1974. Igneous petrology. McGraw-Hill, Inc., New York, 739 p.

Compton, R. R. 1958. Significance of amphibole parageneses in the Bidwell Bar region, California. Amer. Mineral, 43, p. 890-907.

Fawcett, J. J. 1965. Alteration products of olivine and pyroxene in basalt lavas from the Isle of Mull. Mineral. Mag., 35, p. 55-68.

Grapes, R. H. 1975. Actinolite-hornblende pairs in metamorphosed gabbros, Hidaka Mountains, Hokkaido. Contr. Mineral. Petrol., 49, p. 125-140.

Grapes, R. H., Reid, D. L. and McPherson, J. G. 1974. Shallow dolerite intrusion and phreatic eruption in the Alan Hills region, Antarctica. N. Z. J. Geol. and Geophys., 17, p. 563-577.

Hietanen, A. 1974. Amphibole pairs, epidote minerals, chlorite, and plagioclase in metamorphic rocks, northern Sierra, Nevada, California. Amer. Mineral, 59, p. 22-40.

Hess, H. H. 1960. Stillwater igneous complex. Geol. Soc. Amer., Mem., 80.

Hutton, C. O. 1940. Metamorphism in the Lake Wakatipu region, western Otago, New Zealand. N. Z. Dep. Sci. and Ind. Res. Mem., 5, 84 p.

Irvine, T. N. 1970. Crystallization sequences in the Muskox intrusion and other layered intrusions 1. Olivine-pyroxene-plagioclase relations. p. 441-476 in Bushveld igneous complex and other layered intrusions, Symposium, Geol. Soc. S. Africa Spec. Publ., 1.

Irvine, T. N. and Baragar, W. R. A. 1971. A guide to the chemical classification of the common volcanic rocks. Can. J. Earth Sci., 8, p. 523-548.

Irvine, T. N. and Ridler, R. H. 1972. Ultramafic and gabbroic bodies. p. 553-575 in Goodwin, A. M. et al., The Superior Province, p. 527-623 in Price, R. A. and Douglas, R. J. W. (ed.), Variations in tectonic styles in Canada. Geol. Assoc. Canada, Spec. Pap. 11.

Irvine, T. N. and Smith, C. H. 1967. The ultramafic rocks of the Muskox intrusion, Northwest Territories, Canada. p. 38-49 in Wyllie, P. J. (ed.), Ultramafic and related rocks, John Wiley and Sons, New York, 464 p.

Jackson, E. D. 1961. Primary textures and mineral associations in the ultramafic zone of the Stillwater complex, Montana. U. S. Geol. Surv., Prof. Pap., 358, 106 p.

Jackson, E. D. 1967. Ultramafic cumulates in the Stillwater, Great Dyke, and Bushveld intrusions, p. 20-38 in Wyllie, P. J. (ed.), Ultramafic and related rocks, John Wiley and Sons, New York, 464 p.

Jackson, E. D. 1971. The origin of ultramafic rocks by cumulus processes. Fortschr. Mineral., 48, p. 128-174.

Jacques, A. L. 1976. An Archean tholeiitic layered sill from Mt. Kilkenny, western Australia. Geol. Soc. Austral., J., 23, p. 157-168.

Jaeger, J. C. 1958. The solidification and cooling of intrusive sheets, p. 77-87 in Carey, S. W. (ed.) Dolerite - a symposium, Univ. of Tasmania.

Klein, C. Jr. 1968. Two-amphibole assemblages in the system actinolite-hornblende-glaucophane. Amer. Mineral., 54, p. 212-237.

MacRae, N. D. 1969. Ultramafic intrusions of the Abitibi area, Ontario. Can. J. Earth Sci., 6, p. 281-303.

Morse, S. A. 1969. The Kiglapait layered intrusion, Labrador. Geol. Soc. Amer., Mem., 112, 204 p.

Misch, P. 1959. Sodic amphiboles and metamorphic facies in Mount Shuksan belt, northern Cascades, Washington (abstr.). Geol. Soc. Amer., Bull., 70, p. 1736-1737.

Misch, P. 1966. Tectonic evolution of the northern Cascades of Washington State. Canadian Inst. Min. and Metall. Spec. Vol., 8, p. 101-148.

Mueller, R. F. and Saxena, S. K. 1977. Chemical Petrology. Springer-Verlag, New York, 394 p.

Naldrett, A. J. and Mason, G. D. 1968. Contrasting Archean ultramafic bodies in Dundonald and Clergue townships, Ontario. Can. J.

Earth Sci., 5, 111-143.

Papike, J. J., Cameron, K. L. and Baldwin, K. 1974. Amphiboles and pyroxenes: characterization of other than quadrilateral components and estimates of ferric iron from microprobe data. Geol. Soc. Amer. abstr. with programs, 6, p. 946-947.

Peterson, D. W. 1960. Descriptive modal classification of igneous rocks. Geotimes, 5, AGI Data Sheet 23, p. 30-34.

Pollard, D. D. 1973. Derivation and evaluation of a mechanical model for sheet intrusions. Tectonophys., 19, p. 233-269.

Propach, G. 1976. Models of filter differentiation. Lithos, 9, p. 203-209.

Raudsepp, M. 1975. Metagabbro Sill Complex, Favourable Lake area. Center Prec. Stud., 1974 Annual Report, p. 114-120.

Raudsepp, M. 1976. Differentiation in the metagabbro sill complex, Favourable Lake area, Ontario. Center Prec. Stud., 1975 Annual Report, p. 116-124.

Wager, L. R. 1967. Rhythmic and cryptic layering in mafic and ultramafic plutons, p. 445-482 in Hess, H. H. and Poldervaart, A. (ed.), Basalts, v. 2, Interscience, New York, 862 p.

Wager, L. R. and Brown, G. M. 1968. Layered igneous rocks. Oliver and Boyd, Ltd., Edinburgh, 588 p.

Wager, L. R. and Deer, W. A. 1939. The petrology of the Skaergaard intrusion, Kangerdlugssuaq, east Greenland. Medd. om Gronland, Bd., 105, Nr. 4, 335 p.

Wager, L. R., Brown, G. M. and Wadsworth, W. J. 1960. Types of igneous cumulates. J. Petrology, 1, p. 73-85.

Williams, D. A. C. 1971. Determination of primary mineralogy and textures in ultramafic rocks from Mount Monger, western Australia. Spec. Publ. Geol. Soc. Austr., 3, p. 259-268.

Williams, D. A. C. 1972. Archean ultramafic, mafic and associated rocks, Mt. Monger, western Australia. Geol. Soc. Austral., J., 10, p. 162-188.

Williams, D. A. C. and Hallberg, J. A. 1973. Archean layered intrusions of the eastern Goldfields region, western Australia. Contr. Mineral. Petrol., 38, p. 45-70.

Williams, H., Turner, F. J. and Gilbert, C. M. 1954. Petrography, W. H. Freeman and Co., San Francisco, 406 p.

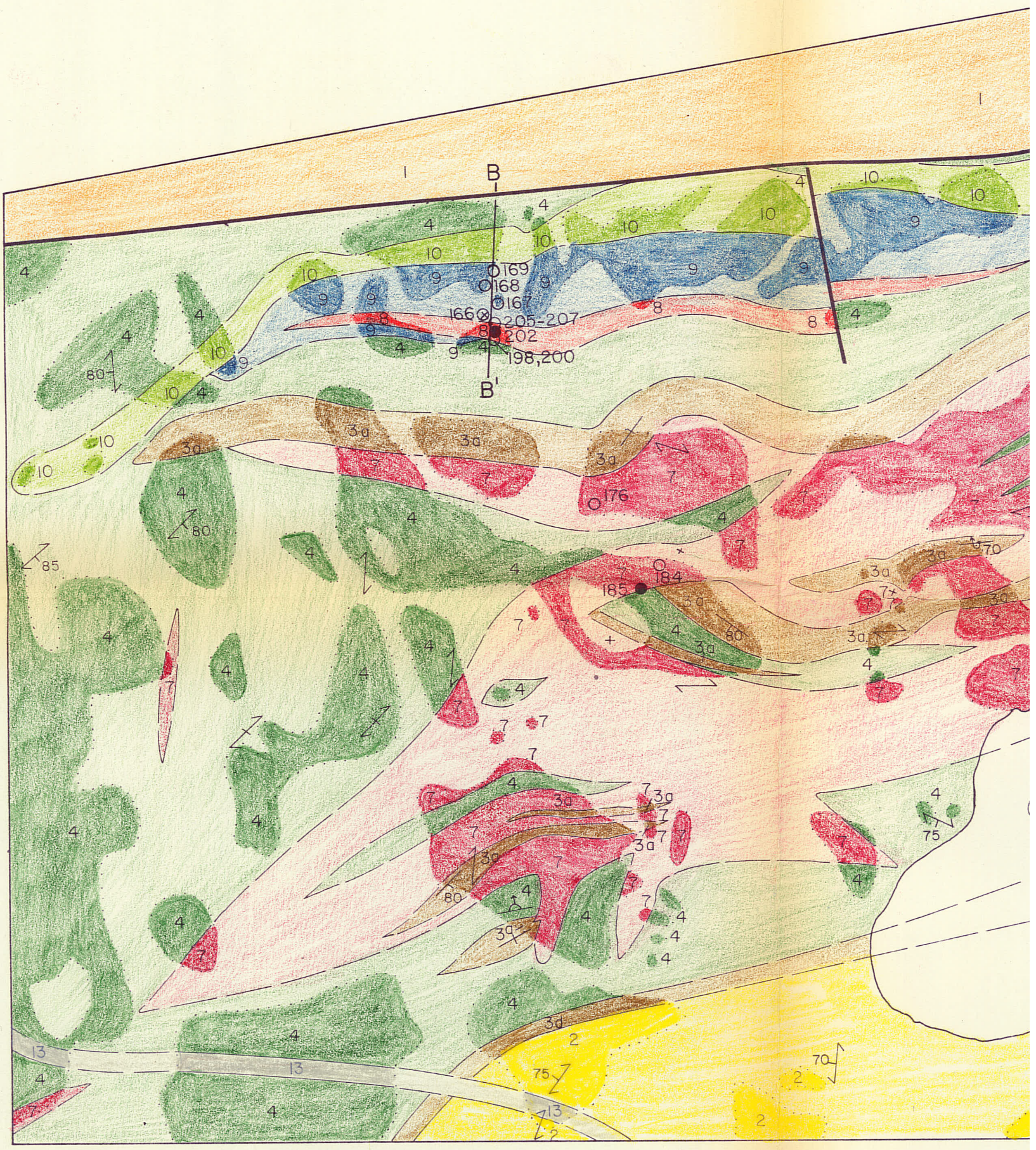

EARLY PRECAMBRIAN[a]

Diabase

13 — 13 Diabase

intrusive contact

Metamorphosed Ultramafic Intrusive Rocks[b]

12 — 12 Metapyroxenite, metaperidotite

intrusive contact

Metamorphosed Mafic to Ultramafic Intrusive Rocks[c]

Phase Z

Mafic Zone

Pegmatitic Metagabbro Member

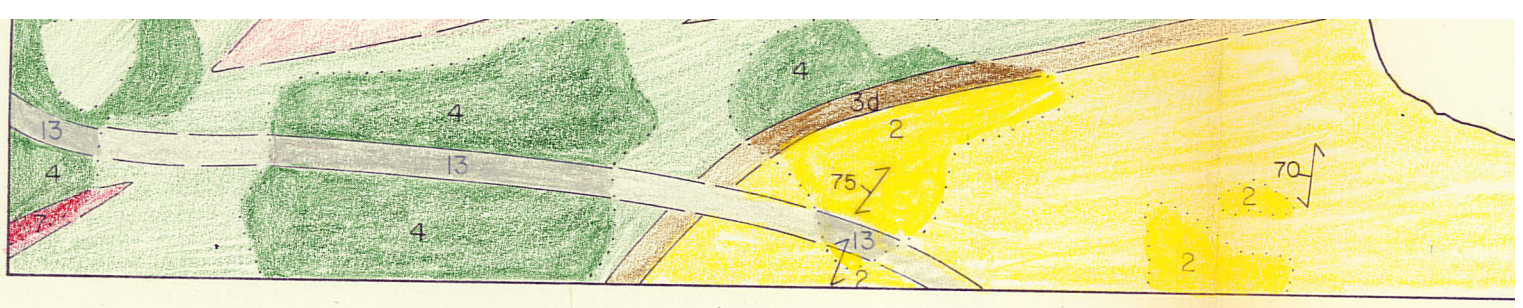

EARLY PRECAMBRIAN[a]

Diabase

13 — 13 Diabase

intrusive contact

Metamorphosed Ultramafic Intrusive Rocks[b]

12 — 12 Metapyroxenite, metaperidotite

intrusive contact

Metamorphosed Mafic to Ultramafic Intrusive Rocks[c]

SILL COMPLEX

Phase Z

Mafic Zone

Pegmatitic Metagabbro Member

11 — 11 Pegmatitic metagabbro

Upper Metagabbro Member[d]

10 — 10 Metagabbro, quartz-bearing metagabbro

Lower Metagabbro Member

9 — 9 Metagabbro

Ultramafic Zone

8 — 8 Metapyroxenite, metaperidotite

intrusive contact

Phase Y

7 — 7 Quartz-bearing metagabbro, metagabbro, q
granophyric metagabbro, rare quartz m

Phase X

Mafic Zones

6 — 6 Metagabbro, feldspathic metapyroxenite, q

Ultramafic Zones

5 — 5 Feldspathic metapyroxenite, metapyroxenit

Formation J Mafic Metavolcanic Rocks[e]

4 — 4 Unsubdivided massive and pillowed flows, l

Figure 2. General geology

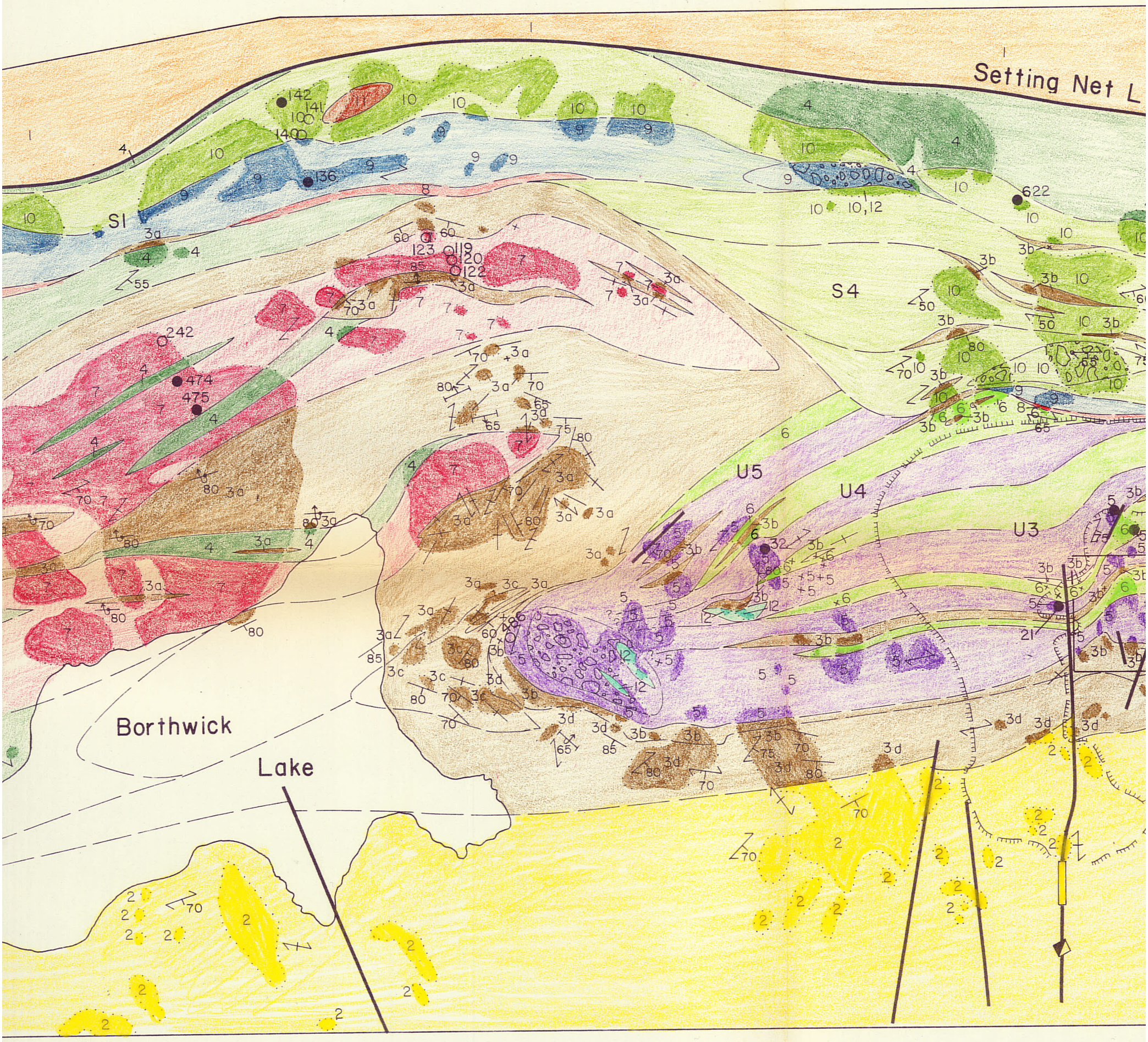

LEGEND

Formation I[e] Clastic and C

3 — 3a Upper clastic u metasiltstone

3b Lacustrine uni intermediate

3c Mafic metacon

3d Lower clastic

Formation H[e]

2 — 2 Felsic to inter

Unsubdivided formations[f]

1 — 1 Unsubdivided n

[a] Bedrock geology. Outc

LEGEND

Formation I^e Clastic and Chemi

3 — 3a Upper clastic units— metasiltstone, inte

3b Lacustrine unit— me intermediate to

3c Mafic metaconglome

3d Lower clastic units-

Formation H^e

2 — 2 Felsic to intermediat

Unsubdivided formations[f]

1 — 1 Unsubdivided metavo

[a] Bedrock geology. Outcrops and light tones of the same

[b] Age relations are uncertain.

[c] In part related to volcanism

[d] Members of the mafic zone

[e] Formation nomenclature after

[f] Both older and younger than intrusions and later granitic

rtz-bearing feldspathic metapyroxenite,
agabbro

rtz-bearing metagabbro, granophyric metagabbro

feldspathic metaperidotite

ally amygdaloidal

rock outcrop, are

geological boundar

70 bedding, top unkno

80 65 bedding, top (arro

lava flow, top (ar

70 schistosity, gneiss

fault

open stope, mine

32 chemically and m

O 176 modally analysed

brecciated area

mill tailings

S2 sill designation,

U2 unit designation,

80 80 bedding top (arro

A—A' cross section

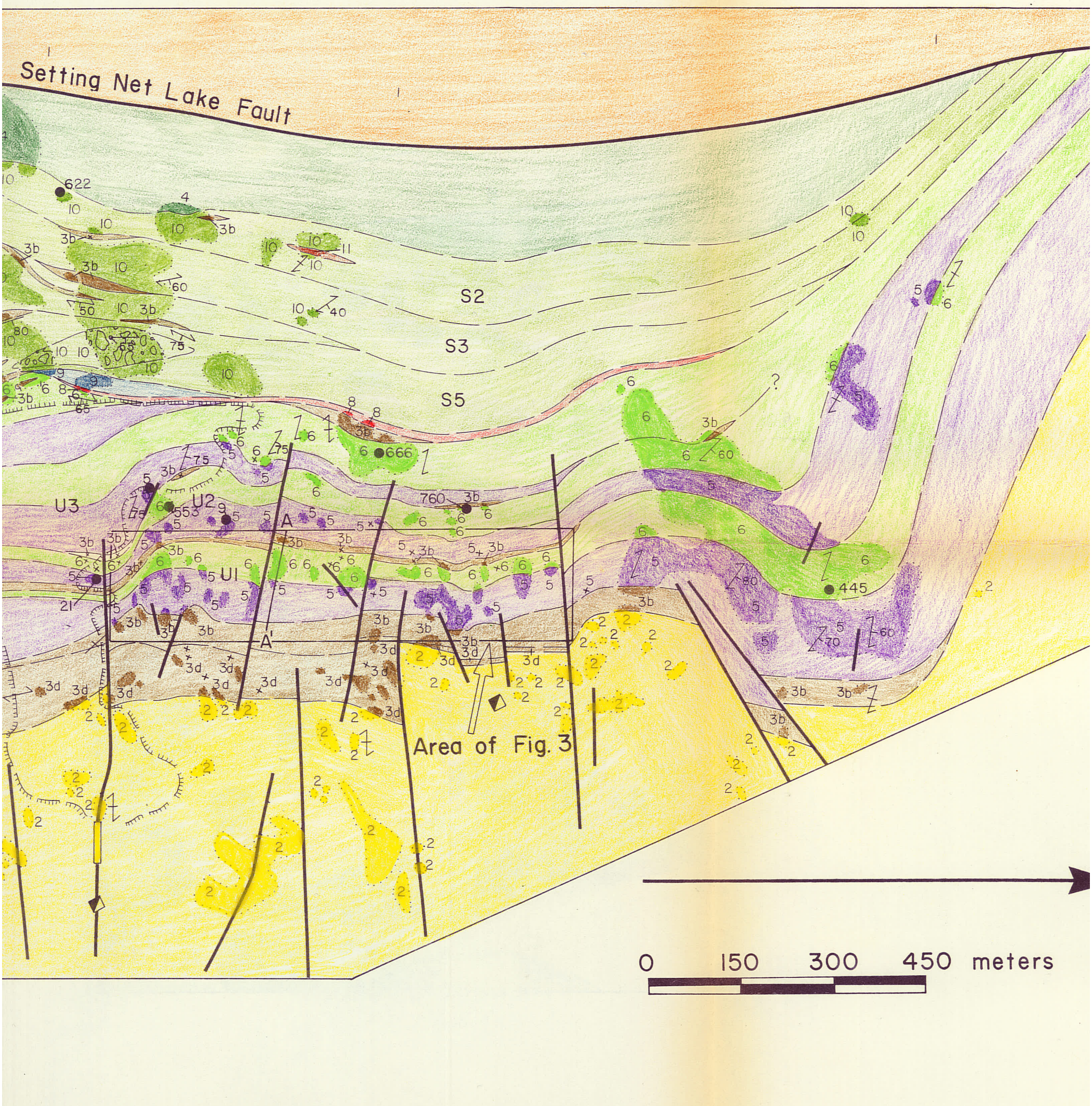

Clastic and Chemical Metasedimentary Rocks

Upper clastic units—immature metasandstone and conglomerate, minor ferruginous metache
metasiltstone, intermediate tuff, felsic tuff

Lacustrine unit—metasiltstone, fine metasandstone, ferruginous metachert, metachert, m
intermediate to mafic tuff and lapilli-tuff

Mafic metaconglomerate derived from formations J and H

Lower clastic units—immature metasandstone and conglomerate derived from formation
e

Felsic to intermediate pyroclastic rocks and flows deposited in caldera

formations[f]

Unsubdivided metavolcanic, metasedimentary, and granitic rocks

eology. Outcrops and inferred extensions of each rock unit are shown, respectively, i
tones of the same colour.
ions are uncertain.

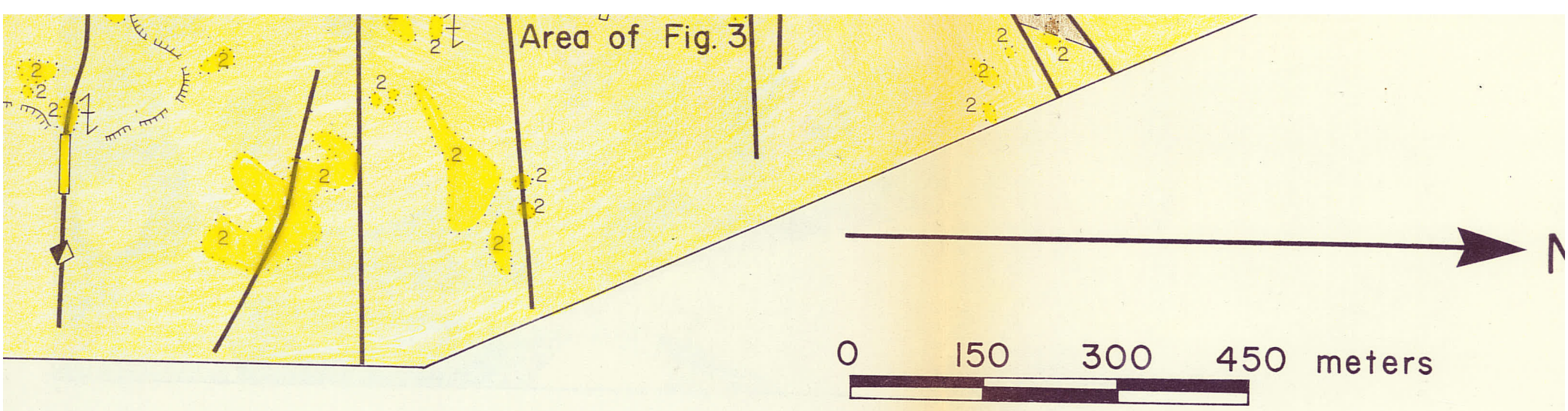

stic and Chemical Metasedimentary Rocks

clastic units—immature metasandstone and conglomerate, minor ferruginous metachert, tasiltstone, intermediate tuff, felsic tuff

strine unit—metasiltstone, fine metasandstone, ferruginous metachert, metachert, marble, ermediate to mafic tuff and lapilli-tuff

metaconglomerate derived from formations J and H

clastic units—immature metasandstone and conglomerate derived from formation H

to intermediate pyroclastic rocks and flows deposited in caldera

ations[f]

divided metavolcanic, metasedimentary, and granitic rocks

y. Outcrops and inferred extensions of each rock unit are shown, respectively, in dee of the same colour.

are uncertain.

l to volcanism.

e mafic zone are not subdivided in sills 2, 3, and 4. Designation 10 is used for er enclature after Ayres (1977).

younger than sill complex. Granitic rocks include both contemporary synvolcanic ater granitic batholiths.

outcrop, area of rock outcrop

ogical boundary (defined, approximate)

ling, top unknown (inclined, vertical, dip unknown)

ing, top (arrow) from cross-bedded relations (inclined, vertical, overturned)

flow, top (arrow) from pillow shape and packing

stosity, gneissosity, cleavage, foliation (inclined, vertical, dip unknown)

stope, mine shaft

ically and modally analysed sample

ally analysed sample

ciated area

tailings

designation, phase Z

designation, phase X

ng top (arrow) from grain gradation (inclined, vertical, overturned)

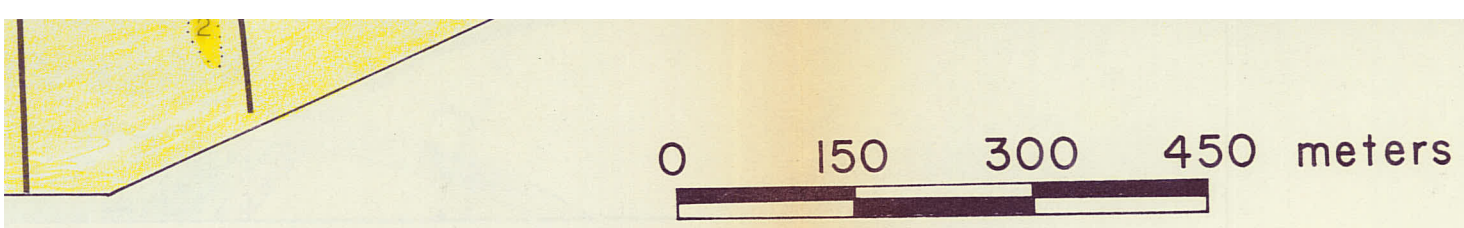

Metasedimentary Rocks

ture metasandstone and conglomerate, minor ferruginous metachert, liate tuff, felsic tuff

stone, fine metasandstone, ferruginous metachert, metachert, marble, tuff and lapilli-tuff

derived from formations J and H

nature metasandstone and conglomerate derived from formation H

yroclastic rocks and flows deposited in caldera

c, metasedimentary, and granitic rocks

inferred extensions of each rock unit are shown, respectively, in deep our.

not subdivided in sills 2, 3, and 4. Designation 10 is used for entire zone. res (1977).

l complex. Granitic rocks include both contemporary synvolcanic oliths.

of rock outcrop

defined, approximate)

(inclined, vertical, dip unknown)

from cross-bedded relations (inclined, vertical, overturned)

) from pillow shape and packing

ty, cleavage, foliation (inclined, vertical, dip unknown)

aft

lly analysed sample

mple

ise Z

ise X

from grain gradation (inclined, vertical, overturned)

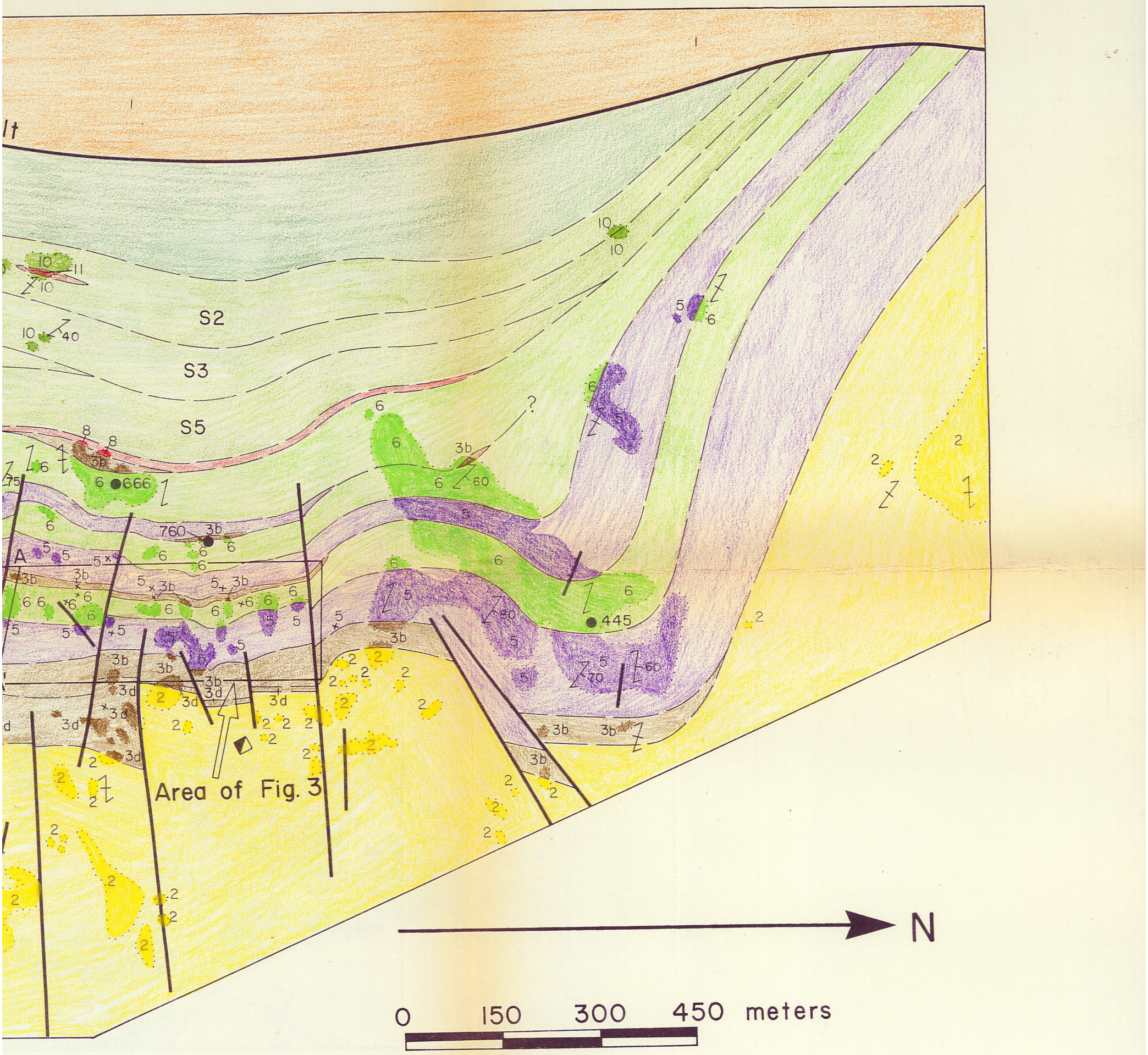

l Metasedimentary Rocks

mature metasandstone and conglomerate, minor ferruginous metachert, nediate tuff, felsic tuff

siltstone, fine metasandstone, ferruginous metachert, metachert, marble, ıfic tuff and lapilli-tuff

ıte derived from formations J and H

immature metasandstone and conglomerate derived from formation H

pyroclastic rocks and flows deposited in caldera

anic, metasedimentary, and granitic rocks

ıd inferred extensions of each rock unit are shown, respectively, in deep colour.